MSc Thesis: Assessment of Hydropeaking Impact on the Ecosystem of the River Meuse

Enhancing Ecological Conditions using Retention

Paul Thönissen

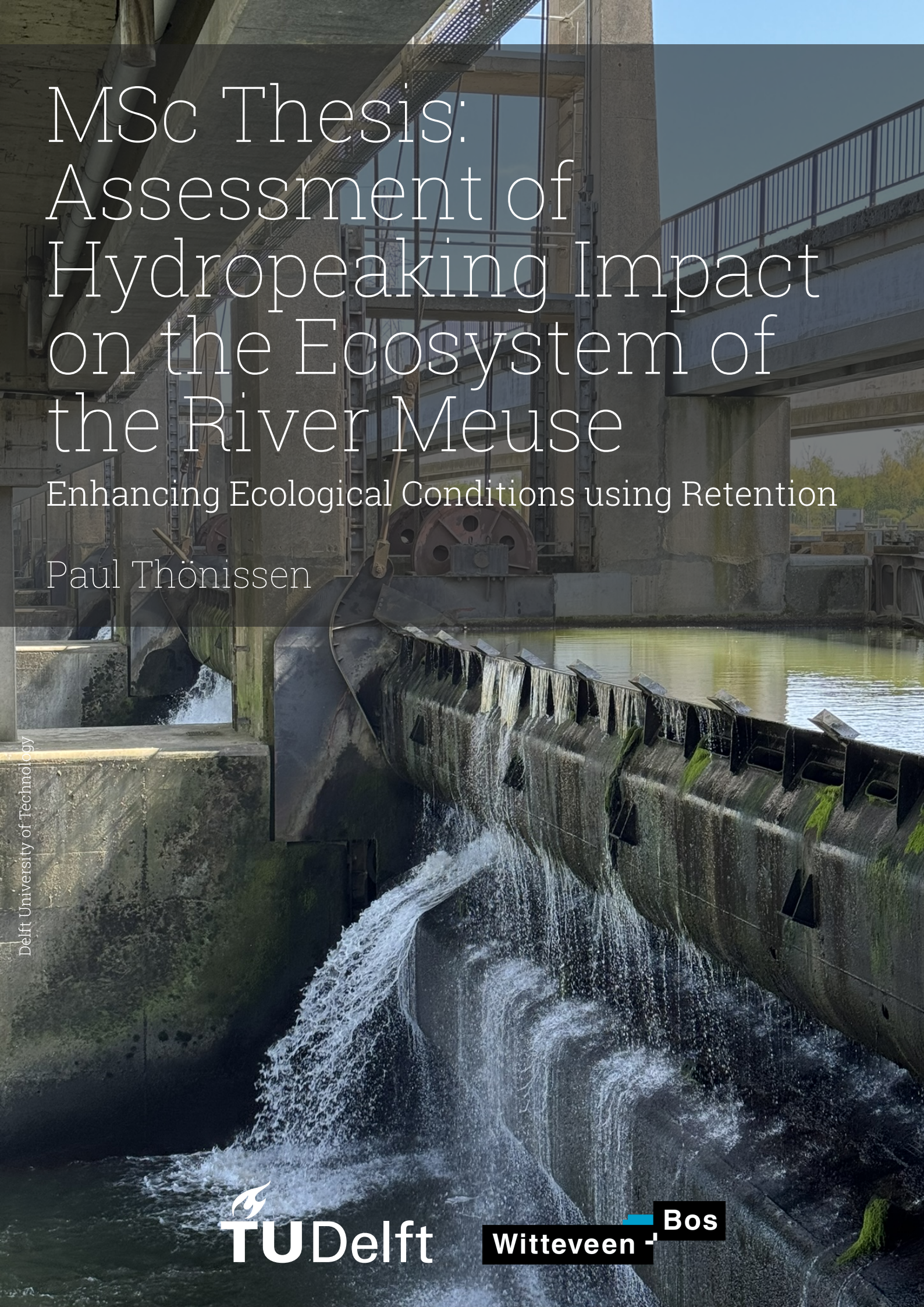

Delft University of Technology

TU Delft

Witteveen + Bos

MSc Thesis: Assessment of Hydropeaking Impact on the Ecosystem of the River Meuse

Enhancing Ecological Conditions using Retention

by

Paul Thönissen

Chair supervisor:	Dr.ir. A. Blom
Daily supervisor:	Dr.ir. E. Mosselman
Supervisor:	Prof.dr. M.E. McClain
Supervisor:	Prof.dr. T.A. Bogaard
Company supervisor:	Ir. M.M.A. Schippers
Project duration:	February, 2025 - August, 2025
Faculty:	Faculty of Civil Engineering & Geosciences, TU Delft

Cover: Weir of Lixhe (by author, 2025)

TU Delft Witteveen + Bos

Preface

This thesis marks the end of my studies at Delft University of Technology. The bachelor programme provided me with a very broad foundation in all Civil Engineering domains. As I found numerous domains interesting, choosing a Master's track was not easy. Ultimately, I chose the Hydraulic Engineering track, which offered fascinating courses. I do not regret the choice, as it led to this interesting thesis. It became quite a multidisciplinary thesis, combining data analysis, ecology, and hydrodynamic modelling.

My graduation committee also became multidisciplinary and relatively large, but in hindsight I am very happy with this. Especially because ecology is not an expertise of mine from the Master's programme, I appreciate having had Michael McClain and Thom Bogaard in my committee. Your ecological insights were extremely helpful. Astrid Blom, thank you for having been the chair of my committee. You were the first person from the university whom I contacted about this thesis topic. I received an enthusiastic reply from you within minutes. I greatly appreciated this positive start. Erik Mosselman, thank you for your daily supervision from the university side. You helped me go in depth while not losing track of my scope and planning at the same time.

Additionally, I would like to thank Pepijn van Denderen (HKV) and Frank Collas (Rijkswaterstaat) for sharing the results and methods of your research on hydropeaking in the Meuse. Especially the wavelet transform method was very useful in my research.

A very warm thank you goes out to Melanie Schippers, for your daily guidance from the side of Witteveen+Bos. I greatly appreciated working with you. Your expertise and experience greatly helped me throughout the research process. Especially when I ran into issues during the modelling part, you helped very well with troubleshooting. I also would like to thank the rest of the Hydrodynamics & Morphology team of Witteveen+Bos and the company in general. I have always felt very welcome and everyone was genuinely willing to help me with my research.

Lastly, I would like to thank my friends and family for their wholehearted support, thoughtful advice, and motivation throughout the graduation process.

It has been a great journey.

Paul Thönissen
Delft, July 2025

Abstract

This thesis investigates the ecological impact of hydropeaking in the Dutch Meuse and explores the effectiveness of retention as a mitigation strategy. While the presence of hydropeaking in the Dutch Meuse is known, there is limited knowledge about the ecological effects of these hydropeaks. In addition, no mitigation measures have been explored yet. This research aims to address these knowledge gaps.

Hydropower plants in the Belgian Meuse are operated to accommodate fluctuating energy demands and release fluctuating discharges as a result. These short-term fluctuations — called hydropeaks — propagate into the Dutch Meuse, where they disrupt aquatic ecosystems.

In this study, hydropeaks are isolated from the hydrograph using a wavelet transform to determine their magnitude and frequency. The wavelet transform method is also used to determine how far downstream hydropeaks reach into the Dutch Meuse. The impact of hydropeaking is assessed by looking at the degree to which protected habitats and species are affected by a median and a 95th percentile hydropeak. The hydropeaks are simulated in D-HYDRO, and the ecological consequences are assessed using three established ecological indicators: disconnected pool formation, wetted river area variation, and bed shear stress fluctuation. These indicators function as objective metrics that show how suited the river is for protected species and habitat types in response to hydropeaking. These species are river lampreys, chabot bullheads, macroinvertebrates, and the habitat type is large pondweed. Finally, the potential of retention is explored by incorporating a retention basin into the D-HYDRO model.

In the Dutch part of the Meuse, hydropeaking is mostly present in the Upper Meuse and the Common Meuse. Median hydropeaks do not cause significant harm to ecology in those reaches, whereas 95th percentile summer hydropeaks do exceed critical ecological thresholds associated with the studied indicators. The wetted river area variation threshold is exceeded at four one-kilometre reaches during an extreme hydropeak, destabilising potential spawning grounds of chabot bullheads and habitats of river lampreys. Retention reduces the number of reaches exceeding the wetted area variation threshold by 75%. At two out of three studied gravel bars, notable disconnected pool areas form that may endanger chabot bullheads, which are reduced by 61% and 67% when implementing retention. Bed shear stresses fluctuate substantially at two out of three gravel bars, compromising macroinvertebrate and chabot bullhead habitats. Retention reduces drift-prone areas at those gravel bars by 54% and 89%.

These results suggest that hydropeaking significantly affects ecology in the Meuse, and that substantial improvements can be achieved when retention is adopted as a mitigation strategy. However, hydropeaking is only one of several factors influencing the river's ecology. Therefore, measures that address hydropeaking impact alone are unlikely to bring the ecosystem to its desired state. An integrated approach is required, focusing on water quality, climatological developments, and ecosystem connectivity, alongside specific measures targeting protected habitats and species as defined by Natura 2000 guidelines (Rijkswaterstaat, 2023). Furthermore, while retention has been explored in a theoretical context in this study, its practical implementation poses significant challenges, making it unlikely to serve as a feasible and effective solution on its own.

The study concludes that the southern part of the Dutch Meuse is adversely affected by extreme hydropeaks, resulting in harm to the local ecosystem. The application of retention could improve ecological conditions. However, further research is required to optimise hydropeaking magnitude predictions, enabling retention based on real-time data. Additionally, impounding using the weir of Borgharen may be considered as an alternative mitigation measure. Enhanced communication between Rijkswaterstaat and Belgian hydropower plant operators can improve effective mitigation, regardless of the type of measure. Any measure should be embedded into a broader strategy which addresses all ecological stressors, such that a sustainable solution is achieved. Finally, as large summer hydropeaks are particularly detrimental to ecology, efforts to limit the formation of such hydropeaks at their source may reduce the need for downstream mitigation measures.

Contents

1 Introduction

1.1. Context

Due to the global shift towards renewable energy and the high flexibility of hydropower in meeting dynamic daily energy demands, the installation of hydropower plants is on the rise. While hydropower offers significant advantages in the transition to cleaner energy sources, it also causes major discharge fluctuations when operated to meet the variable energy demand (Jardim and Colishonn, 2024). The phenomenon whereby hydropower plants cause short but relatively large discharge fluctuations is also known as hydropeaking. These hydropeaking events differ from natural peak flows by exhibiting a shorter, sub-daily period and by causing more rapid changes in flow velocity and water level (Meile et al., 2011).

Hydropeaking severely disrupts aquatic ecosystems, as hydropeaks result in rapid changes in water level and flow velocity, making it challenging for aquatic species to adapt (Schülting et al., 2018). The abundance, diversity, and size of fish and macroinvertebrates are negatively impacted by the disruption of natural flow conditions (Bipa et al., 2023). A rapid decrease in water level can trap fish in shallow areas, as they struggle to reach deeper parts of the river in time (Hoffarth, 2004). This can lead to stranding due to complete dewatering or high stress on fish that are trapped in shallow pools with extreme temperatures and a lack of oxygen (Salmaso et al., 2021). Conversely, a rapid increase in flow velocity can cause macroinvertebrates to drift downstream, as they may fail to find shelter quickly enough. Hydropeaking also leads to less and slower egg hatching, as eggs are flushed away during the rising stage of hydropeaking and desiccated during the falling stage of hydropeaking (Bipa et al., 2023).

Hydropeaks diffuse when travelling downstream due to bed friction and interaction with floodplains and connected ponds. However, when there is a succession of hydropower plants, hydropeaks may be amplified at each plant. Consequently, a hydropeak can persist over a long river reach. This process of hydropeak amplification is visualised in Figure 1.1. The described phenomenon is exactly what occurs in the Belgian Meuse as well: Several hydropower plants in succession cause significant hydropeaks (Asselman et al., 2019). The sequence of hydropower plants in the Belgian Meuse is visible in Figure 1.2. Figure 1.3 shows the hydrograph at Eijsden, which is the most upstream measurement station in the Dutch Meuse, located only one kilometre downstream of the Lixhe hydropower plant. The hydrograph clearly displays many fluctuations on a daily scale, which is in line with the typical hydropeaking wave period of 0.1 to 1.5 days (Van Denderen, 2024). This initial analysis suggests that hydropeaking also occurs in the Dutch Meuse.

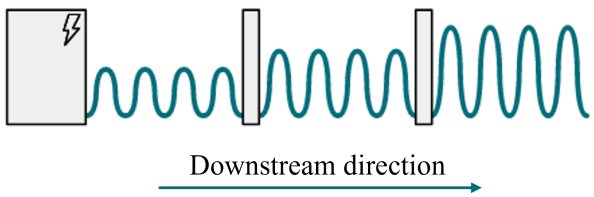

Figure 1.1: Hydropeaking generation and its amplification by successive hydropower plants or weirs. Adjusted from Asselman et al. (2019).

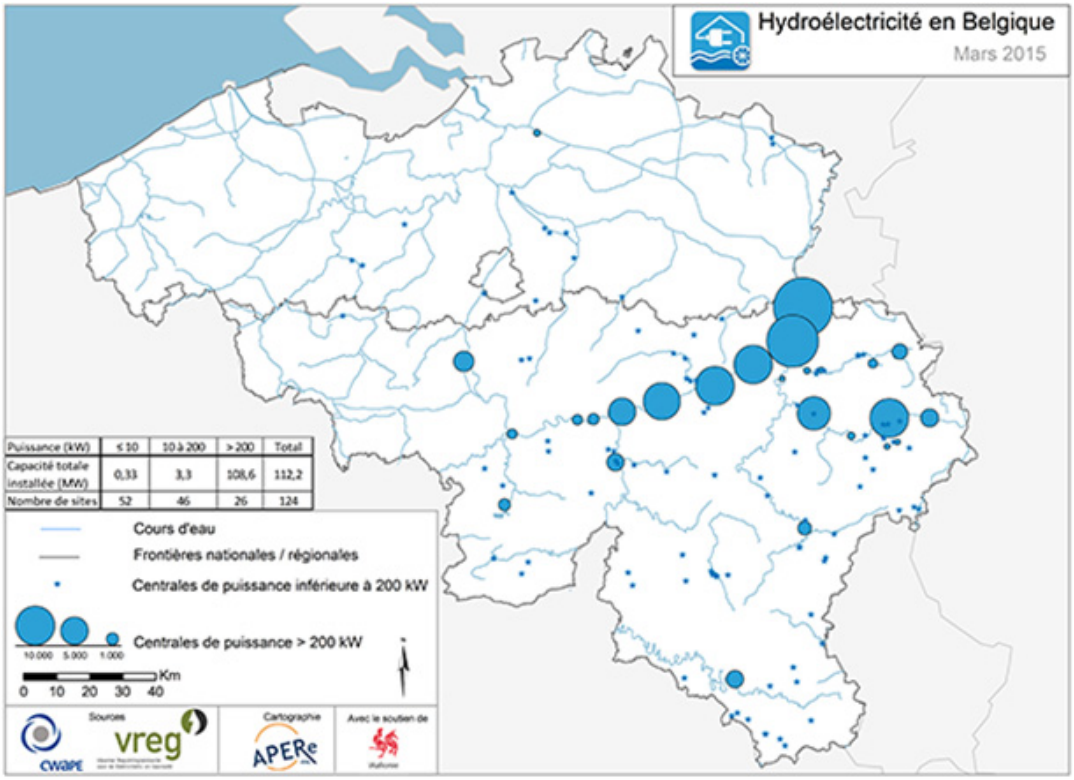

Figure 1.2: Hydropower plants in Belgium. The larger the circle, the greater the nominal capacity of the respective plant. The smallest circles represent plants with a nominal capacity below 200 kW, all other plants have a nominal capacity of above 200 kW (Grenzeloze Schelde, 2016).

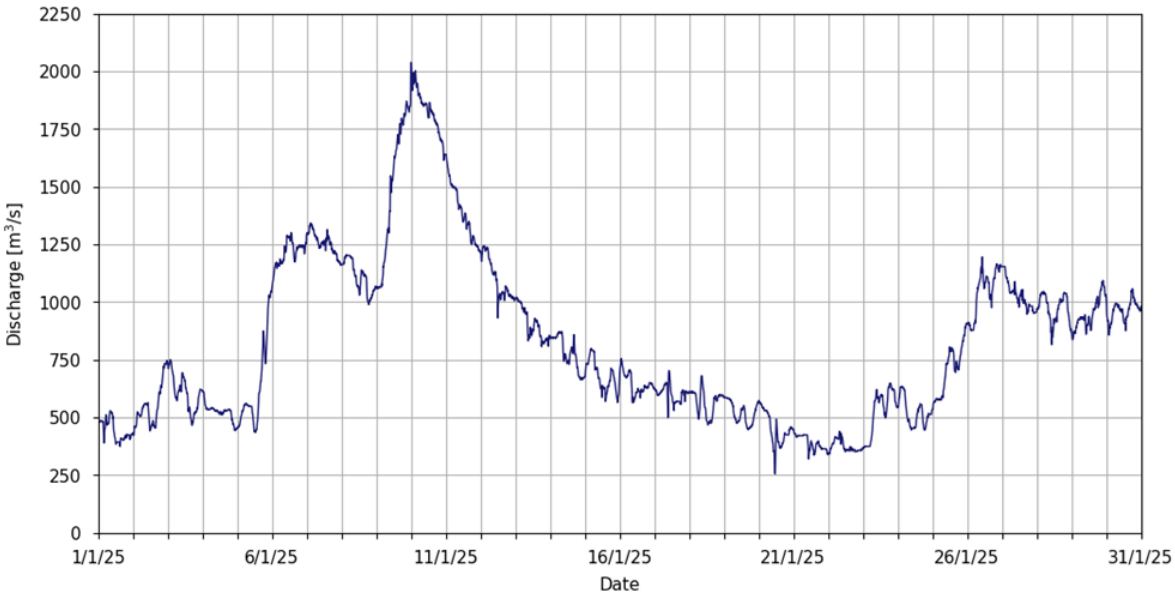

Figure 1.3: Hydrograph of January 2025 at measurement station Eijsden Grens (Rijkswaterstaat, 2025e)

Searching for “hydropeaking” in scientific documents through search engine Scopus gives 435 results between 1991 and 2024 (Scopus, 2025). Figure 1.4 shows a clear increase in mentions over the past decade. This increase may reflect a broader recognition of the ecological impacts of hydropeaking, which is in line with the current trend of dams being dismantled. In 2023 alone, 487 river barriers were

removed in Europe, a 50% increase from 2022, which was already a record year itself (Dam Removal Europe, 2024). In line with that, the European Commission (2020) has set a goal for 2030 to restore at least 25,000 km of European rivers into free-flowing rivers to restore river connectivity by removing obsolete barriers.

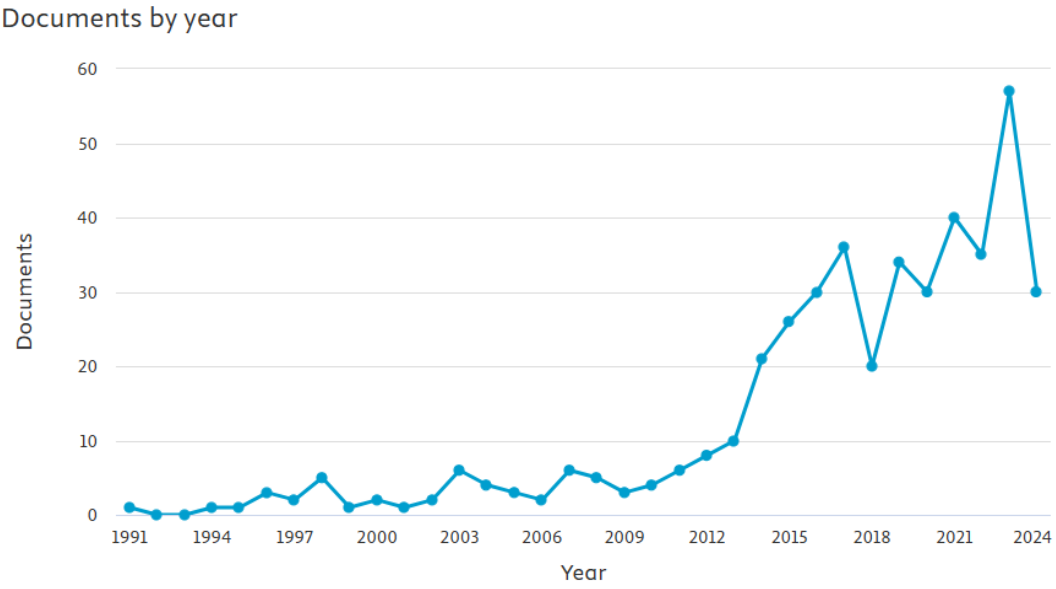

Figure 1.4: Search results for “hydropeaking” in search engine Scopus (Scopus, 2025)

1.2. Problem definition and research objective

Hydropeaking is a well-documented phenomenon that severely disrupts riverine ecosystems. The rapid discharge fluctuations lead to abrupt changes in water level and flow velocity; they threaten aquatic life such as fish and invertebrates through drift; and they cause stranding, egg desiccation, and increased exposure to low-quality water (Schülting et al., 2018; Bipa et al., 2023; Hoffarth, 2004; Salmaso et al., 2021). Hydropeaking occurs in the Dutch Meuse as well, as a consequence of upstream hydropower generation (Asselman et al., 2019; Van Denderen, 2024; Van Neer, 2016).

Despite the scientific consensus that hydropeaking is a serious issue and occurs in the Dutch Meuse, no comprehensive research has been conducted on its ecological impact and on how this impact can be effectively mitigated. Van Denderen (2024) assessed the magnitude of hydropeaking in the Dutch Meuse, and Van Neer (2016) focused on macroinvertebrate abundance in relation to hydropeaking; however, no study has made the link between locally occurring hydropeaks and ecology in a broader sense. Logically, as the extent of hydropeaking impact is not fully clear, mitigation strategies have also not been established.

Reindl et al. (2023) and Tonolla et al. (2017) examined the use of retention basins[1] as a strategy to mitigate hydropeaking impact, with positive outcomes in both studies. Although these case studies focus on mountainous rivers with hydrological and ecological characteristics that differ from those of the Meuse, the results do suggest that retention has potential as a mitigation strategy to prevent ecological impact caused by hydropeaking.

Therefore, this research aims to evaluate to what extent hydropeaking negatively impacts ecology in the Dutch Meuse, and how this negative impact can be successfully mitigated using retention.

[1] “Retention ponds are ponds or pools designed with additional storage capacity to attenuate surface runoff during rainfall events.” (European Commission, 2025)

1.3. Research questions

The research questions of this study are:

- "What part of the Dutch Meuse is affected by hydropeaking and what are the characteristics of these hydropeaks?"
- "In what way is the ecology of the Dutch Meuse affected by hydropeaking?"
- "To what extent could retention be an effective measure to reduce the negative effects of hydropeaking in the Dutch Meuse?"

1.4. Approach

To assess and mitigate the negative ecological impact of hydropeaking in the Dutch Meuse, various steps have to be taken. First, the area of interest is explored, and local river characteristics and ecological circumstances are analysed to identify specific ecological risk factors. From this analysis, ecological indicators are adopted which can be used to objectively assess the extent to which hydropeaks impact the environment. Then, the extent to which hydropeaking occurs in the Dutch Meuse has to be assessed. Signal processing techniques, namely a moving average, a Fourier transform, and a wavelet transform, are tested and compared on their performance to separate hydropeaks from the natural discharge using historic river discharge data. The best performing method is used to separate the hydropeaks and quantify their magnitude.

Hydrodynamic modelling is then used to simulate hydropeaks of various magnitudes, which follow from the data analysis part. The effect of these hydropeaks on ecology is then assessed using the indicators. Subsequently, retention is implemented into the model to evaluate to what extent it can contribute to the mitigation of the negative impact of hydropeaks.

Using this approach, a comprehensive understanding of the ecological impact of hydropeaking in the Dutch Meuse is developed, as well as insight into how well retention basins can be applied as a mitigation strategy.

1.5. Scope

Spatial scope

This research focuses on the southern part of the Dutch Meuse. The area of interest is bounded by the weir of Lixhe upstream, which is located practically on the Dutch-Belgian border, and the point where hydropeaks are negligible downstream. The latter can be determined by analysing hydrographs that are available through Rijkswaterstaat (2025e) at various locations. Near Roermond, large ponds induce substantial peak diffusion (Asselman et al., 2019), which is why hydropeaks are expected to be largely attenuated in this area. The expected study area is visualised in Figure 1.5.

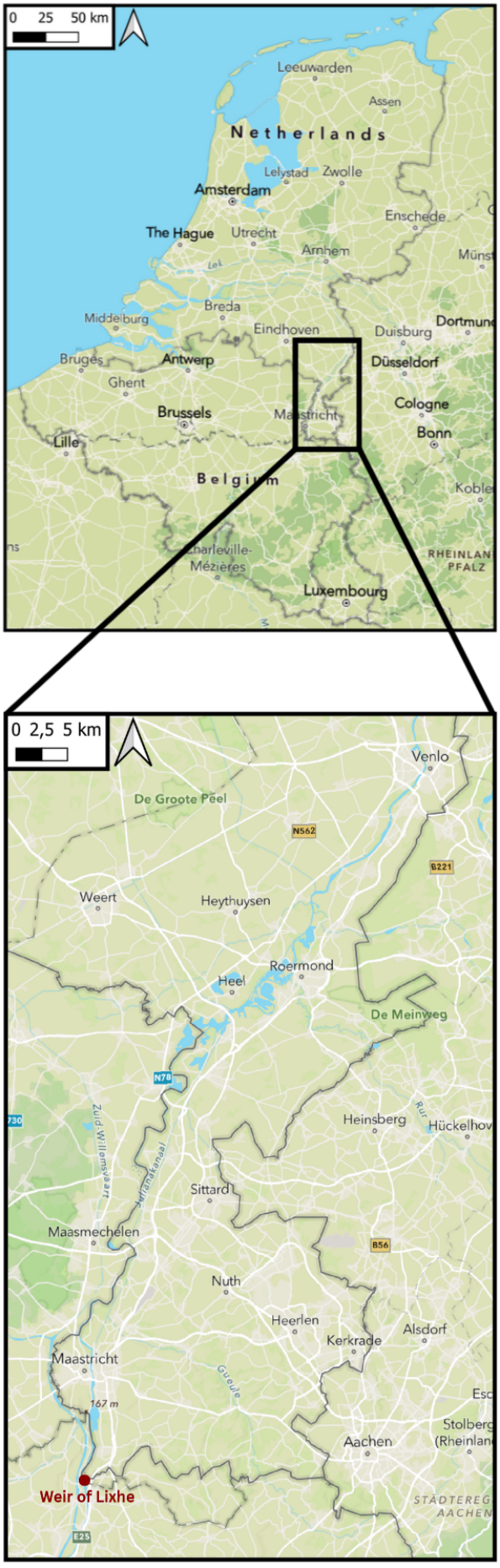

Figure 1.5: Approximate area of interest. Adjusted from Esri (2025a).

Mitigation scope

This study focuses on the application of structural measures to mitigate potential hydropeaking impacts in the Dutch Meuse. Structural measures involve the use of retention basins downstream of the hydropower plant to absorb discharge peaks. These basins can temporarily store peak flows in basins and release them gradually, reducing the abrupt discharge fluctuations caused by hydropeaking (Bipa et al., 2023). Previous research by Ouwerkerk et al. (2021) has shown that there are opportunities for large-scale water storage along the Dutch section of the river Meuse, making structural measures a promising option to explore.

In contrast, operational measures, which involve altering the discharge patterns of the Belgian hydropower plants to return to a more natural flow regime (Bipa et al., 2023), are excluded from the scope of this research. Implementing such measures would require transnational cooperation between Belgium and the Netherlands. This presents significant logistical and political challenges. Moreover, the persistent variability in energy demand, which drives hydropeaking, would require alternative energy sources, an issue beyond the scope of this study.
Morphological measures could also contribute to the mitigation of hydropeaking impact by changing the river geometry to accommodate larger peak flows or provide shelter to aquatic habitats (Kindle et al., 2012). This, nevertheless, lies outside the scope of this study too.

In summary, this research focuses on understanding the extent of hydropeaking impacts downstream of the Lixhe weir and exploring retention as a measure to mitigate these impacts within the defined spatial context of the river Meuse.

1.6. Thesis outline

Chapter 2 covers the area of interest. First, background information about the Meuse is provided, along with ecological attention points. Habitat types and species that are under protection in the Dutch Meuse are studied to determine how they could be affected by hydropeaking and what they require in order to be preserved. These insights are combined with established ecological effects of hydropeaking to define three indicators that support the assessment of hydropeaking impact on the ecosystem. Possible retention locations along the Dutch Meuse are also explored at this stage.

In Chapter 3, various signal processing methods to detect and isolate hydropeaks are proposed and evaluated. These methods are a moving average, a Fourier transform, and a wavelet transform. Subsequently, the most suitable method is applied to the hydrographs along the Meuse to identify the characteristics of hydropeaking in the area of interest.

In Chapter 4, hydrodynamic model runs are performed based on the hydropeaks that are identified in Chapter 3. The indicators of Chapter 2 are then used to evaluate the ecological impact of the hydropeaks. Subsequently, retention is implemented to mitigate potential negative effects. The effectiveness of retention is once again objectively measured using the indicators.

Chapter 5 reflects on the study results and puts them into a broader perspective. Limitations of the used methods are discussed, and the implications of the findings are presented.

Finally, Chapter 6 revisits the research questions and provides the main conclusions of this study. Finally, recommendations are made to involved stakeholders and researchers.

2
The field site

This chapter covers the characteristics of the southern Dutch Meuse and examines the relationship between hydropeaking and the local ecosystem. Section 2.1 describes the properties of the river, including its hydrodynamics, morphology, ecology, and ongoing projects. Section 2.2 addresses the consequences of hydropeaking, both in general and in the local context. In Section 2.3, ecological indicators are established to support the hydropeaking impact assessment. In Section 2.4, hydropeaking impact mitigation strategies are compared. Section 2.5 explores the potential of retention as a mitigation strategy.

2.1. Properties of the southern Dutch Meuse

This section addresses the hydrodynamic, morphological, and ecological properties of the southern Dutch Meuse such that a tailored solution to the ecological effects of hydropeaking can be developed.

The approximate area of interest (Figure 1.5) covers the part of the Meuse that spans from Lixhe to Roermond. This part of the river can be divided into three reaches: the Bovenmaas (or Upper Meuse in English), the Grensmaas (or Common Meuse in English) and the Plassenmaas (has no widely used English name). These reaches are visible in Figure 2.1, and their characteristics are further discussed in Section 2.1.1.

2.1.1. Hydrodynamics and morphology

The Upper Meuse is the most upstream part of the Maas, bounded by Eijsden on the Dutch-Belgian border upstream and the weir of Borgharen downstream. It is the only non-alluvial river reach in the Netherlands (Becker et al., 2022). The bed consists of hard marl with high ecological value that hardly erodes. The downstream part of the Upper Meuse is almost permanently impounded by the weir of Borgharen, making it suitable for navigation. The upstream reach between Eijsden and the Lanayen sluice is shallower and only used for recreational navigation (Asselman et al., 2019).

The Common Meuse is located between Borgharen and Thorn. Most of the 49 km long reach is free-flowing as it is not affected by the weir of Linne downstream. The bed consists of sand and fine gravel, in many places covered by an alluvial layer of coarse gravel. The Common Meuse has many gravel bars and a lot of variation in water depth and flow velocity. This makes the river reach unsuitable for navigation, which is why the parallel Julianakanaal was opened in 1935 (Asselman et al., 2019). The Common Meuse has a relatively steep bed slope of 0.5 m/km (Strijker et al., 2023).

The Plassenmaas is located between Thorn and Roermond. Here, the river is impounded, the bed slope becomes less steep, and large ponds can be found adjacent to the river. These ponds originate from the gravel excavations of the 20th century and contribute to peak attenuation. The bed of the Plassenmaas consists of large amounts of coarse sand and gravel (Asselman et al., 2019).

The Meuse is a pluvial river, i.e. its discharge comes completely from rain and not from melting glaciers (Asselman et al., 2019). Precipitation in the Meuse catchment is nearly constant throughout the entire year, but river discharge is 10 times higher in winter than in summer. This can be fully attributed to a difference in evaporation.

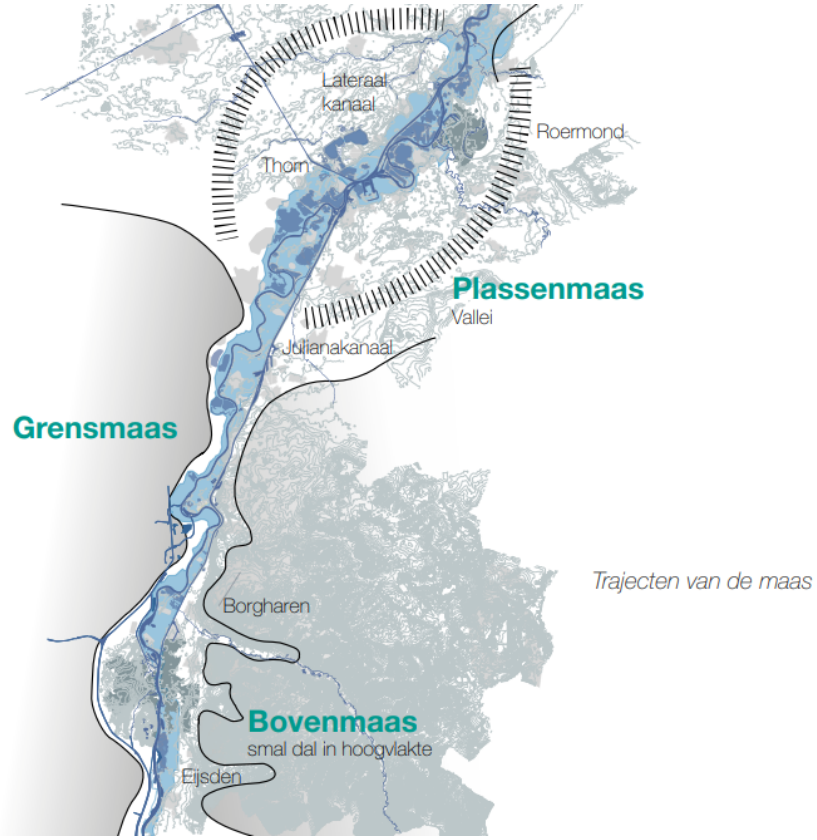

Figure 2.1: Reaches of the southern part of the Dutch Meuse (Asselman et al., 2019)

2.1.2. River training versus dynamics

In the nineteenth and twentieth centuries, the Meuse has been increasingly trained[1] to accommodate ship navigation, and dikes were constructed as a flood protection measure (Asselman et al., 2019). In addition, 7 weirs were installed to facilitate sufficient fairway depths at all times (Rijkswaterstaat, 2025c). The Common Meuse, however, remained free-flowing, as the steep bed slope and meandering character of the reach made it an unsuitable place for inland navigation (Brevé et al., 2014). Instead, a channel, the Julianakanaal, was constructed parallel to the Common Meuse to accommodate navigation (Asselman et al., 2019).

The engineered system worked well for navigation, but flood safety decreased. The increased amount of dikes along the Meuse led to a decrease in floodplain area, and the only way to prevent flooding was continuously heightening the dikes. After the high water events of 1993 and 1995, Dutch scientists and policymakers concluded that the governing approach of flood protection by dike heightening was not desirable anymore (Van Duinhoven, 2004). This led to the 'Room for the River' and 'Maaswerken' programmes, in which space was given back to the Dutch rivers, instead of limiting the space and only focusing on keeping the water between the narrow space between the dikes. The programs encompassed relocating dikes inland, reconnecting the river with the floodplains, lowering existing floodplains, and reconnecting the river with existing ponds (Asselman et al., 2019; Van Duinhoven, 2004).

The Common Meuse remained meandering and free-flowing throughout the river training process, but it was still affected by the engineering activities, as upstream weirs decreased the amount of incoming sediment (Asselman et al., 2019). Additionally, sediment production decreased as well, as commercial gravel extraction left behind large, unerodible rocks (Brevé et al., 2014). 'Project Grensmaas', which is part of the Maaswerken programme, was initiated to restore morphodynamics in the Common Meuse and improve flood prevention. The floodplains are now erodible again, as the top layer of fine gravel and

[1] river training = artificially making a river narrower and straighter (Asselman et al., 2019)

coarse sand is removed and replaced by dredged sand and gravel that are not suitable for commercial purposes (Brevé et al., 2014). The lower floodplains on the Dutch side of the river contribute to flood prevention, as the river is given more space.

2.1.3. Water quality

More extreme river discharges are observed as a result of climate change. Intense rain depressions cause large peak flows, and prolonged dry periods with high temperatures cause critically low flows (Rijksoverheid, 2022). During these low-flow periods, water temperatures rise and oxygen levels drop, harming the aquatic ecosystem. This effect is especially pronounced in the Meuse, as it is a rain river (Asselman et al., 2019).

The water quality of European water bodies is monitored by local water authorities, and assessed according to the standards of the Water Framework Directive (WFD) (European Commission, 2000). This guideline was set up in 2000 by the European Union and is meant to guide the member states of the European Union towards achieving water bodies with adequate ecological and chemical status (Wageningen University & Research, n.d.). The Netherlands ranks lowest among all EU nations in meeting the WFD criteria. Only 1% of the Dutch water bodies have both satisfactory chemical properties and satisfactory ecological properties. The poor water quality can be partly explained by pollutants coming from upstream countries. Additionally, the intensive livestock farming, high population density, and industrial pollution contribute to the issue (Wageningen University & Research, n.d.).

In the Common Meuse specifically, conditions have improved over the past decades. A decrease in chemical pollutants has reduced excessive temperatures and oxygen depletion. However, the ecological status is still unsatisfactory and future water quality is also at risk due to climate change, and persistent agricultural and pharmaceutical pollutants (Rijkswaterstaat, 2023).

2.1.4. Habitats and species

The lack of ship navigation, the presence of gravel bars and the large variety in flow velocity and water depth have resulted in a diverse ecosystem with many habitat types and habitat species in the Common Meuse (Asselman et al., 2019). This great ecological value has resulted in the Common Meuse being named a Natura 2000 area. Natura 2000 is a network of nature reserves set up by the European Union to preserve biodiversity across Europe. Areas that are part of the network have to meet high standards regarding the protection of habitat types and habitat species (Rijkswaterstaat, 2023).

Every Natura 2000 area has its own habitat types and habitat species that have to be protected to preserve a healthy ecosystem and to restore biodiversity in rivers across Europe (Rijkswaterstaat, 2023). For the Common Meuse Natura 2000 area, these types and species are specified in the ’aanwijzingsbesluit’ (Programmadirectie Natura 2000, 2013) and the ’ontwerpwijzigingsbesluit’ (Directie Natuur & Biodiversiteit, 2018).

In the maintenance plan called ’Natura 2000-ontwerpbeheerplan Grensmaas’ (Rijkswaterstaat, 2023), all habitat types and habitat species are discussed in detail. An individual goal is set, their current situation is addressed, their current state of preservation and expected trend are studied, and attention points are mentioned. In this context, a habitat type is an ecosystem with characteristic properties, and a habitat species is any species that is part of European habitat guidelines (Ministerie van Landbouw, Visserij, Voedselzekerheid & Natuur, n.d.).

Table 2.1 shows all habitat types that are to be protected in the along the Common Meuse, and it is stated whether their preservation goal is currently achieved. In addition, the table includes attention points for each habitat type that may be relevant to this research. Table 2.2 is similar, but then for habitat species instead of habitat types.

Table 2.1: Habitat types Natura 2000 Common Meuse (Rijkswaterstaat, 2023)

Habitat type	**Preservation goal achieved?**	**Attention points regarding hydropeaking**
Streams and rivers with water plants, large pondweed	No	Unnatural discharge fluctuations cause high flow velocities and harm young plant roots locally in the southern part of Common Meuse from May to July.
Silty riverbank	Yes	Frequent inundations in summer keep vegetation open. Extreme flow velocities in summer are harmful to young roots. They may drown, break, or get crushed by sediment.
Megaphorbs and fringes, meadowsweet	No	Inundations and water level fluctuations are beneficial to this type, as they deliver nutrients.
Megaphorbs and fringes, tree lines	No	It can withstand inundations and water level fluctuations but does not depend on them.
Moisty alluvial forests, riparian forest	Yes	The increase in low-flow periods in summer forms a threat to this type.
Moisty alluvial forests, streamguiding forests	Yes	It is mostly located along the impounded part of the Common Meuse. Therefore, the water level fluctuations due to hydropeaking barely play a role.

Table 2.2: Habitat species Natura 2000 Common Meuse (Rijkswaterstaat, 2023)

Habitat species	**Preservation goal achieved?**	**Attention points regarding hydropeaking**
River lamprey	No	• Only migration and spawning are observed and pursued. • Migration happens between October and April, spawning between March and May • Reproduction requires shallow (< 1.5 m) fast-flowing sections. • Adults die shortly after spawning. • Infants live in the river bed for 3–4 years • Infant larvae require stable, slow-flowing water, without discharge fluctuations. • River lamprey can withstand low oxygen concentrations, but may be sensitive to pollution.
Salmon	Yes	• Salmon migrates to spawning grounds all year round. • Spawning happens in November and December on a gravel bed in flowing water. • After living for 1–2 years in spawning areas, infants migrate to sea in March to May. • Common Meuse only of use as migration area. Migration happens in spring, early summer and autumn. • Salmon are very sensitive to low oxygen levels and high water temperatures: at 20 °C, migration stops.
Chabot bullhead	No	• Spawning happens in March and April between rocks, river wood, and tree roots. • Chabot bullhead mainly lives in shallow zones near the banks. • Water level fluctuations are detrimental to spawning: spawning grounds fall dry, eggs dry out and silt deposition can suffocate eggs. • Chabot bullheads are very sensitive to oxygen levels and water temperature. • Chabot bullhead's main prey are macroinvertebrates.
Beaver	Yes	• Beaver population is nearly saturated in the Common Meuse. • Beavers mainly live around gulleys and meadowsweet covered river banks. • Grassy banks should not fall dry in summer, so discharge fluctuations are to be avoided.

2.2. Consequences of hydropeaking

The Meuse, being a pluvial river, has a highly variable discharge pattern. There are no glaciers or big lakes in its catchment that ensure a base flow. Meteorological factors such as rainfall and evaporation are the main drivers behind the discharge magnitude (Asselman et al., 2019). For such rivers, impounding water in weirs is a useful way to reduce the variability in discharge and address water scarcity issues. Additionally, water can be released to generate electricity, resulting in hydropeaks. This section elaborates on the consequences of these hydropeaks on ecology.

2.2.1. General ecological consequences of hydropeaking

Besides the advantages of hydropower plants, such as flexible energy generation, also significant negative impacts are associated with the hydropeaks that are produced by hydropower plants. A rapid flow increase causes fish and invertebrates to drift downstream, and a sudden drop in water level leads to species stranding in shallow pools with poor water quality (Auer et al., 2017). Spawning grounds are also at risk during hydropeaks. Eggs can get damaged during the beginning of a hydropeak because of sediment flushing, and spawning grounds may fall dry during the falling stage of a hydropeak (Kopecki et al., 2022). Hydropeaking-affected rivers also often display thermopeaking, a phenomenon where temperature peaks are travelling through the river due to thermal stratification in impounded reaches. These thermopeaks increase the risks of drift and stranding of organisms (Auer et al., 2023). This enumeration highlights key impacts, but it is not exhaustive, as hydropeaking can have additional ecological impacts. Each of the mentioned impacts is addressed below in more detail.

Drift

Catastrophic (involuntary) drift and behavioural (active) drift are natural phenomena for benthic macroinvertebrates. However, hydropeaking increases catastrophic drift and depletes species, leading to a decrease in behavioural drift. The magnitude of the disturbance relative to the baseflow magnitude is the deciding factor in the occurrence of catastrophic drift (Céréghino et al., 2004).

Bed shear stress causes benthic organisms to erode from the river bed. Reaches with high variability in flow velocity often exhibit increased catastrophic drift of species (Lancaster and Hildrew, 1993). Hydropeaks cause rapid changes in bed shear stress, hindering macroinvertebrates from finding refuge from the flow in time. Even though natural high discharges may generate larger shear stresses than hydropeaks, it is the high rate of change of the shear stresses during hydropeaks that poses a threat to macroinvertebrates (Schülting et al., 2018).

Stranding

The phenomenon stranding refers to the occurrence of aquatic animals becoming isolated from the main river stream in shallow pools. These bodies of water typically contain little oxygen and quickly deteriorate in water quality due to a lack of dilution and rising temperatures (Hoffarth, 2004).

Stranding happens during the falling stage of hydropeaking, when water levels drop quickly. Reducing these large down-ramping rates during hydropeaking events should reduce fish mortality as well (Bradford et al., 1995).

Juvenile fish are more susceptible to stranding than adult fish, as young fish prefer slow-flowing areas and these are areas that are particularly prone to stranding (Moore and Gregory, 1988; Grimardias et al., 2012).

Reduction in amount of spawning grounds

Hydropeaking reduces the quantity of potential spawning grounds, as these habitats more frequently inundate and desiccate in a hydropeaking-affected area (Moreira et al., 2018). Additionally, instantly flushing blocked sediment through a river poses the risk of damaging eggs (Panthi et al., 2022).

Reductions of water level fluctuations and controlled sediment transport should therefore be pursued to optimise spawning conditions.

Thermopeaking

Hydropeaking leads to rapid changes in water temperature as well. This phenomenon, called thermopeaking, is caused by the stratification of water temperatures in impounded reaches. Cold thermopeak-

ing, a sudden decrease in water temperature, usually occurs in summer, and warm thermopeaking, a sudden increase in water temperature, usually occurs in winter (Zolezzi et al., 2011).

Both cold and warm thermopeaking increase downstream drift and stranding of fish significantly. Auer et al. (2023) showed that cold thermopeaking leads to a 51% drift increase and a 31% stranding increase. Warm thermopeaking leads to a 27% drift increase and a 14% stranding increase. The experiment by Auer et al. (2023) was conducted on the European grayling.

2.2.2. Ecological consequences of hydropeaking for the Dutch Meuse

During low and average discharge levels, the water level in the Common Meuse is considerably influenced by incoming hydropeaks, whereas the water levels of the impounded river reaches are not (Asselman et al., 2019).

To prevent the lowering of groundwater levels on the Belgian side of the Common Meuse due to the Maaswerken programme, gravel sills have been constructed to maintain a sufficient water level during low-discharge periods. However, the effect of these measures remains uncertain, and they cause disconnected pools during low discharges, especially in combination with discharge fluctuations such as hydropeaks (Asselman et al., 2019). These pools are harmful to water quality, as they are oxygen-depleted and the water temperature is high, leading to algae bloom (Rijkswaterstaat, 2023; Asselman et al., 2019).

The water quality also deteriorates due to industrial wastewater that is discharged into the Meuse. During low-discharge periods, wastewater cannot properly dilute with the river discharge and causes high water temperatures, leading to oxygen depletion, algae bloom and botulism. Hydropeaking shortly decreases river discharge magnitude even further during low-flow periods, increasing the risks associated with waste discharges as well (Asselman et al., 2019).

Barbels (rheophilic fish) struggle to find suitable spawning grounds in the Common Meuse. During April and May, which is usually their spawning period, daily water level fluctuations of 0.2 to 1.6 m may occur, which can suddenly result in spawning grounds becoming too deep or spawning grounds running dry just after spawning, leading to a notable loss in barbel spawn (Asselman et al., 2019).

Van Looy et al. (2007) have demonstrated that beetle species abundance strongly correlates with discharge fluctuations in the Common Meuse. In their research, they established a 30% increase in discharge in an hour as a turning point, beyond which species presence declines significantly.

Very few species in the Common Meuse are able to cope with the fluctuating discharges that are caused by hydropower plants. Spawning grounds frequently flood and fall dry, making them unsuitable as eggs will either dry out or flush away. Even adult organisms cannot always withstand the stress that is exerted by the incoming hydropeaks and involuntarily drift downstream (Rijkswaterstaat, 2023).

Van Neer (2016) sampled macroinvertebrates at gravel banks in the Meuse, as hydropeaking is known to cause macroinvertebrate drift by rapid changes in bed shear stress (Schülting et al., 2018). The study found more characteristic species downstream. This could have led to the conclusion that hydropeaking causes less species abundance, as diffusion would make a hydropeak's magnitude and impact smaller downstream. However, the exact extent to which hydropeaking was responsible remains unclear, as the influence of other factors, such as tributaries, was not fully known. Van Denderen (2024) briefly addressed the influence of hydropeaks on bed shear stress. The study illustrated that hydropeaking leads to a substantial, rapid increase in bed shear stress in the Meuse. However, no link was made to specific species.

2.3. Indicators of hydropeaking impact

The 'Natura 2000-ontwerpbeheerplan Grensmaas' (Rijkswaterstaat, 2023) is used as the primary ecological guideline for this study. This means that the preservation goals of habitat types and habitat species that are identified to be of major importance in the Common Meuse in this plan are the focus points when assessing the impact of hydropeaking and a possible intervention. The main objective is to achieve the preservation goals of types and species that are currently not achieved yet, indicated by a 'No' in the third column of Table 2.1 and Table 2.2. However, achieving these goals should not

compromise the habitat area and habitat quality of the types and species whose preservation goal is already achieved.

An additional Natura 2000 area is present along the Dutch side of the river Meuse, called 'Maas bij Eijsden'. All habitat types and species that have to be protected here according to Becker et al. (2022), are also in 'Natura 2000-ontwerpbeheerplan Grensmaas' (Rijkswaterstaat, 2023), except habitat type 'moisty alluvial forests, ash-elm forests'. However, this type is not affected by hydropeaking as it is located highly elevated on the floodplains (Becker et al., 2022). Therefore, the habitats of the Natura 2000 Common Meuse area are also representative for the Natura 2000 Maas bij Eijsden area regarding hydropeaking. On the Belgian side of the Upper Meuse and Common Meuse there are also two Natura 2000 areas. They are called 'Basse Meuse et Meuse mitoyenne' (European Environment Agency, n.d.[a]) and 'Uiterwaarden langs de Limburgse Maas met Vijverbroek' (European Environment Agency, n.d.[b]). The species and types that are to be protected there, have similar ecological requirements as those on the Dutch side. Therefore, intervening in the system to improve the quality of the Dutch side of the ecosystem is expected to improve the Belgian side as well. That is why using the 'Natura 2000-ontwerpbeheerplan Grensmaas' (Rijkswaterstaat, 2023) as the primary ecological guideline for this study is considered appropriate.

Three indicators are used to assess how mitigation solutions can improve the state of the habitat types and species from Table 2.1 and Table 2.2 for which the preservation goal is not yet met. These indicators are:

- Disconnected pool formation (Section 2.3.1)
- Wetted river area variation ΔA_w (Section 2.3.2)
- Bed shear stress fluctuation $\Delta \tau_t$ (Section 2.3.3)

The indicators are set up using the knowledge about local circumstances (Section 2.1), as well as known consequences of hydropeaking, both in general and in the Meuse (Section 2.2). They are meant to address the negative effects hydropeaking has on organisms and the environment. Note, good scores on the indicators do not mean that the desired ecosystem is reached. It means that hydropeaking impact is minimal and the ecosystem partially improves, but other stressors such as pollution or temperature extremes due to climate change may persist. The indicators are used in the modelling section to objectively ascertain hydropeaking impact and to assess the effect of potential mitigation solutions.

2.3.1. Disconnected pool formation

This indicator is relevant for the habitat species chabot bullhead, as it is sensitive to temperature and oxygen levels in water. Hydropeaks are a common cause of disconnected pools in the Meuse during low-flow conditions (Asselman et al., 2019). These pools have increased temperatures and contain less oxygen, making it challenging for organisms to survive. Disconnected pools also form during natural flow fluctuations, but during hydropeaking it happens more rapidly, causing chabot bullheads to be cut off from the main stream. Moreover, hydropeaking frequency is significantly higher than natural peak flow frequency, so the hydropeaking-induced pools form more often.

Chabot bullheads are sensitive to both dissolved oxygen levels and extreme water temperatures. The lower and upper thermal limits of the chabot bullhead are 2.5 °C and 27.6 °C, respectively (Elliot and Elliot, 1995). The daily average air temperature at Maastricht in summer is close to the upper limit (Koninklijk Nederlands Meteorologisch Instituut, 2025). This makes the occurrence of disconnected pools with excessive water temperatures a serious risk for chabot bullheads in the Meuse. Furthermore, the presence of coarse gravel on the Common Meuse bed (Asselman et al., 2019) can cause quick drainage of water into the subsurface.

This indicator is relevant all year long. The goal is to reduce the amount of disconnected pools as much as possible. There is no specifically desired threshold value.

2.3.2. Wetted river area variation ΔA_w

The most important attention point for the habitat species river lamprey is addressed in this indicator. A low wetted river area variation should ensure that the water level fluctuations that occur during a hydropeak are not so large that they compromise potential river lamprey larvae habitats by frequently

drying and wetting the river bed. The larvae live in the river bed for several years, which means that the indicator is relevant for them all year long (Rijkswaterstaat, 2023). This indicator is also important to prevent chabot bullhead egg suffocation due to sediment deposition in March and April (Rijkswaterstaat, 2023). When spawning is followed by low-flow conditions, the risk of egg desiccation also increases as spawning sites fall dry (Saltveit and Brabrand, 2013). The primary concern is whether the river bed remains submerged or not, rather than the occurrence and magnitude of water level fluctuations. Therefore, the indicator is defined in terms of the maximum allowable variation in wetted river area.

Inspired by Baumann et al. (2012), Equation 2.1 represents the wetted river area variation indicator.

$$\Delta A_w = \frac{A_w^{\text{max}} - A_w^{\text{min}}}{A_w^{\text{max}}} \cdot 100 \ (\%) \tag{2.1}$$

Here, A_w^{max} and A_w^{min} denote the maximum wetted river area during a hydropeak cycle and the minimum wetted river area during a hydropeak, respectively.

In Switzerland, 30% is employed as the maximum allowable variation of wetted river area[2] (Baumann et al., 2012). Exceeding this limit results in an unsatisfactory ecological status. Although morphological properties such as bed slope and bed material may differ between Switzerland and the Netherlands, the ecological importance of having low wetted river area variation remains. Therefore, the Swiss limit of 30% wetted river area is adopted as a general guideline for the desired range of variation in this study. The optimal result in the Meuse is achieved by reducing the variation of wetted river area as much as possible during the entire year. In practice, low-discharge periods are expected to be most critical, as dry areas are more likely to occur during such periods than during high-discharge periods.

2.3.3. Bed shear stress fluctuation $\Delta\tau_t$

Finally, the third indicator is meant to maintain the population of macroinvertebrates, which are the main prey of chabot bullheads (Rijkswaterstaat, 2023). Moreover, macroinvertebrates are vital in the functioning of aquatic ecosystems and their abundance is often used as an indicator of water quality (Kenney et al., 2009). Bed shear stress is what causes macroinvertebrates to drift downstream involuntarily (Lancaster and Hildrew, 1993). During hydropeaking, it is the rate of change of bed shear stress during the ramping stage that forms the biggest risk, as macroinvertebrates may not manage to find refuge in time when the base flow magnitude is low. During high-discharge periods, macroinvertebrates tend to be more active and require less time to find refuge, or have already sought refuge (Schülting et al., 2018; Miller and Judson, 2014). Hence, although absolute bed shear stress is what drifts macroinvertebrates downstream, it is the rate of change of bed shear stress that plays a pivotal role during a hydropeak.

The attention point of the habitat type 'Streams and rivers with water plants, large pondweed' is also addressed in this indicator. Limiting bed shear stress fluctuations during the growing season, which is from May to July (Rijkswaterstaat, 2023), would prevent damage to young plant roots .

Equation 2.2 represents the bed shear stress fluctuation indicator.

$$\Delta\tau_t = \frac{\tau_{\text{max}} - \tau_{\text{base}}}{\Delta t} \quad (\text{Pa/h}) \tag{2.2}$$

In this context, τ_{max} and τ_{base} denote the maximum bed shear stress during a hydropeaking cycle, and the bed shear stress during base flow, respectively. The substrate structures of the gravel bars in the Meuse provide high ecological value, which is why they are usually inhabited by macroinvertebrates (Van Neer, 2016). Therefore, the focus lies on the bed shear stresses at these locations.

The amount of literature on tolerable limits to bed shear stress fluctuations for macroinvertebrates is limited. However, it is known that an absolute shear stress value of 10 N/m² causes all macroinvertebrate species to drift involuntarily (Hauer et al., 2012). Locations with low bed shear stress before a hydropeak arrives could become unsafe to macroinvertebrates if the hydropeak causes the bed shear

[2] This threshold is established to reduce stranding risk in Switzerland (Baumann et al., 2012).

stress to rapidly increase to a value above the threshold of 10 N/m². Therefore, focus lies on such locations.

The three species types and the habitat type that are protected using these indicators are illustrated in Figure 2.2. Note, the species types and the habitat type in the figure may not exactly match the types that are present in the Meuse.

Figure 2.2: Habitats and species of Common Meuse that are affected by hydropeaking. Top left: chabot bullhead (Animalia, n.d.). Top right: river lamprey (Herasimtschuk, n.d.). Bottom left: macroinvertebrates (Carter, n.d.). Bottom right: large pondweed (Jakubec, n.d.).

2.3.4. Remaining preservation goals

The preservation goal of the habitat type 'Megaphorbs and fringes, meadowsweet' has not yet been achieved. Remarkably enough, this habitat type is positively affected by hydropeaking's water level fluctuations (Rijkswaterstaat, 2023). Inundations that are necessary for nutrient delivery would still occur naturally when hydropeaking is reduced. The absolute water level fluctuations that are caused by hydropeaking are of a smaller scale than natural, rain-induced water level fluctuations and are therefore deemed to be of lesser importance for nutrient delivery. That is why no indicator is proposed that specifically targets this habitat type.

The status of the habitat type 'Megaphorbs and fringes, tree lines' is not at a satisfactory level currently either. Yet, it is located at such a high altitude that hydropeaking does not affect it (Rijkswaterstaat, 2023). Consequently, no measures are necessary to directly address this habitat type.

2.4. Hydropeaking mitigation measures

Person (2013) describes three types of hydropeaking mitigation measures: structural measures, operational measures, and morphological measures. Structural measures decrease the magnitude of hydropeaks by using retention basins to flatten a steep discharge peak (Schweizer et al., 2008). Operational measures directly prevent the formation of hydropeaks at the source by changing the way hydropower plants release water. Morphological measures decrease the effect of hydropeaking by changing the river geometry such that the river reacts differently to flow fluctuations or such that aquatic organisms benefit from additional sheltered habitats (Kindle et al., 2012).

Operational measures may be the most logical type of measure. This way, the problem would be tackled at its source. However, the hydropower plants where the problem stems from are located in Belgium,

so this would require transnational cooperation. That is why this type of measure is outside the scope of this research.

Morphological measures are not as straightforward as the other measures when it comes to tackling negative effects. For example, when creating gravel sills to create shelter from shear stress for invertebrates, locations with a high risk of disconnected pools are simultaneously created. This is exactly what has happened in the Common Meuse (Asselman et al., 2019).

Person (2013) explored numerous hydropeaking mitigation measures using a model that focused on both economic viability and ecological effectiveness. Among the investigated options, the application of retention basins consistently showed the best cost/benefit ratio, as it combines habitat improvement with operational feasibility. This study focused on the Vorderrhein and Hasliaare Rivers in Switzerland.

Reindl et al. (2023) examined the use of retention basins to mitigate hydropeaking in the Upper Inn River in Austria. The effect of the basin on the discharge fluctuations, which are caused by the Silz hydropower plant, was considered positive. Retention basins, particularly a 300,000 m^3 basin at the Silz hydropower plant, effectively reduced discharge fluctuations without limiting energy production. The effectiveness of the retention basins was assessed through hydrological modelling. The study highlights retention basins as a flexible solution for alpine rivers, especially where land constraints and operational constraints restrict other mitigation options. One should note that the above examples are from mountainous regions, unlike the southern part of the Netherlands. This difference works in favour of the Meuse, however, as a gentle slope results in greater peak attenuation than a steep slope.

2.5. Exploration of retention possibilities along the Meuse

Ouwerkerk et al. (2021) conducted an exploratory study into retention basins along the Dutch Meuse, on both the Dutch and Belgian sides. The primary objective of this study was to identify potential drought mitigation measures, more specifically locations where water can be stored for several months. These basins may also be suited for hydropeaking mitigation, in which case they would be utilised for a shorter period of time. Therefore, the nine locations that were identified by Ouwerkerk et al. (2021) are now further explored as potential retention locations.

Ouwerkerk et al. (2021) selected potential locations such that it would result in a diverse collection of storage options with consideration given to storage type, geographical location along the river, and the size of each location. For these nine locations, a geomorphic analysis has been conducted to assess the suitability of the subsurface for water storage, i.e. to determine the presence of impermeable layers, and to estimate the cost of any additional layers, along with an exploration of the possible storage volumes.

Figure 2.3 shows the nine locations that were identified by Ouwerkerk et al. (2021). Possible locations include ponds and lowlands that can be enclosed using dikes. Within the hydropeaking mitigation context, locations 7, 8, and 9 may be dismissed because of their location. They are located downstream of the Common Meuse, the reach with the highest ecological value, and the reach where most problems are expected to occur as a result of hydropeaking.

Figure 2.3: Possible retention locations (Ouwerkerk et al., 2021). Adjusted from Esri (2025a).

The pond near Stevensweert, location 6, is also dismissed as it is far more expensive than the other locations. Ouwerkerk et al. (2021) estimated that 143 million euros are required to apply an impermeable layer at the pond. Moreover, it is located at the end of the Common Meuse, which considerably reduces its functionality. The remaining five locations are used in the rest of this study. An overview of these five locations, together with their storage volumes, is provided in Table 2.3.

Table 2.3: Retention locations and their potential storage volume (Ouwerkerk et al., 2021)

Location	1 ENCI-groeve	2 Borgharen	3 Borgharen–Itteren (op-, in de Weerd)	4 Grevenbicht (Bichterweerd)	5 Grevenbicht (Koeweide + Visserweert)
Volume (m^3)	7,577,371	208,109	795,409	2,557,604	1,829,529

Location 1 stands out among the five remaining locations. The ENCI-quarry (Figure 2.4) has by far the largest storage space. This former quarry, located just upstream of Maastricht at rkm[3] 9, is very deep due to marl extraction. The deepest point in the quarry is elevated at NAP[4]+7 m (Ouwerkerk et al., 2021), while the river bed at rkm 9 is elevated at approximately NAP+39 m (Rijkswaterstaat, 2025a). The storage space, together with the location being the one that is the most upstream of all potential retention locations identified by Ouwerkerk et al. (2021), makes it a suitable place to store water during a hydropeak. Therefore, the ENCI-quarry is selected to be used as retention location in Chapter 4.

[3]rkm = rivierkilometer/river kilometre/river chainage

[4]NAP = Normaal Amsterdams Peil, the reference level used in the Netherlands. NAP+0 m is approximately equal to the average sea level in the North Sea (Rijkswaterstaat, 2025d).

Figure 2.4: ENCI-quarry (by author, 2025)

3
Hydropeaking identification

In order to reduce the negative impact of hydropeaking, hydropeaks have to be isolated first. When their magnitude and characteristics are known, the impact assessment can commence, followed by the design of mitigation strategies. This chapter covers the separation of the hydropeaking signal from the natural hydrograph that would occur if there were no barriers in the river. Section 3.1 explores various signal processing techniques to assess what the most suitable way of hydropeaking isolation is. Section 3.2 examines the key characteristics of the isolated hydropeaks and discusses their implications.

3.1. Hydropeaking isolation from natural hydrograph

Three methods are compared to determine what the best way is to separate natural and artificial fluctuations. These methods are compared based on the following criteria:

- *Effectiveness of signal classification*: How well is the natural signal visually separated from the hydropeaking signal? In general, the period of a hydropeak can be up to a week (Déry et al., 2021), though it is usually smaller than a day (Carolli et al., 2015).
- *Sensitivity to parameter selection*: How sensitive is the method to changing parameters that may be uncertain (e.g. frequency limits)?
- *Computational efficiency*: How much computational power is required to carry out the analysis?

Besides, the characteristics of the hydropeaks that emerge from each method are examined to assess which method produces the most realistic results.

Data used for this part is 15-year discharge data (2009-2023) from measurement station Eijsden Grens (Rijkswaterstaat, 2025e) with a continuous sampling interval of 10 minutes. Eijsden is just downstream of the Lixhe hydropower plant, so any hydropeak that is produced by the plant should be present in the hydrograph.

All three signal processing methods are frequency-based separation methods, which is because hydropeaks are known to have high frequencies (Meile et al., 2011).

3.1.1. Moving average

A simple way to detach long, natural discharge peaks from short, unnatural hydropeaks would be to use a moving average. If the period of a hydropeak is known, the window size of the moving average can be set equal to the hydropeak period. Then, the moving average can be seen as the natural signal, and the remaining signal can be considered to be the hydropeaking signal[1].

Figure 3.1 shows the separation of the natural signal and the hydropeaking signal using a window size of exactly 1 day at the measurement station Eijsden Grens for a 7-day period in November 2022. The reconstructed hydrograph is, by definition, equal to the original hydrograph when using this method.

The method successfully detaches the high-frequency signals from the low-frequency signals. However, the natural signal is still influenced by hydropeaks, which can be seen in Figure 3.1 around the 25th of November. The natural signal displays a small peak, as it is surrounded by two short peaks,

[1] When this study refers to a 'natural signal' or 'hydropeaking signal', it should be noted that these are approximations, and not exact representations of reality.

which are likely hydropeaks. This influence can be attributed to the fact that the hydropeaking period is not constant. So when using a moving average, the window size cannot be set equal to the exact hydropeak period at each point. This means that the natural signal will always be influenced slightly by the hydropeaking signal, and they cannot be fully detached. Without any frequency domain analysis techniques such as a Fourier transform or wavelet transform applied to the data to determine the dominant hydropeaking frequency of hydropeaking, the choice for a window size is arbitrary and affects the results.

The moving average method is computationally efficient. The signal separation of the Eijsden Grens hydrograph is completed within a few seconds.

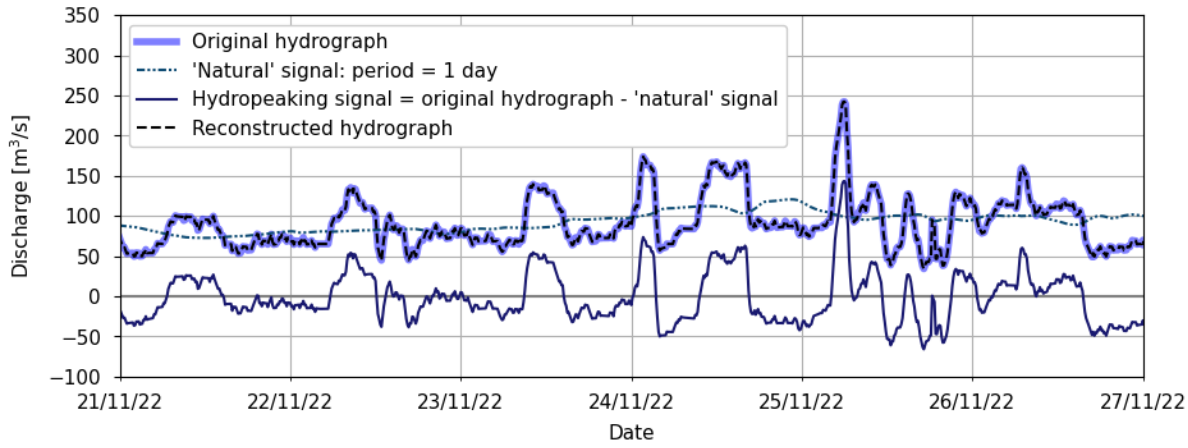

Figure 3.1: Signal separation using a moving average at Eijsden Grens

3.1.2. Fourier transform

Another method frequently used in signal processing is the Fourier transform. The Fourier transform method uses sinusoidal waves with an infinite duration to fit a signal, making it suitable for periodic signals (Sifuzzaman et al., 2009). The continuous Fourier Transform of the 15-year hydrograph at Eijsden Grens (Rijkswaterstaat, 2025e) is visible in Figure 3.2. Low frequencies contribute large-amplitude sinusoids to the reconstructed signal, which can be explained by the yearly discharge cycle, with high discharges in winter and low discharges in summer. Additionally, around a frequency of approximately 0.25 cycles per day, a small peak is visible. This is probably caused by rain depressions that have a period of a few days to a week. At a frequency of 1 cycle per day, another peak is visible. This peak is likely caused by hydropeaking. Apart from this small peak, no clear boundaries are visible that could indicate what the frequency window of hydropeaks is. Instead, many frequencies contribute equally to the Fourier transform. An explanation for this could be that many artificial sinusoids are required to fit sharp transitions in the hydrograph. A Fourier transform assumes stationarity (Sifuzzaman et al., 2009), which is not actually the case in a river hydrograph, requiring many artificial frequencies to fit sharp transitions.

Using the inverse Fourier transform with only a lower bound cut-off frequency equal to $\frac{1}{\text{day}}$ and no upper bound cut-off frequency for the hydropeaking signal, this method also delivers a perfectly reconstructed hydrograph in Figure 3.3.

The lower bound cut-off frequency is set equal to $\frac{1}{\text{day}}$, as hydropeaks usually have a sub-daily period (Carolli et al., 2015). However, having no upper bound cut-off is unrealistic, as this would suggest that there are hydropeaks having an infinite frequency. This would mean that some hydropower plants are only opened for an infinitesimally short period of time; the hydropeaking signal in Figure 3.3 tracks even the smallest and fastest fluctuations in the original hydrograph. Nevertheless, any choice for an upper bound cut-off frequency would be arbitrary, as the Fourier transform in Figure 3.2 gives no clear indication of frequencies that are more present than others. The fact that all frequencies contribute to the hydrograph also means that choosing an upper bound cut-off frequency would significantly influence the separation of the signals when using this method.

The Fourier transform method requires little computational capacity. The signal seperation of the Eijsden Grens hydrograph is completed in less than a minute.

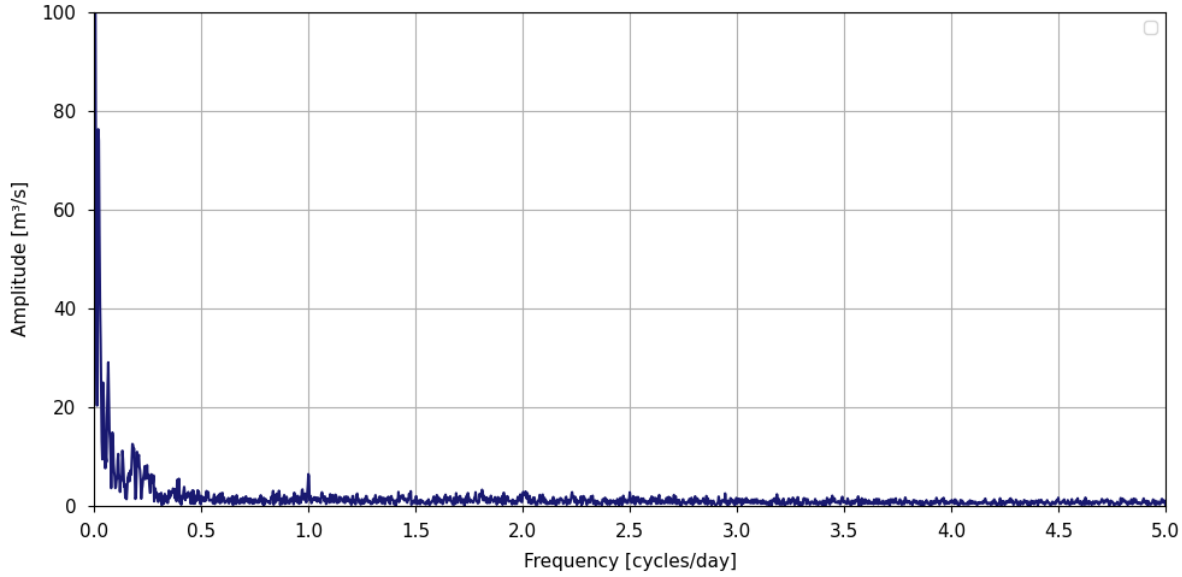

Figure 3.2: Normalised Fourier transform of 15-year hydrograph at Eijsden Grens

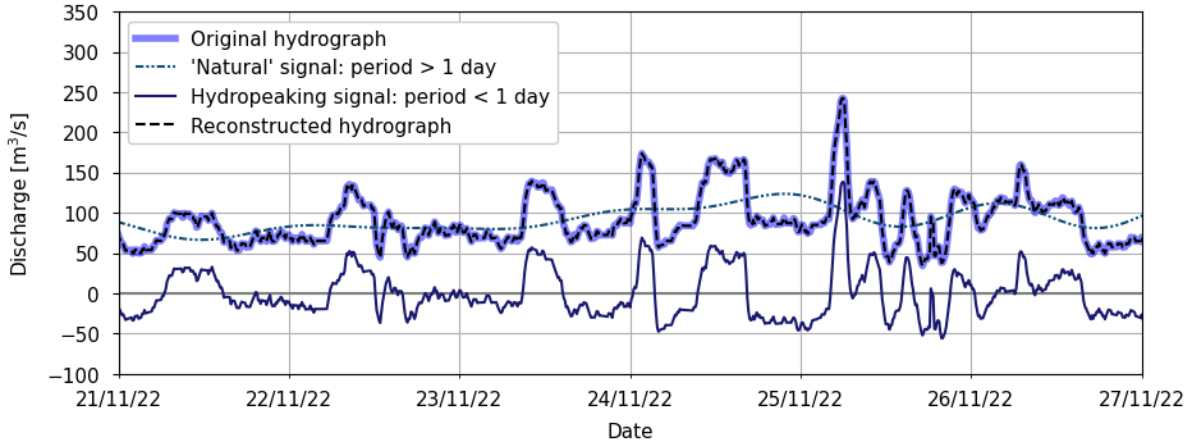

Figure 3.3: Signal separation using an inverse continuous Fourier transform at Eijsden Grens

3.1.3. Wavelet transform

Another frequency analysis technique is the wavelet transform. The wavelet transform is similar to the Fourier transform, but it is localised in time, making it more suitable for non-stationary signals (Sifuzzaman et al., 2009). Less artificial frequencies are needed to smoothen the hydrograph compared to the Fourier transform, yielding a frequency spectrum that should have distinct peaks and a clear frequency range where hydropeaks are recognisable.

The wavelet transform method was successfully applied to identify hydropeaking in the Meuse by Van Denderen (2024). Their approach is adopted here as well. By integrating it into this chapter, a validation of the approach is performed, and it can be directly compared to the other two signal processing techniques. Various types of wavelet bases are available, all differing in shape and frequency. Van Denderen (2024) used the Morlet wavelet, as this wavelet provides a balance between time resolution and frequency resolution (Torrence and Compo, 1998). Figure 3.4 shows the Morlet base wavelet, which is

scaled, shifted, and summed throughout the time domain for many different frequencies to reconstruct the original signal.

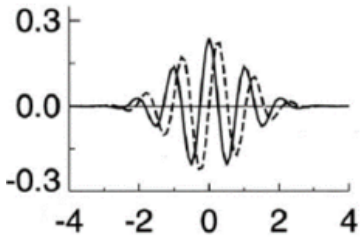

Figure 3.4: Morlet base wavelet (Torrence and Compo, 1998)

The Morlet wavelet is applied to the discharge data at Eijsden Grens (Rijkswaterstaat, 2025e); a continuous wavelet transform with the 'power' that is present across different frequencies over time is visible in Figure 3.5. Wavelet power is a signal processing concept that represents the variance magnitude of a specific frequency at a particular moment in time (Torrence and Compo, 1998). Three distinct areas can be detected in the spectrum. Seasonal variations are well visible by the clear presence of signals with a period between 10^2 days and 10^3 days. Daily weather depressions are visible at periods between 1 day and 10 days. Lastly, the presence of signals with a period between approximately 0.1 day and 1.5 days can be observed everywhere in Figure 3.5, except during dry periods in summer. Hydropeaks are usually associated with sub-daily periods (Carolli et al., 2015), or in some cases with weekly periods (Déry et al., 2021). This indicates that this band could very well correspond with the hydropeaking signal. The absence of hydropeaking during summers can be explained by the fact that during periods of low discharge, there is simply less water available for impoundment and subsequent release. The clear presence and absence of frequencies in the wavelet transform of Figure 3.5 reduces the sensitivity of the results to the choice of cutoff frequencies.

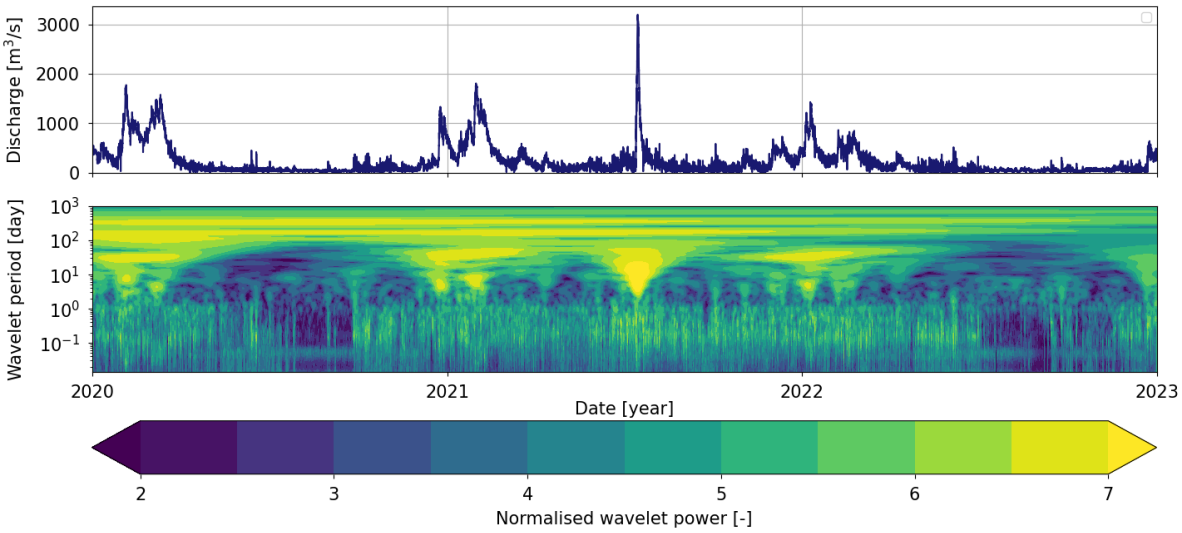

Figure 3.5: Hydrograph and continuous wavelet transform at Eijsden Grens. Adjusted from Van Denderen (2024)

Figure 3.6 shows the separation of the natural signal and the hydropeaking signal at Eijsden Grens using the Morlet wavelet, using a lower bound cut-off frequency of $\frac{1}{1.5\text{day}}$ and an upper bound cut-off frequency of $\frac{1}{0.1\text{ day}}$ for the hydropeaking signal. The hydropeaking signal does not follow all small high-frequency fluctuations anymore because of the upper bound cut-off frequency.

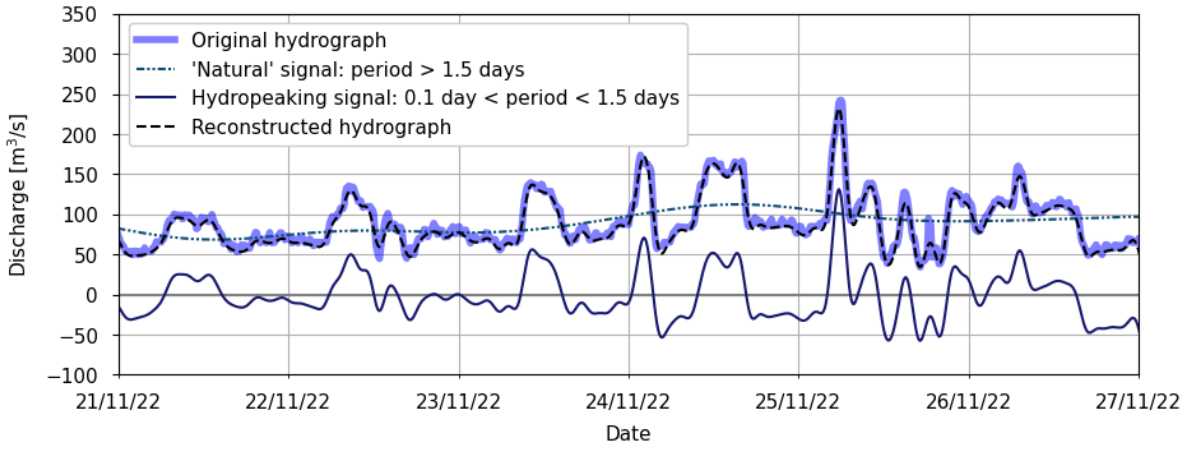

Figure 3.6: Signal separation using an inverse continuous wavelet transform at Eijsden Grens

The wavelet transform method requires more computational capacity than the previous techniques. The signal separation of the Eijsden Grens hydrograph is completed in five minutes.

3.1.4. Hydropeaking signals

The hydropeaking signals of all three methods and the original hydrograph are visualised for a day in September 2012 in Figure 3.7. One can clearly see that the wavelet transform signal is much smoother than the other two signals, which contain a lot of high frequencies.

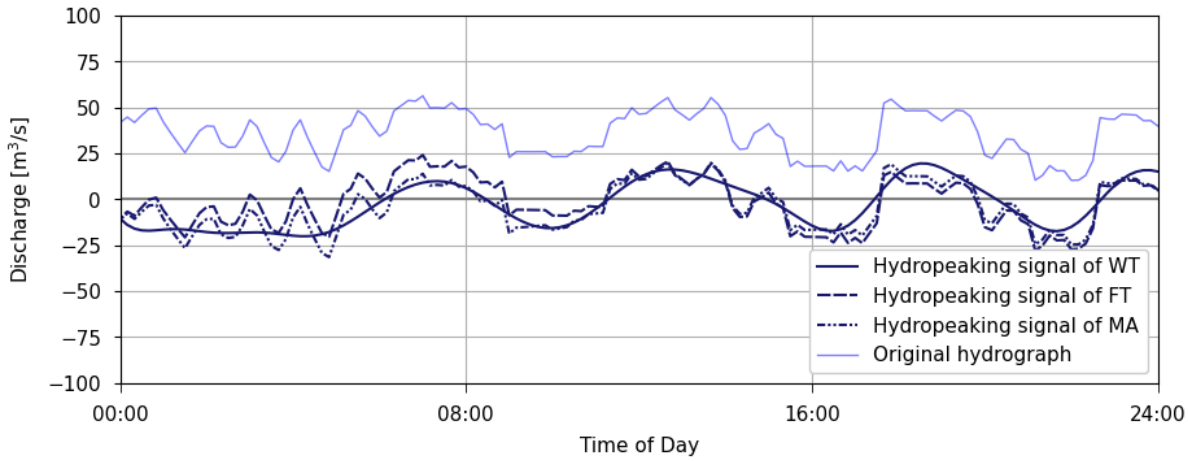

Figure 3.7: Hydropeaking signal of all three methods

In this study, a single hydropeak is defined to start at the point where the hydropeaking signal crosses $Q = 0$ m^3/s with a positive time derivative, and it ends the subsequent time this happens. Using this approach on the 15-year-long discharge data at Eijsden Grens, 34891 hydropeaks have been identified using the moving average approach, 37408 hydropeaks using the Fourier approach, and 13002 hydropeaks using the wavelet approach. These differences can be explained by the differences in cut-off frequencies that are used in the methods. The wavelet method has an upper-bound cut-off frequency of $\frac{1}{0.1 \text{ day}}$, while the other methods have no upper-bound cut-off frequency. Those methods therefore cross $Q = 0$ m^3/s more frequently, resulting in a greater number of peaks.

The volume of a hydropeak can be calculated by integrating either the positive part or the negative part of a single hydropeak. Here, a trapezoidal integration is used on the positive part of the hydropeaks (see Figure 3.8).

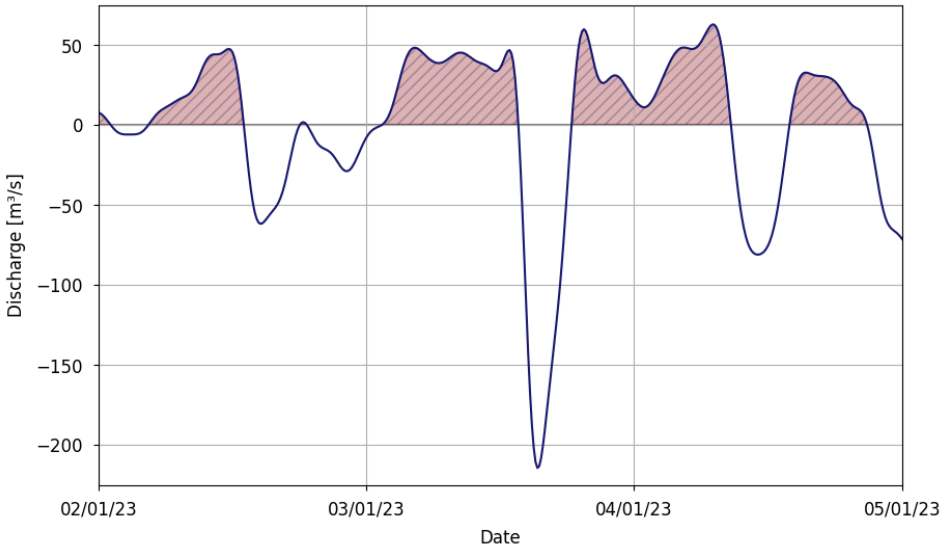

Figure 3.8: Trapezoidal integration on the positive part of hydropeaks

Statistics of the peak values and peak volumes of the 15-year-long discharge data at Eijsden Grens (Rijkswaterstaat, 2025e) can be found in Table 3.1 and Table 3.2, respectively. It is clear that the values of the moving average method and the Fourier transform method are very much affected by the number of small, high-frequency peaks they contain. The 5th percentiles, the 50th percentiles, the 95th percentiles and the average values of the wavelet transform are significantly larger than those of the other two methods.

Table 3.1: Hydropeak peak values (m^3/s)

Signal processing method	5th percentile	50th percentile	Average	95th percentile	Maximum
Moving average	0.7	12	25	98	727
Fourier transform	0.7	12	24	92	725
Wavelet transform	1.3	28	41	129	648

Table 3.2: Hydropeak volumes (m^3)

Signal processing method	5th percentile	50th percentile	Average	95th percentile	Maximum
Moving average	111	15,557	164,533	925,253	9,295,692
Fourier transform	109	15,430	139,510	759,219	5,331,339
Wavelet transform	2,934	216,034	405,502	1,421,859	5,524,753

3.1.5. Conclusion

All three methods that have been tested to detach the hydropeaking signal from the natural signal have their pros and cons regarding the criteria of Section 3.1. They are now be evaluated one by one.

The moving average method is a very simple and computationally efficient method to separate high-frequency signals from low-frequency signals. It uses data points close to the point of interest to smoothen the signal. The larger the window size, the less sensitive the moving average becomes to individual data points. The method could have been used in this context if hydropeaks had a fixed frequency. However, this is not the case, causing the natural signal to still be influenced by hydropeaks if this method is applied. Moreover, the choice for a window size is too arbitrary without any frequency domain analysis carried out. Therefore, the moving average method is not suitable to detach the hydropeaking signal from the natural signal.

The continuous Fourier transform method assumes the signal is made up of many sinusoidal waves that last forever (Sifuzzaman et al., 2009). The method reconstructs the original hydrograph very well, as it sums many frequencies. It also creates artificial frequencies to fit the signal, yielding a Fourier transform that does not show a clear hydropeaking frequency window (see Figure 3.2). Therefore, the cut-off frequencies of hydropeaking cannot be chosen with certainty. Moreover, choosing a cut-off frequency influences the separation of the signal too much. Therefore, the Fourier transform method is also less suitable to detach the hydropeaking signal from the natural signal.

The continuous Morlet wavelet transform method uses time-localised frequency decomposition of the hydrograph, i.e. it decomposes the original signal into signals with varying frequencies that last for a finite duration (Van Denderen, 2024). This application is useful for non-stationary signals (Sifuzzaman et al., 2009), such as a hydrograph. The wavelet transform in Figure 3.5 gives a clear range of periods where hydropeaking is present, which can be used to separate the signals. The risk of leakage remains, but the clear band reduces the sensitivity to slightly changing the cut-off bounds. All in all, the wavelet transform is the most reliable way of separating the hydropeaking signal from the natural signal. Therefore, it is used as hydropeaking isolation method in this study.

Table 3.3 summarises how well each method performs on the criteria that were established in Section 3.1.

Table 3.3: Signal processing performances. ++ = very good; + = good; 0 = neutral; - = poor; - - = very poor

Signal processing method	Effectiveness of signal classification	Sensitivity to parameter selection	Computational efficiency
Moving average	-	- -	++
Fourier transform	+	-	++
Wavelet	++	+	++

3.2. Hydropeaking characteristics

Using the wavelet transform, various hydropeak characteristics can be deduced from the river discharge data. The histogram in Figure 3.9 shows the total amount of identified hydropeaks throughout the day between 2009 and 2023. Hydropeaking clearly occurs more frequently during daytime than during nighttime, with maxima occurring in the morning and evening. This pattern corresponds with observed fluctuations in energy demand, which also typically peak during the morning and evening (ENTSO-E, 2025).

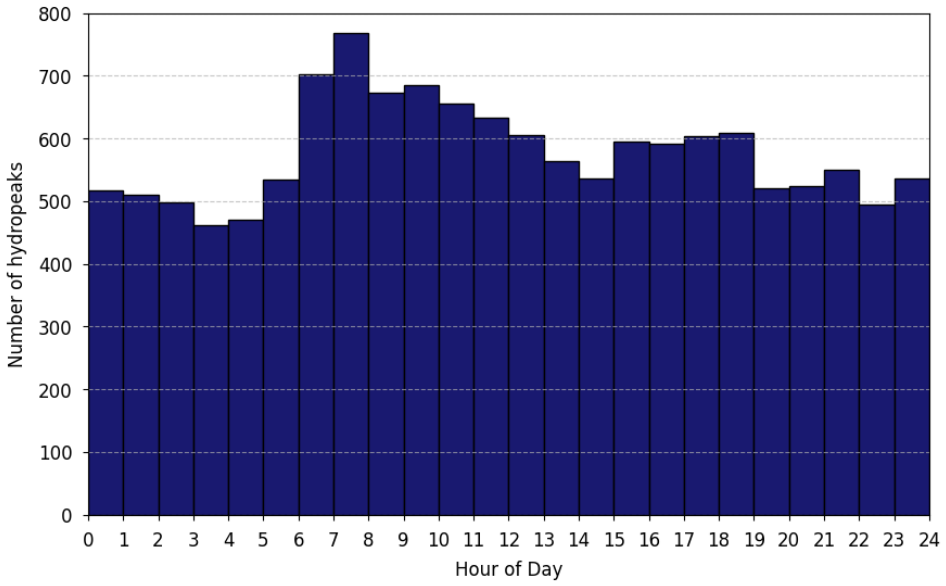

Figure 3.9: Histogram of hydropeak peak times throughout the day at Eijsden Grens (2009-2023)

The bar diagram in Figure 3.10 shows how many hydropeaks are detected during each month of the year, together with the average hydropeak volume of every month. The number of peaks per month is fairly constant, but their average volume is smaller during the summer months.

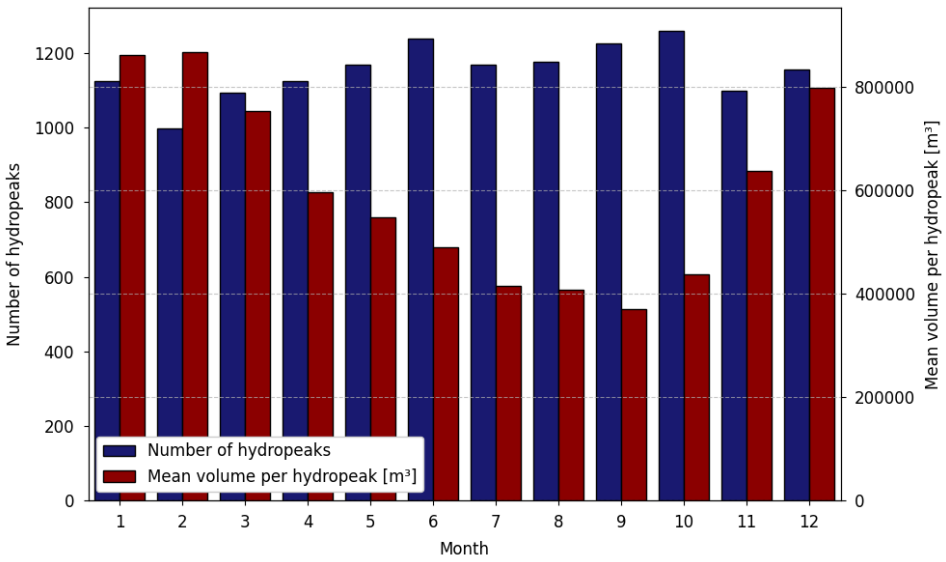

Figure 3.10: Bar diagram of hydropeak occurrences throughout the year and the average volume per hydropeak in each month at Eijsden Grens (2009-2023)

Figure 3.11 shows the number of identified hydropeaks per year and the combined volume of all of these hydropeaks per year at Eijsden Grens from 2009 up to and including 2023. The number of identified hydropeaks per year and the total hydropeak volume per year have a Pearson correlation coefficient of 0.06, suggesting no linear relation between the two quantities. Hence, a high number of hydropeaks in a year does not necessarily imply a high total hydropeak volume. A larger number of hydropeaks in a year is thus likely to be caused by many small peaks. Neither of the variables in Figure 3.11 displays a clear trend.

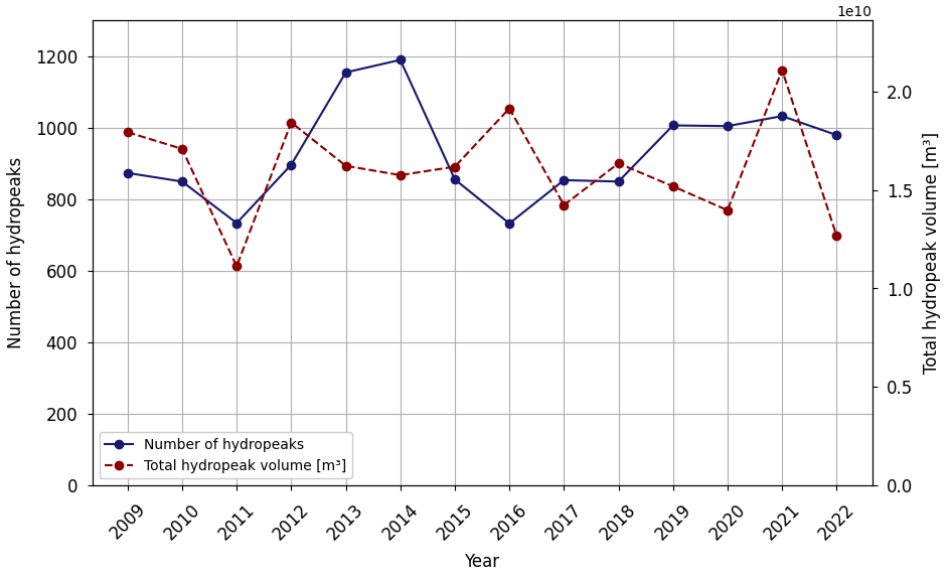

Figure 3.11: Number of hydropeaks over the years and total hydropeak volume per year at Eijsden Grens (2009-2023)

The histogram in Figure 3.12 shows the period distribution of identified hydropeaks at Eijsden Grens. The mode of the periods, i.e. the most common period, is 3 to 4 hours, and the average hydropeak period is 9.43 hours. There are few hydropeaks detected that last longer than a day. One should note that this period analysis is biased due to the frequency-based signal decoupling method. All wavelets with periods between 0.1 day and 1.5 days were identified as hydropeaks, so it may not be a surprise that most hydropeak periods fall into that range.

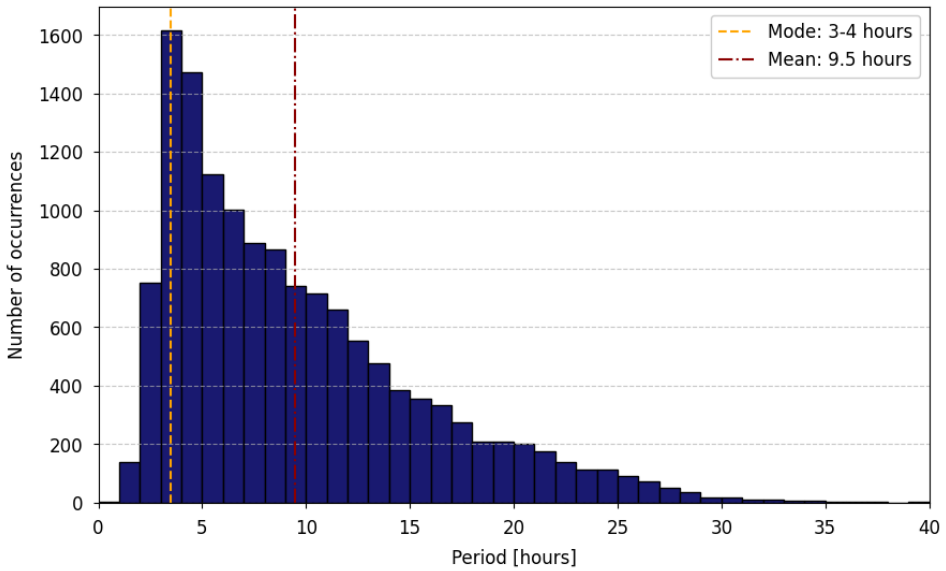

Figure 3.12: Histogram of hydropeak periods at Eijsden Grens (2009-2023)

The density scatter plot in Figure 3.13 demonstrates the relationship between natural discharge and hydropeak peak values. Every point in the figure represents a single hydropeaking event. An examination of the median hydropeak line reveals that the hydropeak peak value quickly increases with increasing natural discharge, but it stabilises around 45 m^3/s beyond a natural discharge of 100 m^3/s. Apparently, the hydropower plant of Lixhe does not produce larger hydropeaks when the base discharge increases. This can likely be attributed to the fact that at a natural discharge of 100 m^3/s, sufficient flow can be

diverted through the hydropower outlet to induce the most efficient electricity generation. So when base flow increases, there is no need to impound more water.

The number of hydropeaking events decreases as natural discharge increases, which is simply because high discharges are rarer. There are very few days with a discharge above 1000 m^3/s (Rijkswaterstaat, 2025e).

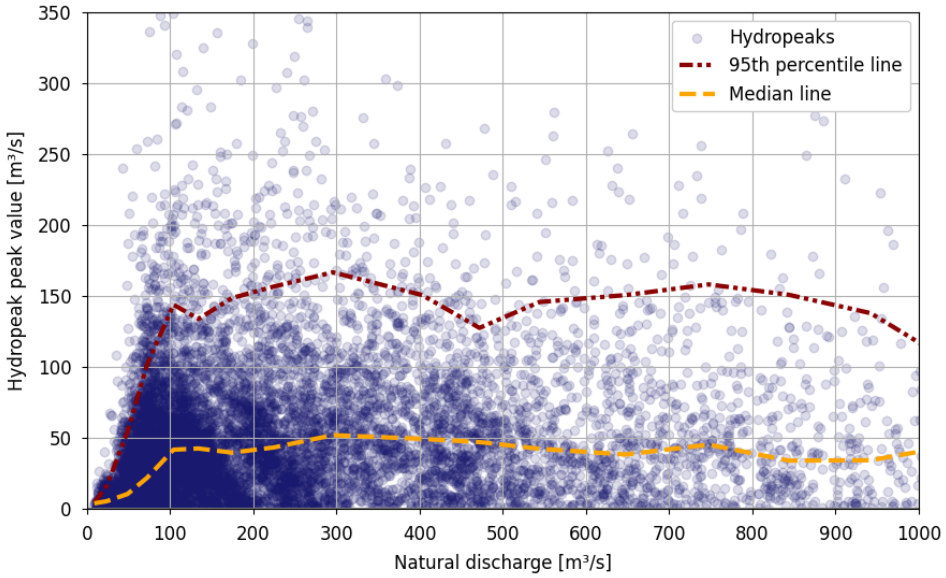

Figure 3.13: Density scatter plot of natural discharge and hydropeak peak value at Eijsden Grens (2009-2023)

In Chapter 4, various combinations of natural base flow and hydropeaking magnitude are combined and assessed on their impact. The relative contribution of hydropeaking to the total discharge is largest when the base flow magnitude is small. Figure 3.14 displays the 5% largest hydropeaks corresponding to a natural discharge between 50 m^3/s and 150 m^3/s. Figure 3.15 shows the average number of occurrences of such hydropeaks per month. These hydropeaks, which are expected to be most harmful to ecology because of their relatively large contribution to the total discharge, mainly occur between May and October. Their average return period during these months is equal to 9 days.

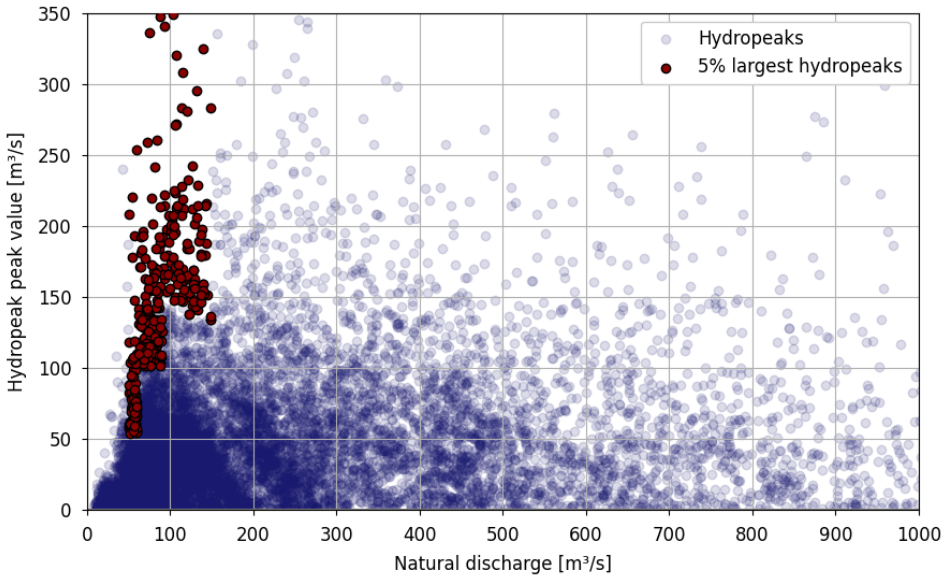

Figure 3.14: 5% largest identified hydropeaks when base flow magnitude is between 50 m^3/s and 150 m^3/s

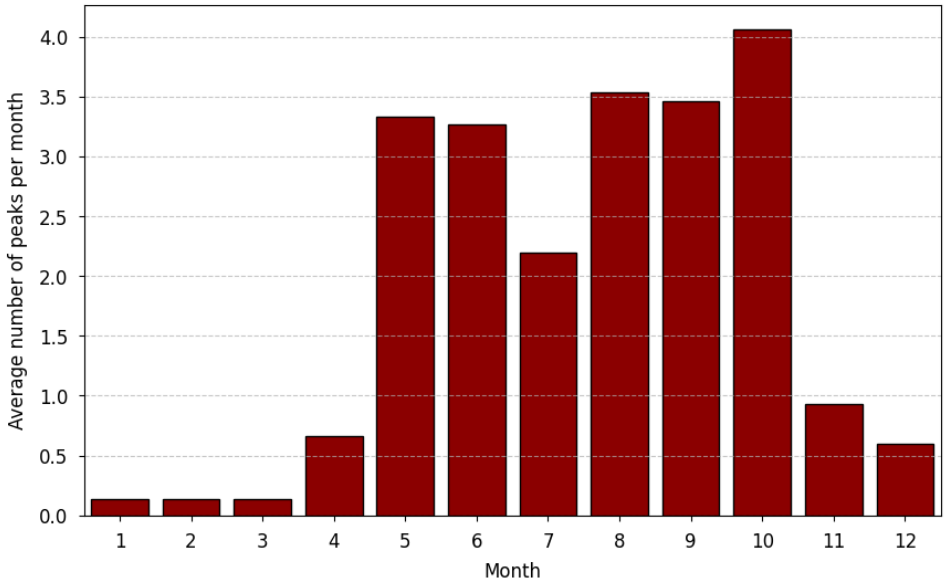

Figure 3.15: Histogram of occurrence of 5% largest identified hydropeaks when base flow magnitude is between 50 m^3/s and 150 m^3/s

4

Hydrodynamic simulations of various hydropeaks

This chapter examines the impact of hydropeaking using hydrodynamic modelling. In Section 4.1, a model choice is made. Section 4.2 outlines the different model runs. Section 4.3 describes the initial and boundary conditions of these runs. Section 4.4 focuses on model calibration and validation. Section 4.5 gives a detailed description of how the model results are evaluated. Finally, Section 4.6 presents the simulation results.

4.1. Selection of model

To quantify the negative impact of hydropeaking and to assess the performance of mitigation measures quantitatively, hydrodynamic modelling is required. This section covers the model choice.

4.1.1. Selection of hydrodynamic model

Selecting a suitable hydrodynamic model is essential in order to accurately represent hydropeaking effects. First, the preferred dimensionality (1D/2D/3D) has to be determined; then a suitable software program can be selected.

A 1D hydrodynamic model would be too simplistic, as the relevant phenomena of hydropeaking cannot be properly studied in a 1D model. Studying bed shear stress requires a 2D domain and both longitudinal and lateral flow. The variation in wetted river area and the occurrence of disconnected pools are also 2D processes. 2D models usually follow a depth-averaged approach, assuming that the time-averaged horizontal flow velocities are of a much larger scale than the time-averaged vertical flow velocities (Glock et al., 2019). This is an acceptable assumption in this application, as the wavelength of a hydropeak is much larger than the water depth in the Meuse. Therefore, a 2D model may be adopted.

Various software programs could be used. One option is the water modeling software program MIKE. The MIKE tool that is the most suitable to model hydropeaks and to test the effectiveness of hydropeaking mitigation measures is the MIKE+ Rivers tool. This tool is useful for river engineering applications and ecological purposes (DHI Group, 2025).

Another possibility is the TELEMAC-2D tool of the Open TELEMAC-MASCARET software program. This numerical modelling tool simulates free-surface flows in the horizontal plane. It may be used to focus on e.g. river flow, bed friction and dry areas (TELEMAC, 2025). Hence, it could be useful in this study .

Thirdly, D-HYDRO Suite 2D3D is considered. This open-source tool, developed by Deltares, is suitable for simulating river flow and the interaction between hydrodynamic and ecological processes (Deltares, 2025b). Additionally, Deltares and Rijkswaterstaat (2025b) have published a schematisation of the watershed of the Meuse, including a grid, a topography, weirs, sluices, inlets, and outlets. This adds value to this particular software program, which is why it is chosen to be used during the modelling phase.

4.1.2. Selection of submodel

Several 2D D-HYDRO models of the Dutch Meuse are available, each covering different reaches of the river (Deltares and Rijkswaterstaat, 2025b). Submodel A covers rkm 2 to rkm 85 (see Figure 4.1),

submodel B spans rkm 67 to rkm 165, and submodel C extends from rkm 144 to rkm 247. There is also a model that covers the entire Dutch Meuse. The submodels have a resolution that is 4 times larger than the resolution of the total model, as their mesh size is 2 times smaller (20 m versus 40 m). This is supposed to improve the river roughness representation in the model (Deltares and Rijkswaterstaat, 2025b).

The wavelet transform is applied to discharge data (consistent with the approach described in Section 3.1.3) at four measurement stations along the Dutch Meuse to assess how far downstream hydropeaks reach. The four measurement stations are denoted in Figure 4.1.

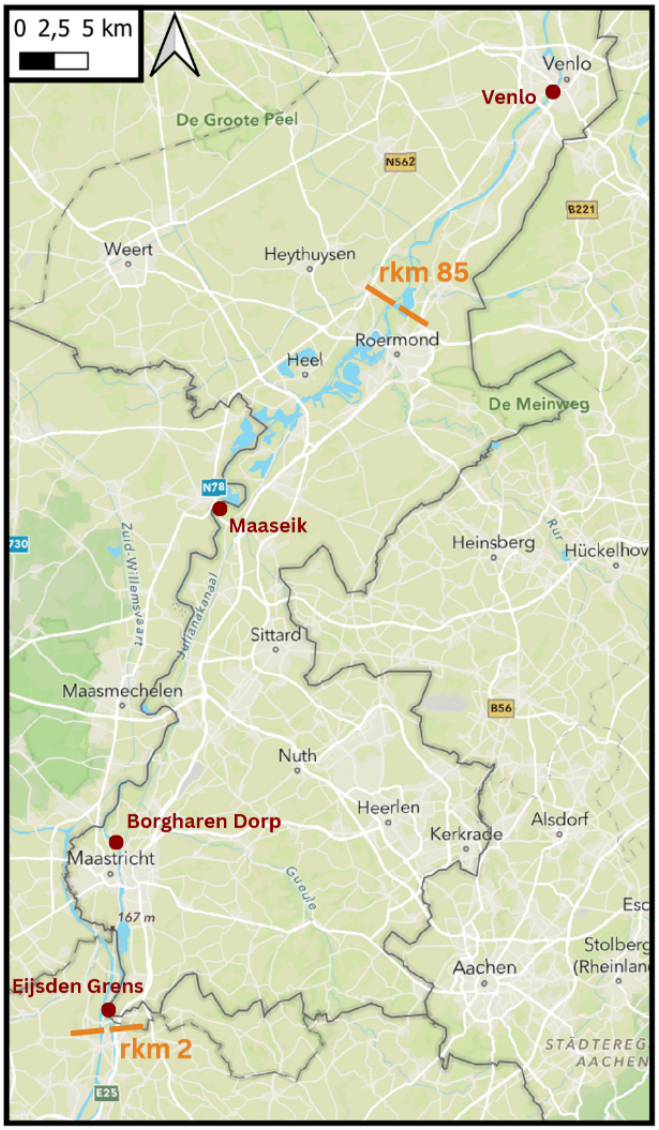

Figure 4.1: Boundaries of submodel A (indicated in orange) and locations of measurement stations along the Dutch Meuse (indicated in dark red). Adjusted from Esri (2025a).

Figure 4.2 shows the hydrograph at Eijsden Grens, along with its wavelet transform and those of the three downstream measurement stations. At Eijsden Grens and Borgharen Dorp, a clear band is visible between a period of 0.1 day and 1.5 days. This signal is already substantially reduced at Maaseik, and is further diminished at Venlo. The latter dissipation can be explained by the big lakes around Roermond that were formed due to gravel extraction (Asselman et al., 2019). The reappearance of a signal at wavelet periods shorter than 0.1 day may be attributed to the weirs of Linne, Roermond, and Belfeld, which are located between Maaseik and Venlo (Rijkswaterstaat, 2025c).

Hydropeaking appears to be most prominently present in the Upper Meuse and Common Meuse, i.e. from the Belgian border until approximately rkm 65 (GeoWeb Rijkswaterstaat, 2025). Submodel A covers this entire reach and is therefore selected for use in this study.

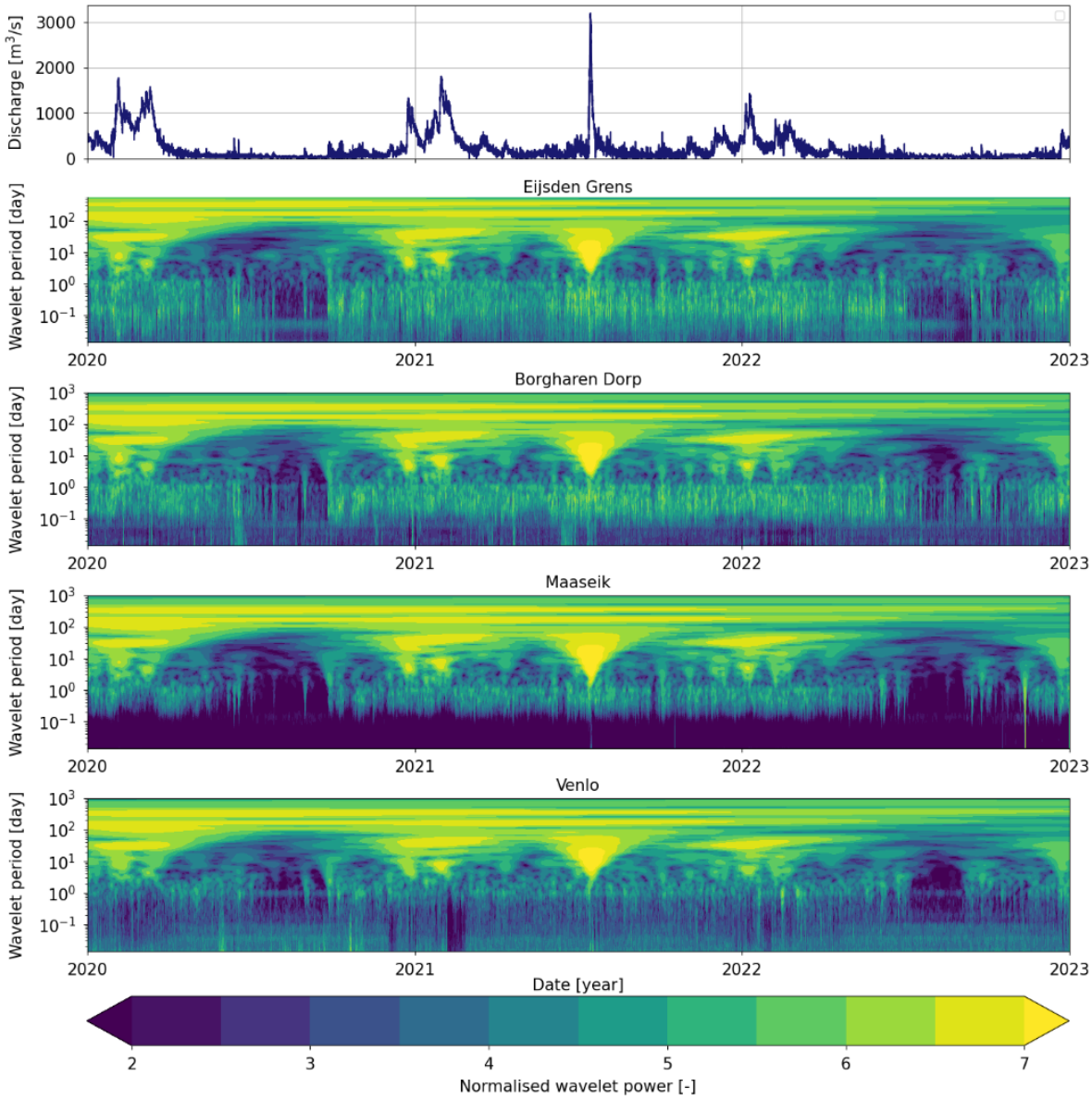

Figure 4.2: From top to bottom: hydrograph at Eijsden Grens, wavelet transform at Eijsden Grens, wavelet transform at Borgharen Dorp, wavelet transform at Maaseik and wavelet transform at Venlo. Adjusted from Van Denderen (2024)

4.2. Simulation run plan

The relative magnitude of hydropeaks is the largest during low base flows, and their effect is expected to be most notable then as well. Involuntary drift of invertebrates due to rapid changes in bed shear stress, egg desiccation due to high wetted river area variation, and formation of disconnected pools with poor water quality: all of these phenomena are more likely to occur during low-discharge periods than during high-discharge periods. Therefore, model runs are performed with low base flow (100 m^3/s) and two different hydropeaks added on, namely a median hydropeak and a 95th percentile hydropeak (see Figure 4.3). They are used in order to capture both a common and an extreme case. Additionally, a third run is executed with retention applied to the 95th percentile hydropeak. This is done because measures are expected to be most urgently needed for extreme events.

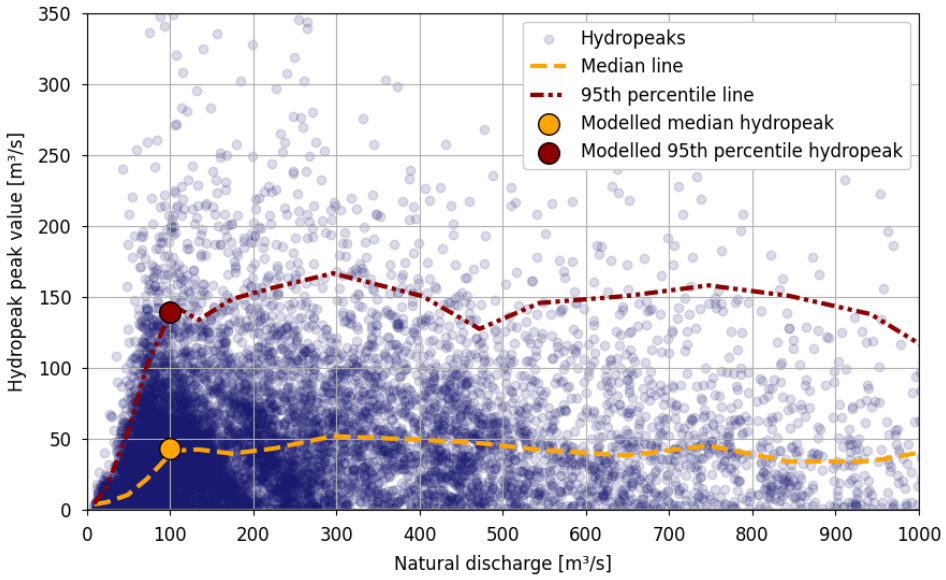

Figure 4.3: Density scatter plot of natural discharge and hydropeak peak value at Eijsden Grens (2009-2023). Modelled median and 95th percentile hydropeaks at a base flow of 100 m^3/s are indicated in orange and red.

4.2.1. Run 1: median hydropeak

The first run that is executed in D-HYDRO is a median hydropeak that happens around a natural discharge of 100 m^3/s. The median hydropeak peak value at a natural discharge of 100 m^3/s is equal to 42.35 m^3/s.

The wavelet transform method (Van Denderen, 2024) is used to isolate hydropeaks, as described in Section 3.1.3. After separating the hydropeaking events, they are filtered on peak values and natural discharge values within the range of a median hydropeak. All identified hydropeaks between 2009 and 2023 with a peak value between 41 m^3/s and 44 m^3/s, and a natural discharge between 97 m^3/s and 103 m^3/s, are listed in Table 4.1. From these hydropeaks, the hydropeak of the 9th of April 2021 is modelled in D-HYDRO. It is detached from the natural signal and summed up to a constant discharge of 100 m^3/s. The upstream boundary condition of the median hydropeak is visible in Figure 4.4. First, nearly three days with constant discharge are applied, allowing the model to stabilise before the hydropeak starts.

Table 4.1: Median hydropeaks at 100 m^3/s at Eijsden Grens (2009–2023)

Peak Time	Peak Value (m^3/s)	Volume (m^3)	Natural Discharge (m^3/s)	Period (hours)
2014-08-08 10:10:00	41.87	1.5×10^5	97.02	3.89
2014-12-06 10:10:00	42.66	3.7×10^5	97.07	7.04
2019-05-06 05:30:00	41.32	2.6×10^5	97.35	4.64
2021-04-09 22:30:00	43.07	2.7×10^5	102.97	4.50
2021-11-20 07:40:00	43.58	6.8×10^5	98.83	12.05

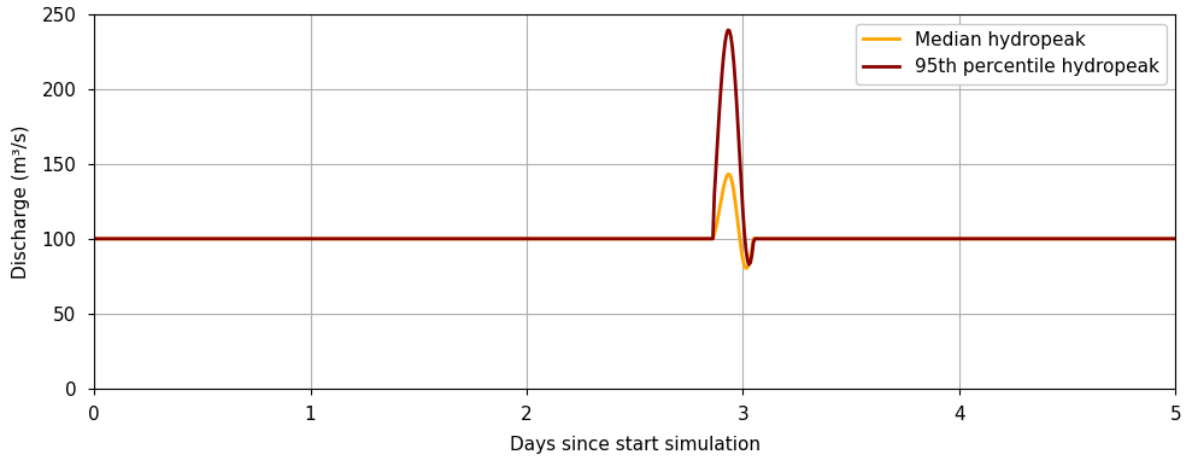

Figure 4.4: Upstream boundary conditions

4.2.2. Run 2: 95th percentile hydropeak

Additionally, a 95th percentile hydropeak around a natural discharge of 100 m^3/s is modelled. The 95th percentile hydropeak peak value at a natural discharge of 100 m^3/s is equal to 137.8 m^3/s. Using a similar approach as during the median hydropeak, all identified hydropeaks with a peak value between 135 m^3/s and 140 m^3/s and a natural discharge between 97 m^3/s and 103 m^3/s are listed in Table 4.2. From these two hydropeaks, the hydropeak of the 27th of November 2022 is modelled in D-HYDRO. It is again detached from the natural signal and summed up to a constant discharge of 100 m^3/s. The upstream boundary condition of the 95th percentile hydropeak is also visible in Figure 4.4.

Table 4.2: 95th percentile hydropeaks at 100 m^3/s at Eijsden Grens (2009–2023)

Peak Time	Peak Value (m^3/s)	Volume (m^3)	Natural Discharge (m^3/s)	Period (hours)
2015-08-28 17:00:00	136.17	1.2×10^6	97.10	8.58
2022-11-27 04:10:00	139.46	1.1×10^6	100.62	4.66

4.2.3. Run 3: retention basin

Subsequently, retention is added to the model. This is done using the 'Sources and sinks' option in D-HYDRO (Deltares, 2025a). The ENCI-quarry is used as a retention basin (see Figure 4.5). It is selected because of its upstream location and large storage volume (see Section 2.5).

Figure 4.5: ENCI-quarry and 'source' & 'sink' locations. Background map: Airbus (2024).

First, it must be determined when water storage starts and ends. The choice is made to start storing water in the quarry when, within half an hour, the discharge at the measurement station closest to the retention location has increased by 10%. If we keep storing water until the discharge undershoots the discharge magnitude at which storage started, the entire peak should be extracted. If this approach is applied to the 95th percentile hydropeak, the required storage volume would be equal to 9.34 x 10^5 m^3. The available storage space at the ENCI-quarry is equal to 7.58 x 10^6 m^3 (Ouwerkerk et al., 2021), which suffices, assuming the entire quarry is used for retention.

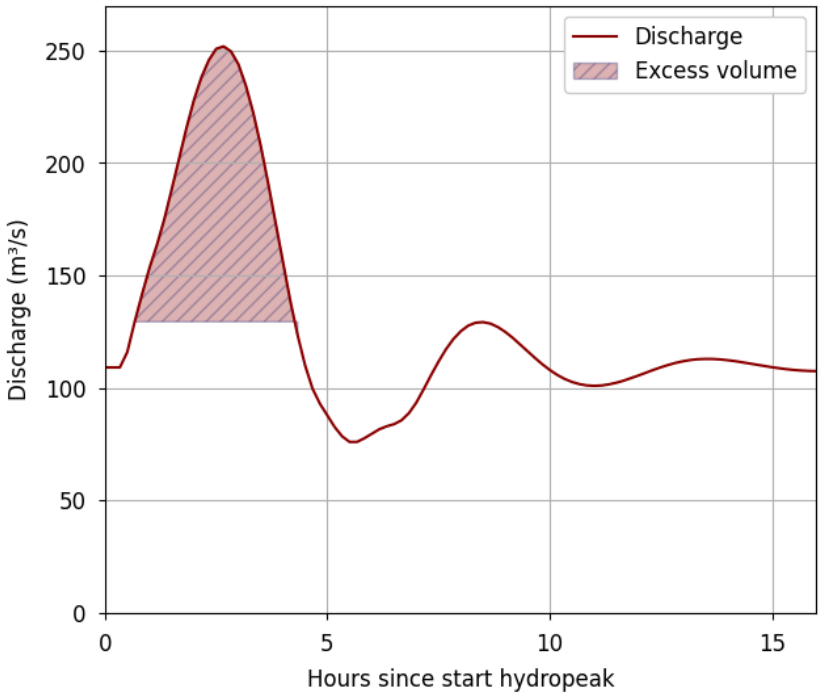

Figure 4.6: Water storage of 95th percentile hydropeak when cutting of entire peak

Theoretically, cutting off the entire hydropeak as described would work well when using a weir with a varying crest level to extract the right amount of water. In hindsight, it is clear that the entire peak can be cut off. However, the hydrograph is only fully known in hindsight, and we are only modelling a simple, single hydropeak, without natural variation. Maybe, in reality, the discharge would not undershoot the limit anymore, and one cannot tell when the hydropeak is over. Therefore, it may be more sensible to predict what the peak value and period of a hydropeak are going to be based on the local rate of change of water level or discharge and based on upstream measurements, and then control the weir such that water is extracted with a parabolic extraction quantity that follows the shape of the hydropeak. This way, the weirs can be controlled based on real-time data. Figure 4.7 displays the correlation between a hydropeak's rise speed and its peak value. They are strongly correlated: their Spearman's rank correlation coefficient is equal to 0.86. This illustrates that real-time monitoring can possibly be useful in predicting a hydropeak's shape. Note, these correlations are based on the separated hydropeak signal, not on a full hydrograph. Optimisation of the extracted and released discharge quantities is outside the scope of this research.

Instead of artificially cutting off the entire peak, water is extracted with a parabolic extraction rate by using a weir with a varying crest level. This requires less storage volume, which could become important if a hydropeak is followed by a new hydropeak, as then the storage volume should be available again. As discussed earlier in this section, the ENCI-quarry offers sufficient storage volume, reducing the need for rapid release. However, that estimation was based on the assumption that the entire quarry can be used for storage. This may not be feasible in practice, as releasing water that is stored in the deepest parts of the quarry requires substantial pumping capacity. Using a smaller, higher-elevated volume would be more cost-effective, though this reduces storage space.

When implemented correctly, the hydropeak will become much smoother. If the release of the stored water is timed correctly, the 'trough' of the hydropeak can be filled with it. Note, this timing is risk-prone, as premature release could amplify the hydropeak, which would aggravate the hydropeak magnitude. Figure 4.8 shows how the retention basin should theoretically affect the hydrograph of the 95th percentile when applied in the described manner. Instead of a large peak discharge followed by a steep drop, two small peaks are observed with a less rapid increase and decrease in discharge.

The quick release of water may not be needed at the ENCI-quarry due to large retention space. In reality,

however, not all storage volume may be used for the purpose of retention. Storing at the deepest parts of the quarry probably requires pumping to release the water again, making it expensive.

Clearly, the practical applicability is highly location-dependent. And if retention is used at another location, there will probably not be so much storage volume available.

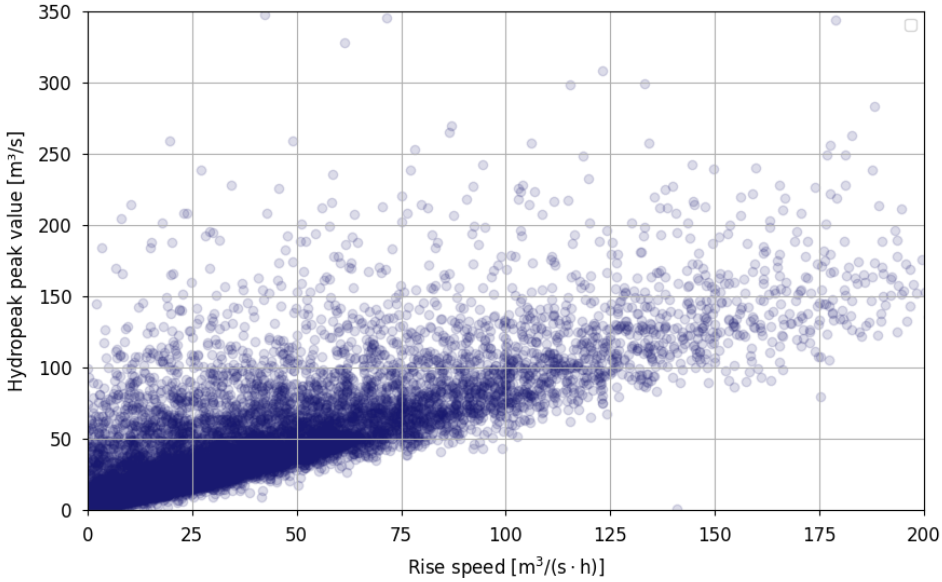

Figure 4.7: Correlation between the rise speed of a hydropeak during the first half an hour and the peak value of that hydropeak. Each dot represents one hydropeaking event.

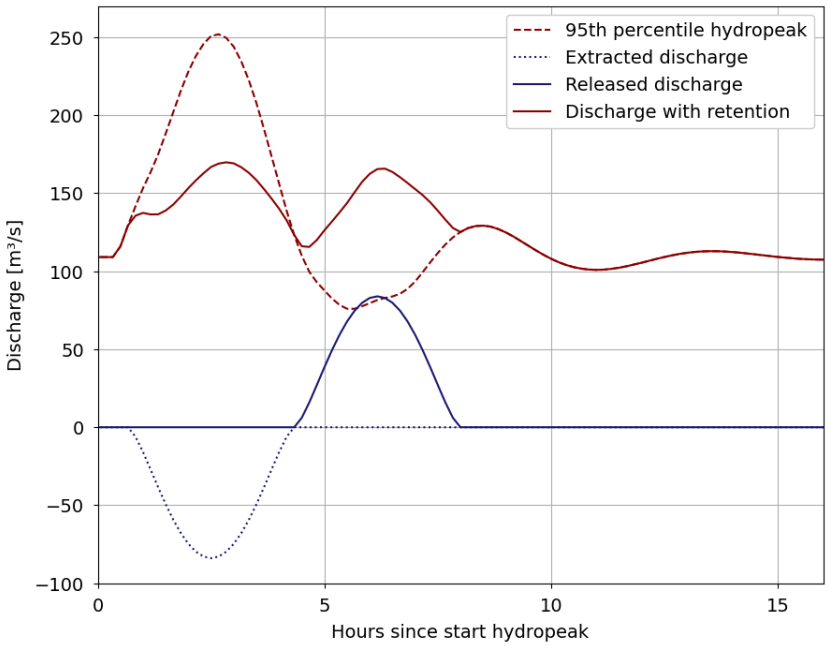

Figure 4.8: Extraction and release of water applied to 95th percentile hydropeak

4.3. Initial and boundary conditions

The model is initialised by applying an upstream discharge boundary condition of 100 m^3/s for 30 days, tributary inflows that correspond to a discharge of 100 m^3/s, and no initial water level.

Downstream, at rkm 84.6, a stage-discharge relation is applied as a boundary condition. This stage-discharge relation is deduced from Betrekkingslijnen Maas 2023-2024 (Rijkswaterstaat, 2025b). At every rkm, water levels are given that correspond with a certain discharge upstream at measurement station 'Sint Pieter Noord'. The discharges that would appear downstream are calculated by adding tributary inflows to the upstream discharges. Tributary inflows of some discharges have been provided by Rijkswaterstaat together with the D-HYDRO submodel. Tributary inflows of any remaining discharges are calculated by using either interpolation or extrapolation. This type of stage-discharge derivation is needed because the submodel comes with only stationary water levels belonging to some discharges and not with a stage-discharge relation.

By using no initial water level, the river reaches upstream of the weirs slowly fill, and no disconnected pools are formed. The latter could happen when starting with too high initial water levels.

After 30 days, the model is in equilibrium, i.e. it shows no variation in discharge and water level anymore. The end result of this run is used as a restart file for the runs with hydropeaking. Doing the latter still results in a small spin-up phase, during which discharge magnitudes and water levels fluctuate throughout the entire model.

During the hydropeak runs, a constant discharge of 100 m^3/s is first applied as an upstream boundary condition at Lixhe. After a few days, when conditions are steady, the isolated hydropeaks are added onto the base discharge.

4.4. Model calibration and validation

The D-HYDRO model is not independently calibrated or validated as part of this research. Calibration of submodels A (which is used here), B and C is not possible because they contain future geometry, i.e. they contain measures that are currently being implemented. Therefore, there is no data with which the model outcomes can be compared (Deltares and Rijkswaterstaat, 2025b).

Validation of the submodels has been carried out by Rijkswaterstaat and Deltares by comparing the results of the submodels with those of the total model. Submodel A shows the largest deviations in water level compared to the total model. Additionally, Submodel A displays unrealistically little peak attenuation. That is why submodel A is suitable for the assessment of relative effects, but should be used with caution when looking at absolute effects (Deltares and Rijkswaterstaat, 2025b).

4.5. Evaluation method

The results of the model runs are compared by assessing how they perform on the indicators that were established in Section 2.3. This section explains in more detail how these indicators are practically used in the model.

4.5.1. Disconnected pool formation

Disconnected pools are identified as any grid cell or collection of grid cells in the model output that is not connected to the main stream and has no flow velocity. Cells that meet these conditions are a threat to the chabot bullhead, as the water temperature may quickly rise above the upper thermal limit of the chabot bullhead in those locations (see Section 2.3.1).

Because chabot bullheads mainly live in shallow zones and because their main prey are macroinvertebrates, which tend to live near gravel bars, these gravel bars are the most critical locations to check for the occurrence of disconnected pools (Rijkswaterstaat, 2023). Moreover, the permeability of gravel would cause drainage of the pool, compromising the habitat even further. Therefore, the occurrence of pools is checked at multiple gravel bars in the Common Meuse (see Figure 4.9, Figure 4.10 and Figure 4.11). These gravel bars are identified using satellite imagery from the summer of 2023 (Airbus, 2023). This collection of gravel bars does not comprise all gravel bars in the Meuse, but their vast size and the fact that these three are spread out throughout the Meuse makes them representative for the present study. The studied gravel bars are located at Borgharen (rkm 17), Meers (rkm 32) and Grevenbicht (rkm 47).

Figure 4.9: Gravel bar at Borgharen. Adjusted from Airbus (2023).

Figure 4.10: Gravel bar at Meers. Adjusted from Airbus (2023).

Figure 4.11: Gravel bar at Grevenbicht. Adjusted from Airbus (2023).

The D-HYDRO bed topography is relatively coarse: 20×20 m in the winter bed, and between 5×20 m and 20×20 m in the summer bed (Deltares and Rijkswaterstaat, 2025b). Because of this grid coarseness, not all potential disconnected pools are identifiable from the D-HYDRO model output. This is because the pools may be smaller than the resolution of the grid cell at that location. The D-HYDRO bed topography is interpolated from a Baseline[1] bed topography with a finer resolution of 5×5 m (Deltares and Rijkswaterstaat, 2025b) throughout the entire grid. In Figure 4.12, the effect of this interpolation is visualised in a cross-sectional bed level profile near the gravel bar of Borgharen. It is clear that the interpolation masks the presence of deeper parts that are surrounded by shallower parts, which are especially potential disconnected pools. Therefore, the disconnected pool analysis is not conducted solely based on D-HYDRO output, but it is combined with Baseline topography. Furthermore, the spin-

[1] Baseline is a geodatabase containing geographical information that is used in Rijkswaterstaat models (Deltares and Rijkswaterstaat, 2025a)

up phase during the beginning of each simulation complicates pool detection when relying solely on D-HYDRO, as pools already form during spin-up. As a result, the specific effect of the hydropeaks on pool formation cannot be isolated.

At the three studied gravel bars, water level data throughout each run is retrieved from the D-HYDRO output. The maximum water level of each peak, and the base flow water level (which is the same during every run) together give the variation in water level that occurs at the bars. The Baseline topography is used to accurately tell which cells are connected to the main stream at each water level. Figure 4.13 shows which Baseline cells are connected to the main stream at the peak of the 95th percentile hydropeak and which cells are connected to the main stream during base flow. When the water level drops from the former situation to the latter, disconnected cells emerge. These are identified at each bar for each unique run.

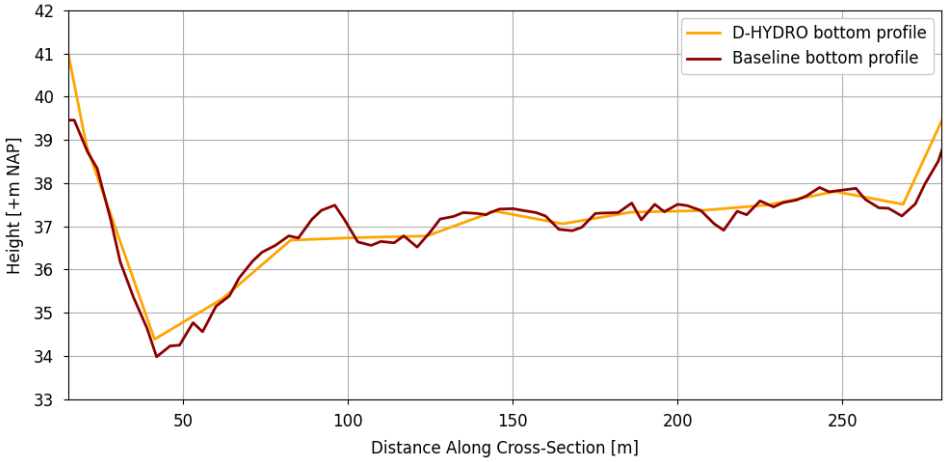

Figure 4.12: Cross-sectional bed level profiles from D-HYDRO and Baseline near Borgharen

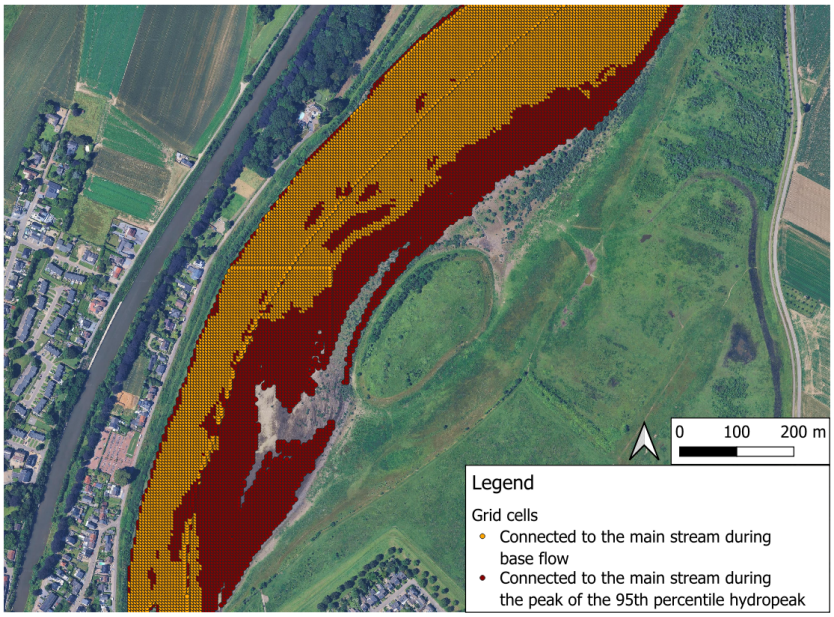

Figure 4.13: Grid cells that are connected to the main stream during the peak of the 95th percentile hydropeak and during base flow at Borgharen. Background map: Airbus (2024).

4.5.2. Wetted river area variation

The variation in wetted river area (Equation 2.1) is a measure of habitat availability for protected species. River lamprey larvae and chabot bullhead eggs both require a constantly submerged river bed (see Section 2.3.2). A threshold value of 30% is adopted from Swiss legislation (Baumann et al., 2012). The wetted river area variation is examined in the Upper Meuse and Common Meuse, as these are the reaches where hydropeaking is mostly active.

First, the river is divided into sections of 1 km. Within these sections, all grid cells within the river banks, including connected lakes, are included in a polygon (example in Figure 4.14). Within such a polygon, all cells that are wet (depth > 0.01 m) are calculated throughout the hydropeak, so that at any moment, the wetted area can be calculated (example in Figure 4.15). Subsequently, the variation in wetted area throughout the hydropeak is calculated for each section, according to Equation 2.1. Figure 4.16 and Figure 4.17 illustrate what a wetted river area variation looks like in plan view.

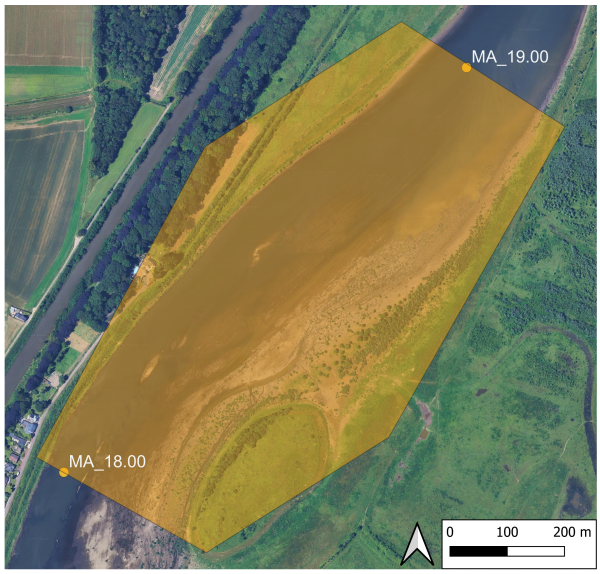

Figure 4.14: Polygon of rkm 18 — rkm 19. Background map: AND (2007).

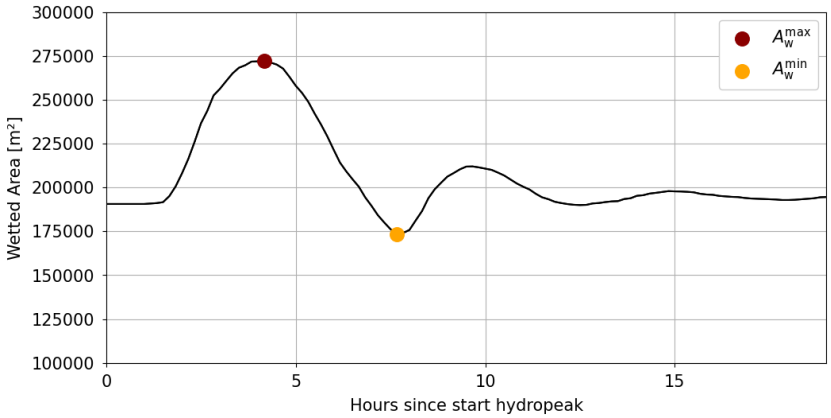

Figure 4.15: Wetted river area over time of rkm 18 — rkm 19

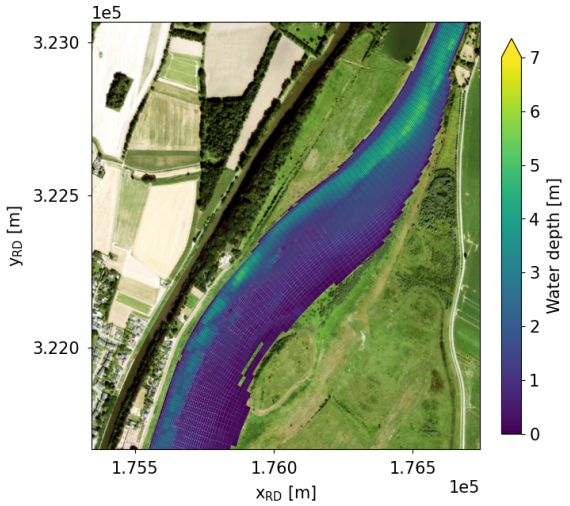

Figure 4.16: Wet cells between rkm 18 and rkm 19 at the moment of $A_{\mathrm{w}}^{\mathrm{max}}$. Background map: Esri (2025b).

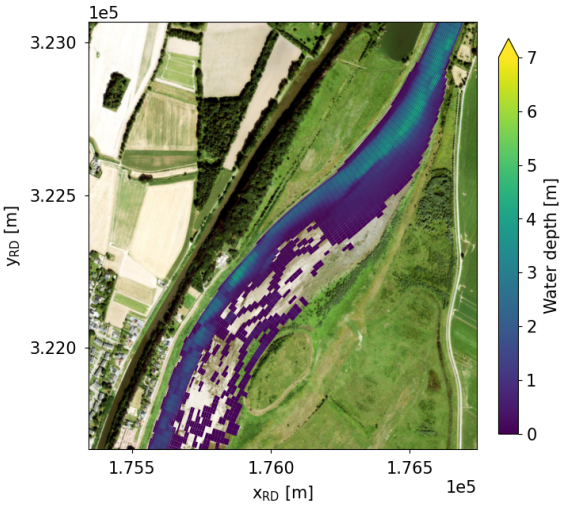

Figure 4.17: Wet cells between rkm 18 and rkm 19 at the moment of $A_{\mathrm{w}}^{\mathrm{min}}$. Background map: Esri (2025b).

4.5.3. Bed shear stress fluctuation

The gravel bars in the Meuse provide great ecological value for macroinvertebrates (Van Neer, 2016). That is why the bed shear stresses right before the hydropeak are compared with those at the peak of the hydropeak at the gravel bars of Figure 4.9, Figure 4.10 and Figure 4.11. The rate of change of bed shear stresses at the gravel bars is important as under low-flow conditions macroinvertebrates may not be active and are vulnerable to high shear stresses if they were to occur quickly. If during the peak of a hydropeak the absolute bed shear stress threshold value of 10 N/m² for macroinvertebrate drift is exceeded, the specific location could form a threat to these species if the bed shear stress was low before the hydropeak (see Section 2.3.3). Macroinvertebrates may be able to seek refuge in time, but the shear stress fluctuations still remain a stress factor. Such periods could, for instance, hinder the quest for food. Limiting bed shear stresses between May and July should also reduce damage to roots of large pondweed, as that is the growing season of this protected habitat (Rijkswaterstaat, 2023).

Figure 4.18, Figure 4.19 and Figure 4.20 display how the bed shear stress fluctuation is quantitatively examined. Figure 4.18 shows the bed shear stress right before the median hydropeak arrives at Borgharen, Figure 4.19 shows the bed shear stress during the peak of the median hydropeak at Borgharen, and Figure 4.20 shows the difference in bed shear stress between the two moments, only at locations with low bed shear stress (< 1 Pa) before the hydropeak arrives. Dark red areas are areas with large fluctuations in bed shear stress during a hydropeak, posing a risk to macroinvertebrates. In Section 4.6, no absolute bottom shear stresses are shown; only the differences in bed shear stress are visualised. The total drift-prone area is stated, allowing for a quantitative comparison of the results across the different runs. The area of all individual cells is known, so the area of all cells with excessive shear stresses is added to obtain this total drift-prone area around a gravel bar. This approach is applied to all three gravel bars and all three runs.

It should be noted that this evaluation method assumes macroinvertebrates are equally abundant across an entire gravel bar. However, in reality, they may be more likely to inhabit wet parts of the riverbed than dry parts. Therefore, the identified extent of drift-prone areas might be slightly overestimated.

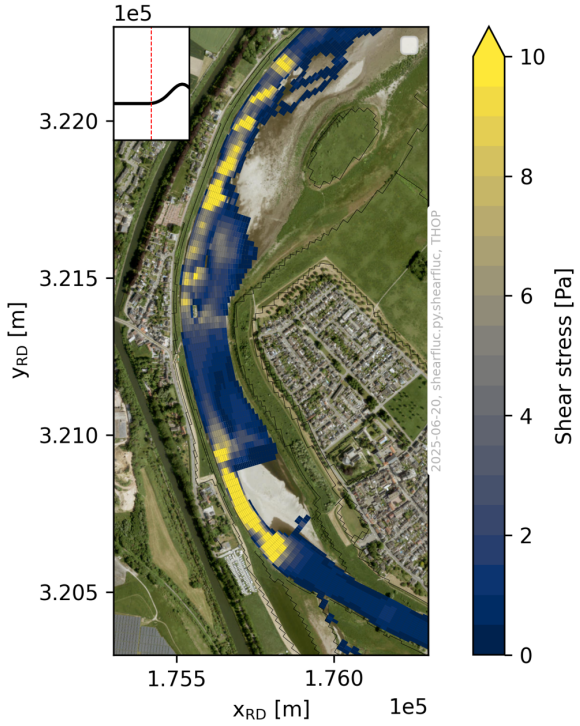

Figure 4.18: Bed shear stress right before median hydropeak at Borgharen. The moment in time is visualised in the hydrograph in the top left corner. Background map: Esri (2025b).

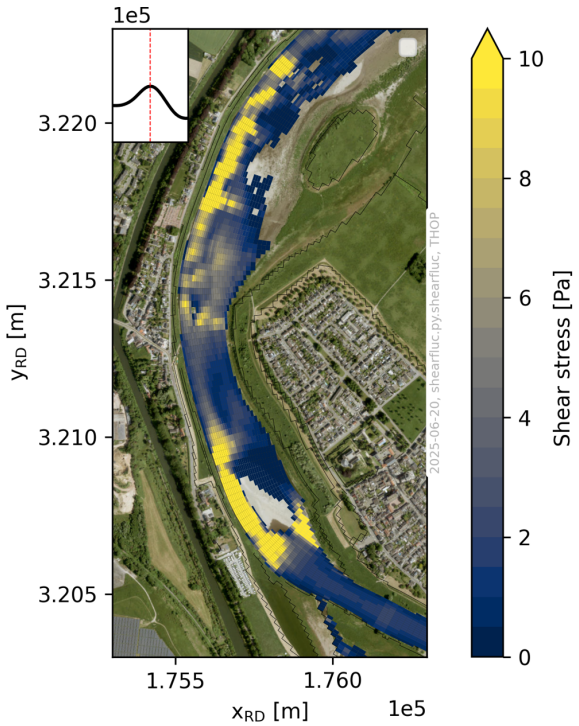

Figure 4.19: Bed shear stress during peak of median hydropeak at Borgharen. The moment in time is visualised in the hydrograph in the top left corner. Background map: Esri (2025b).

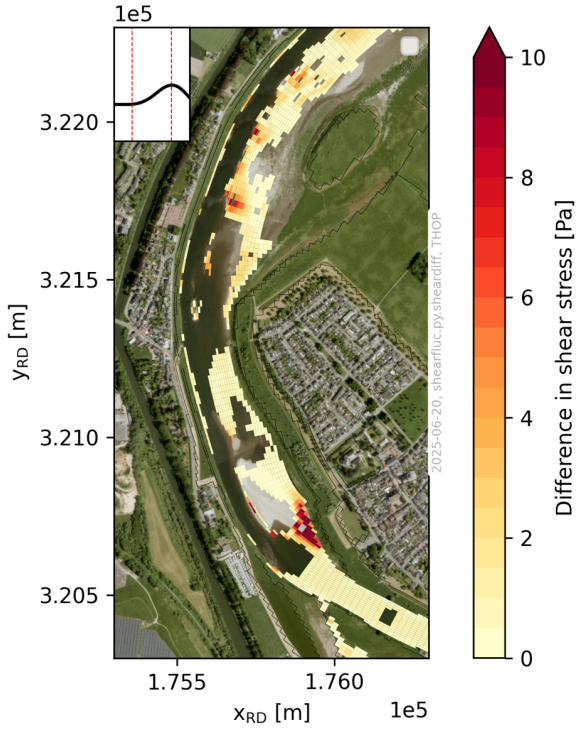

Figure 4.20: Difference in bed shear stress between base flow and peak of median hydropeak at Borgharen at locations with low bed shear stress (< 1 Pa) before hydropeak. The moments in time are visualised in the hydrograph in the top left corner. Background map: Esri (2025b).

4.6. Simulation results

Before diving into specific ecological indicators, it is useful to observe what happens to each peak when travelling through the river. The focus is first on the shape of the peaks at rkm 11, which is just downstream of the location where extraction and release happen during the run with retention. Figure 4.8 illustrates the predicted hydrograph; Figure 4.21 presents the actual hydrographs at rkm 11 that are produced by the D-HYDRO model simulations. As expected, using retention results in two moderate peaks rather than one large peak.

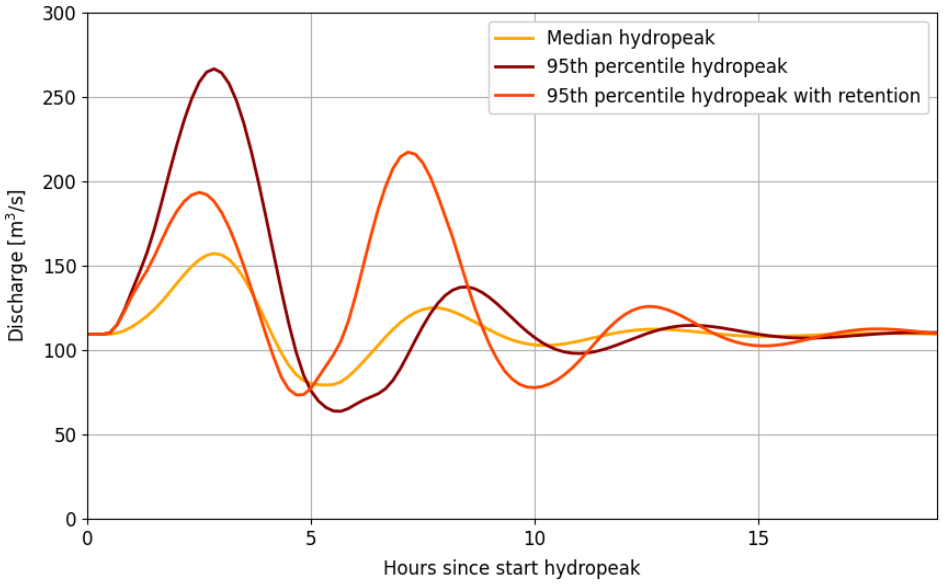

Figure 4.21: Discharge of the three runs at rkm 11

Figure 4.22, Figure 4.23, and Figure 4.24 show how the water level varies throughout the Upper Meuse and Common Meuse during each run. The effects of the weir of Borgharen at rkm 15 and the weir of Linne at rkm 68 are clear: upstream of the weirs, the water levels are practically constant as the measurement locations are impounded, and the water levels of consecutive measurement stations are nearly the same. In the free-flowing section of the Common Meuse, from rkm 18 to rkm 51 in the figures, peak attenuation is observed.

The median hydropeak barely causes any water level variation anymore in the lower part of the Common Meuse. The other two runs still display some variation, though they also began with a larger disturbance upstream. In both cases, the peak height significantly reduces throughout the Common Meuse.

Derived by De Jong and Asselman (2019), Equation 4.1 gives a theoretical formula for the relative wave height reduction with respect to the water depth for river flood waves. A higher wave results in an increased h in the numerator of the equation. The modelled median hydropeak and the modelled 95th percentile hydropeak have a similar period (see Section 4.2). L_{wave} of the 95th percentile hydropeak will therefore be higher, as a wave with a larger amplitude will have a greater propagation speed. Because L_{wave} is in the demoninator, the relative wave height reduction is not necessarily higher for the 95th percentile hydropeak.

$$\frac{\Delta h}{h} = -\frac{4\pi^2}{3\, i_b}\, h\, \frac{L_{\text{reach}}}{L_{\text{wave}}^2} \tag{4.1}$$

Where:
- Δh = wave height reduction (m) over L_{reach}
- h = water depth (m)
- i_b = bed slope (-)
- L_{reach} = reach of interest (m)
- L_{wave} = wavelength (m)

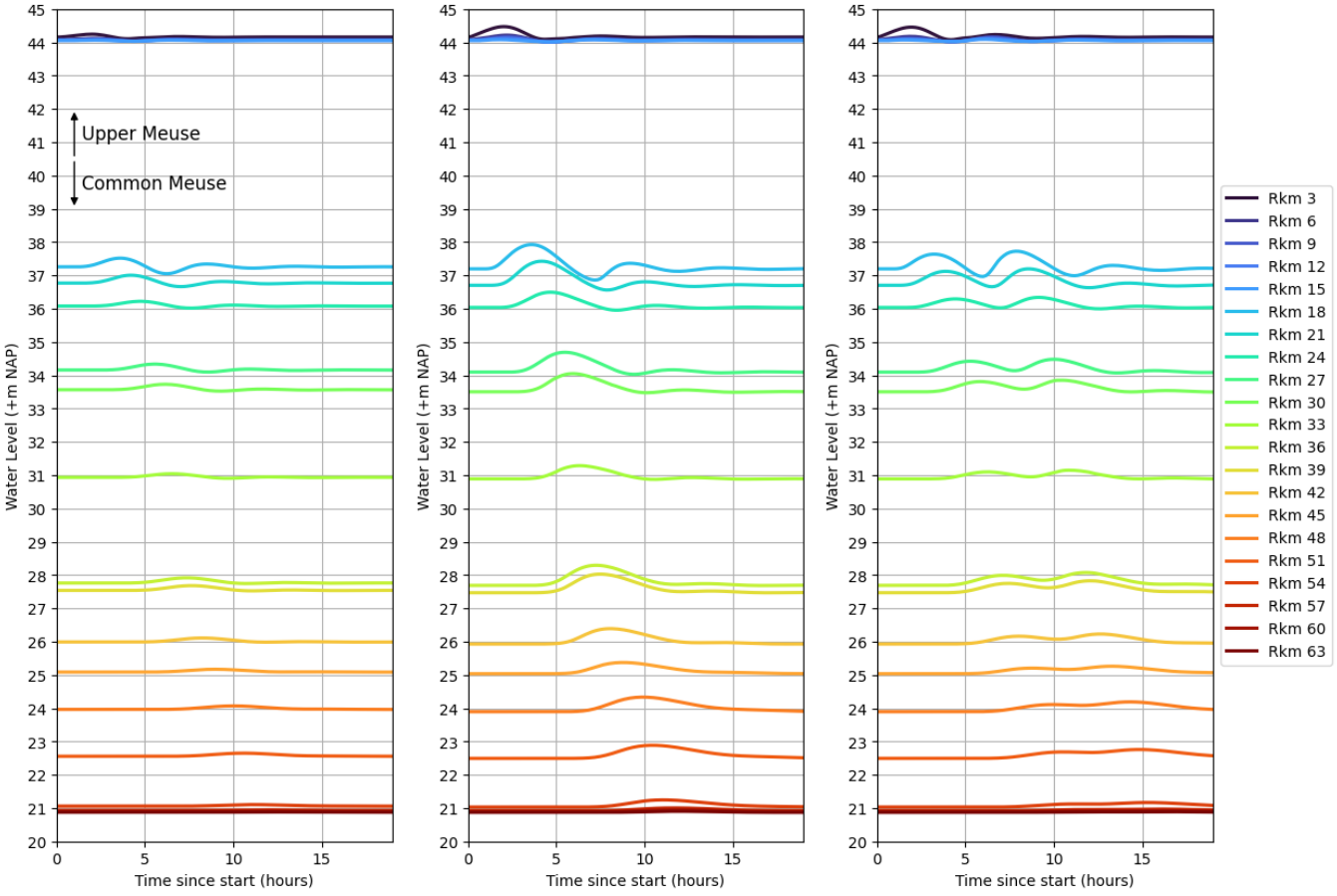

Figure 4.22: Water level development during the median hydropeak throughout the Upper Meuse and Common Meuse.

Figure 4.23: Water level development during the 95th percentile hydropeak throughout the Upper Meuse and Common Meuse.

Figure 4.24: Water level development during the 95th percentile hydropeak with retention throughout the Upper Meuse and Common Meuse.

4.6.1. Disconnected pool formation

Borgharen

At Borgharen, several disconnected pools form during each of the runs. These are visible in 4.25. Especially near the right bank, a few gulleys form after the water level drops. All cells in the pools have a water depth of less than 0.5 m, which could quickly drain into the coarse gravel bed, depending on the soil saturation. During the median hydropeak, 4,600 m^2 of pools form in the studied area. During the 95th percentile hydropeak, the total disconnected pool area equals 16,575 m^2, which is reduced by 61% to 6,525 m^2 of disconnected pools when retention is implemented. One could say that retention works well in mitigating pool formation; however, the influence of the base water level may not be overlooked. As can be seen in the cross-sectional bed level profile of Figure 4.12, water level variations between

NAP+37 m and NAP+38 m carry the risk of pool formation, whereas variations between NAP+36 m and NAP+37 m or NAP+38 m and NAP+39 m do not carry the same risk.

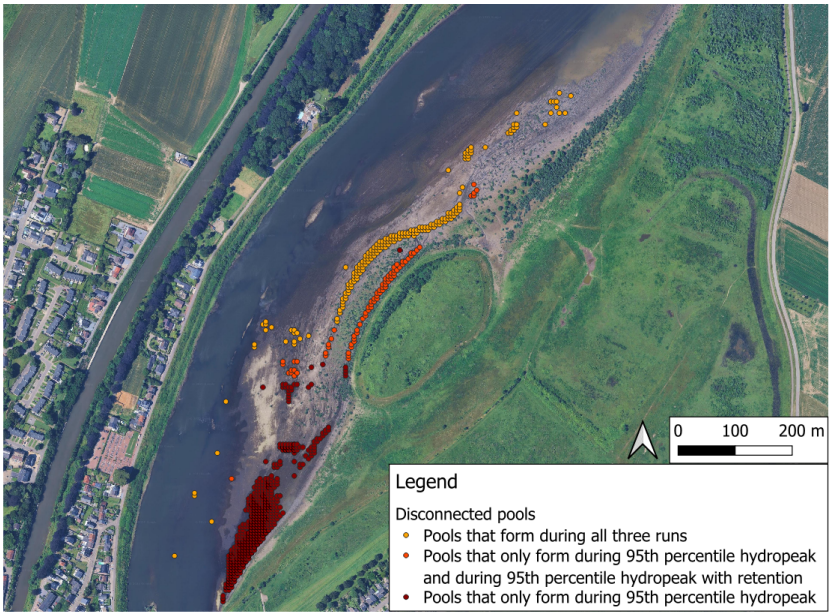

Figure 4.25: Disconnected pools at Borgharen. Background map: Airbus (2024).

Meers

Figure 4.26 shows the pools that form at Meers. Here, very few pools form, even though the satellite map may give the impression that more pools should form near the gravel bars. During the median hydropeak, 250 m^2 of disconnected pools form, especially in the middle of the river near the gravel bars. This increases to 1350 m^2 during the 95th percentile hydropeak and reduces by 30% to 950 m^2 when retention is implemented.

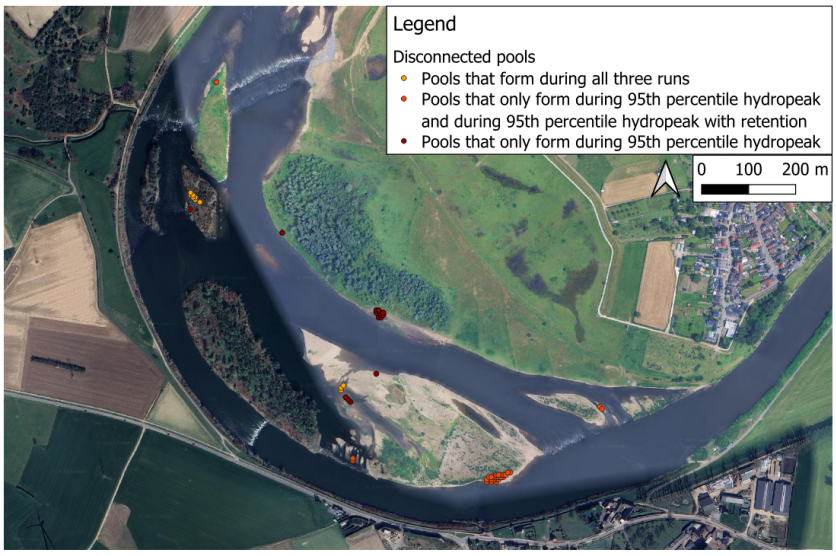

Figure 4.26: Disconnected pools at Meers. Background map: Airbus (2024).

Grevenbicht

At Grevenbicht, surprisingly, a more pronounced effect is observed (Figure 4.27) than at Meers, even though it is located downstream of Meers. During the median hydropeak, 1850 m^2 of disconnected

pools forms. The 95th percentile hydropeak causes 7375 m^2 of pools, which is reduced by 67% to 2425 m^2 when retention is used. The fact that more pools form at Grevenbicht than at Meers can be explained by differences in local bed topography. Here, gulleys form when water levels drop, similarly to what happens at Borgharen (Figure 4.25).

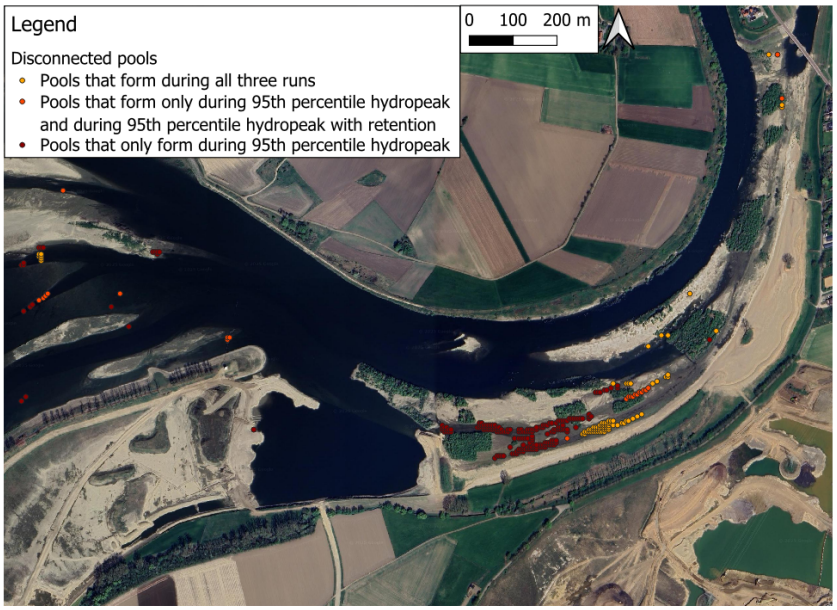

Figure 4.27: Disconnected pools at Grevenbicht. Background map: Airbus (2024).

Table 4.3 presents an overview of the disconnected pool area per gravel bar and model run. The largest pool areas are found at Borgharen, and Grevenbicht has more pools than Meers, despite being located further downstream. This highlights the relevance of local bed topography and base flow magnitude in pool formation.

Table 4.3: Disconnected pool area (m^2) per gravel bar and model run

Gravel bar	Median hydropeak (m^2)	95th percentile hydropeak (m^2)	Retention (m^2)	Difference (%)
Borgharen	4,600	16,575	6,525	-61%
Meers	250	1,350	950	-30%
Grevenbicht	1,850	7,375	2,425	-67%

4.6.2. Wetted river area variation

Median hydropeak

Figure 4.28 shows the wetted river area variation throughout the Upper Meuse and Common Meuse during the median hydropeak. The Upper Meuse spans from rkm 2 until rkm 15, which is visible well in the figure. As it is mostly impounded, there is little variation in water level and, as a result, there is also little variation in wetted river area. The Common Meuse spans from rkm 16 until rkm 64, where the free-flowing character results in significantly higher variations in wetted river area. In the most downstream part of the Common Meuse, the hydropeak has diffused to such an extent that it barely causes a variation in wetted river area anymore. The 30% threshold is not exceeded anywhere during the median hydropeak.

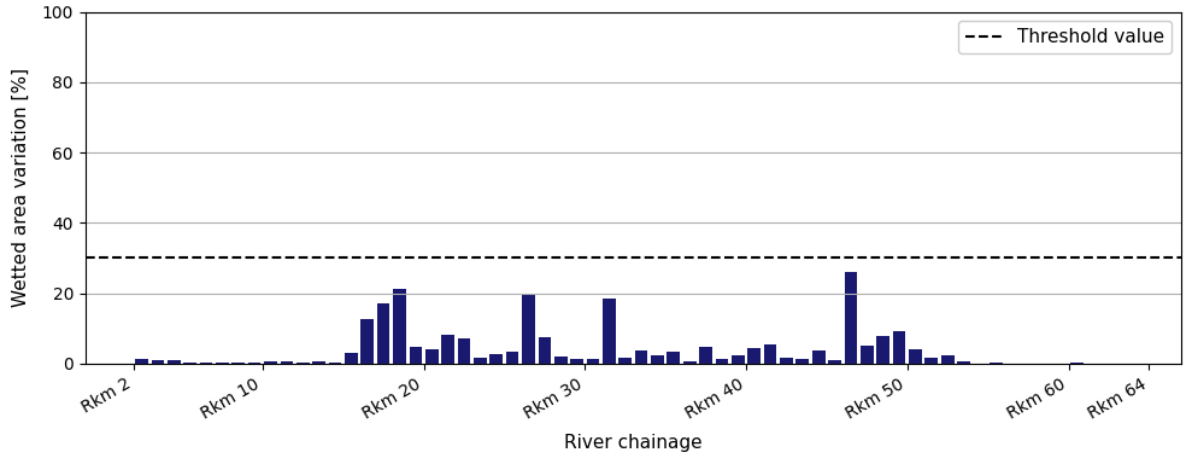

Figure 4.28: Wetted river area variation per 1 km reach during a median hydropeak

95th percentile hydropeak

The wetted river area variation during the 95th percentile hydropeak is significantly larger than during the median hydropeak. At 4 reaches, the critical threshold of 30% is exceeded (see Figure 4.29). However, it is still not an issue in the Upper Meuse nor in the lower part of the Common Meuse. In the remaining part of the Common Meuse, the high variation that occurs at the 4 reaches are a problem for the chabot bullhead, whose eggs may suffocate or desiccate, and for the river lamprey larvae, which require constantly wet habitats.

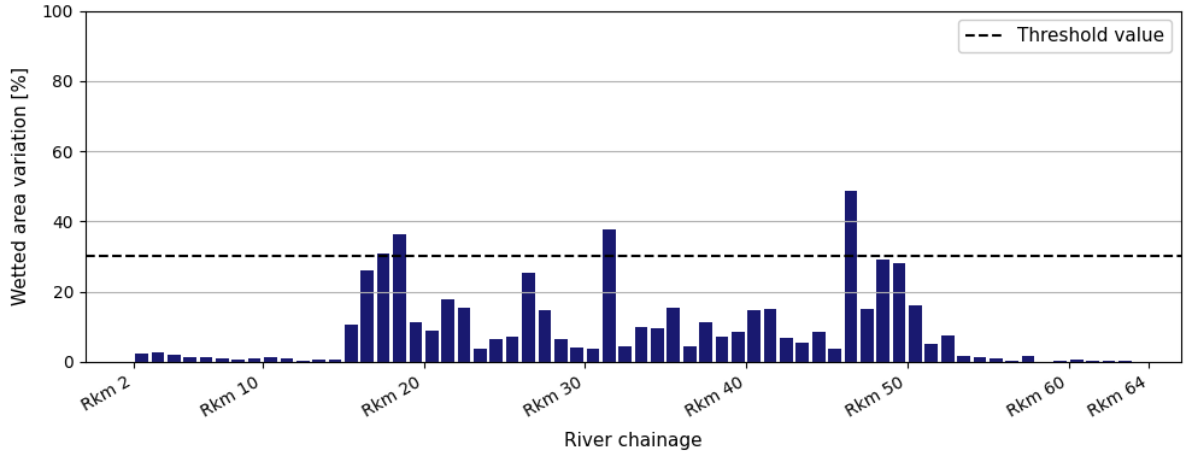

Figure 4.29: Wetted river area variation per 1 km reach during a 95th percentile hydropeak

Retention basin

Figure 4.30 shows the wetted river area variation during the 95th percentile hydropeak with a retention basin at the ENCI-quarry included. At 3 out of the 4 reaches where problems arose during the 95th percentile hydropeak run, the variation is now below the 30% threshold, which is a 75% improvement. Only the reach between rkm 46 and rkm 47 displays such an amount of wetted area variation that it cannot be classified as a suitable habitat.

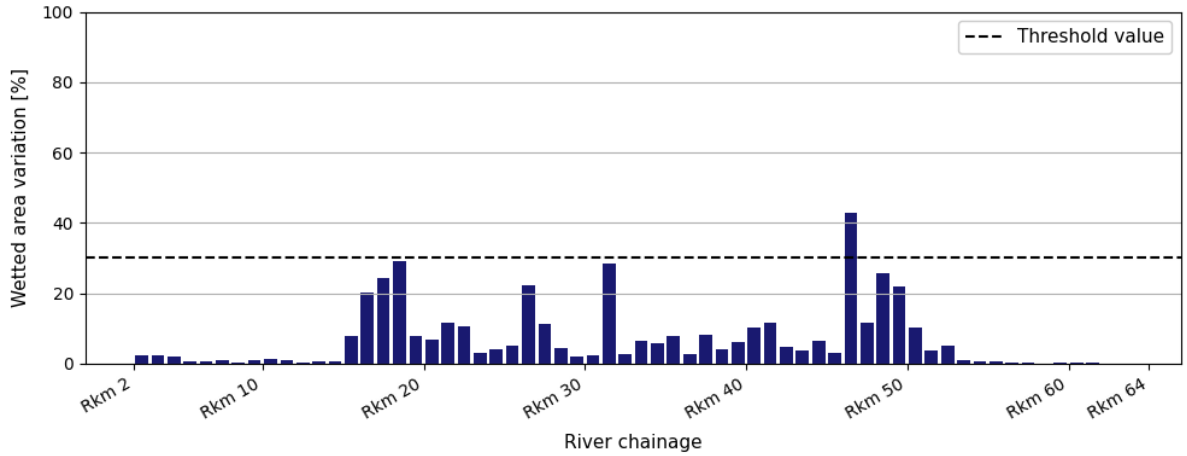

Figure 4.30: Wetted river area variation per 1 km reach during a 95th percentile hydropeak with retention basin

4.6.3. Bed shear stress fluctuation

Borgharen

The bed shear stress fluctuation of the median hydropeak at Borgharen is visible in Figure 4.31. The area where the drift risk is high is equal to 3,004 m^2, located mainly at the lower gravel bar. During the 95th percentile hydropeak, the high-risk area increases to 15,166 m^2. From Figure 4.32, it can be seen that there are now large areas with significant increases in bed shear stress at both the lower and upper gravel bar. The implementation of retention in combination with the 95th percentile hydropeak yields the bottom shear stress fluctuation of Figure 4.33. By visual comparison with Figure 4.32, it can already be seen that a considerable decrease in problematic areas is ensured by using a retention basin. This is underlined by the quantitative decrease: a 54% decrease, with now 7047 m^2 of high-risk area.

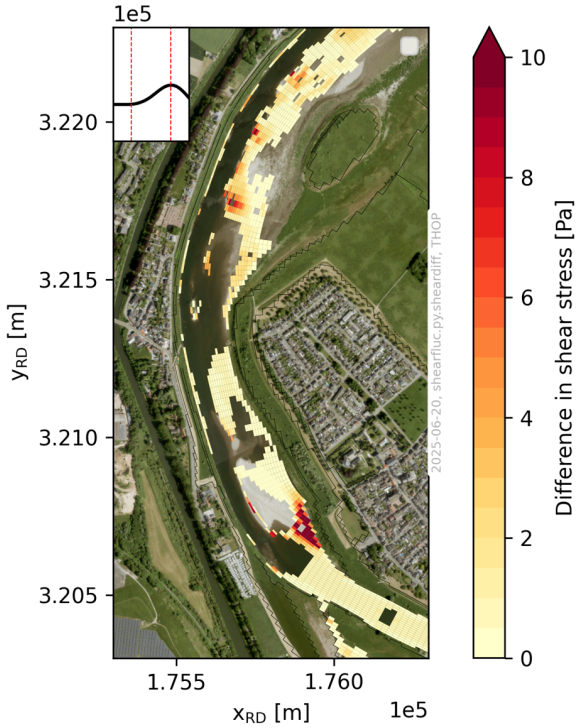

Figure 4.31: Difference in bed shear stress between base flow and peak of median hydropeak at Borgharen at locations with low bed shear stress (< 1 Pa) before hydropeak. The moments in time are visualised in the hydrograph in the top left corner. Background map: Esri (2025b).

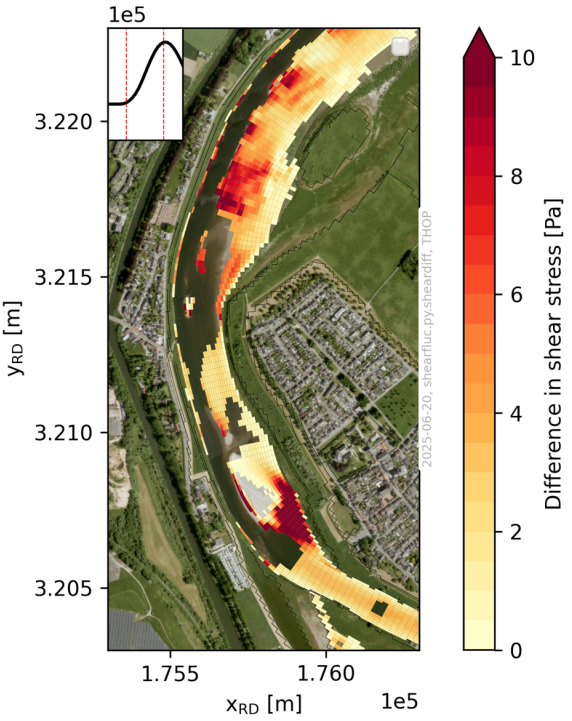

Figure 4.32: Difference in bed shear stress between base flow and peak of 95th percentile hydropeak at Borgharen at locations with low bed shear stress (< 1 Pa) before hydropeak. The moments in time are visualised in the hydrograph in the top left corner. Background map: Esri (2025b).

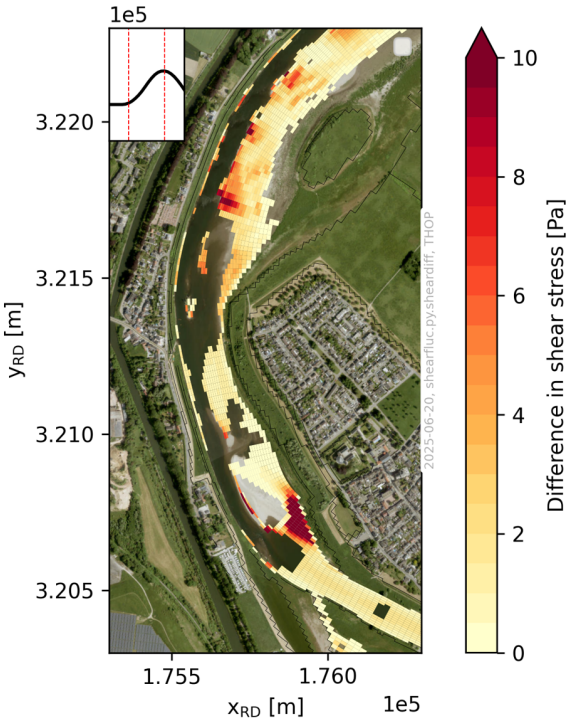

Figure 4.33: Difference in bed shear stress between base flow and peak of 95th percentile hydropeak with retention at Borgharen at locations with low bed shear stress (< 1 Pa) before hydropeak. The moments in time are visualised in the hydrograph in the top left corner. Background map: Esri (2025b).

Meers

Figure 4.34 shows the bed shear stress fluctuations that occur at Meers during a median hydropeak. The high-risk area is equal to 136 m^2. From Figure 4.35, it can be seen that significantly more problematic areas arise during the 95th percentile hydropeak: 5,165 m^2. With the implementation of retention, 89% of these areas are resolved and only 574 m^2 of high-risk area remains. In general, all runs show less pronounced bed shear stress fluctuations at Meers than at Borgharen, which illustrates the diffusion of hydropeaks. Note, however, that the fluctuations also strongly depend on the local topography of the focus areas, as regions with more variation in bed level will display more pronounced fluctuations in bed shear stress than regions which have a very clear distinction between deep and shallow parts.

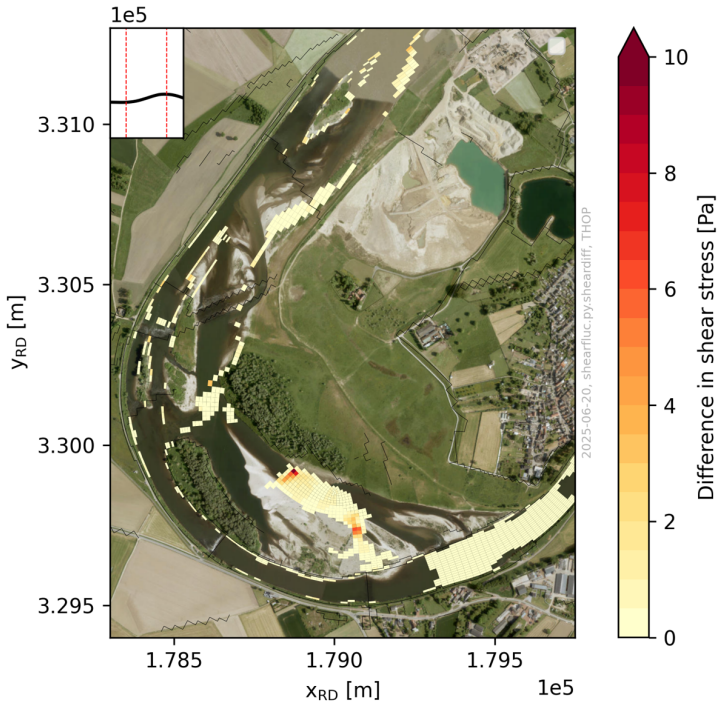

Figure 4.34: Difference in bed shear stress between base flow and peak of median hydropeak at Meers at locations with low bed shear stress (< 1 Pa) before hydropeak. The moments in time are visualised in the hydrograph in the top left corner. Background map: Esri (2025b).

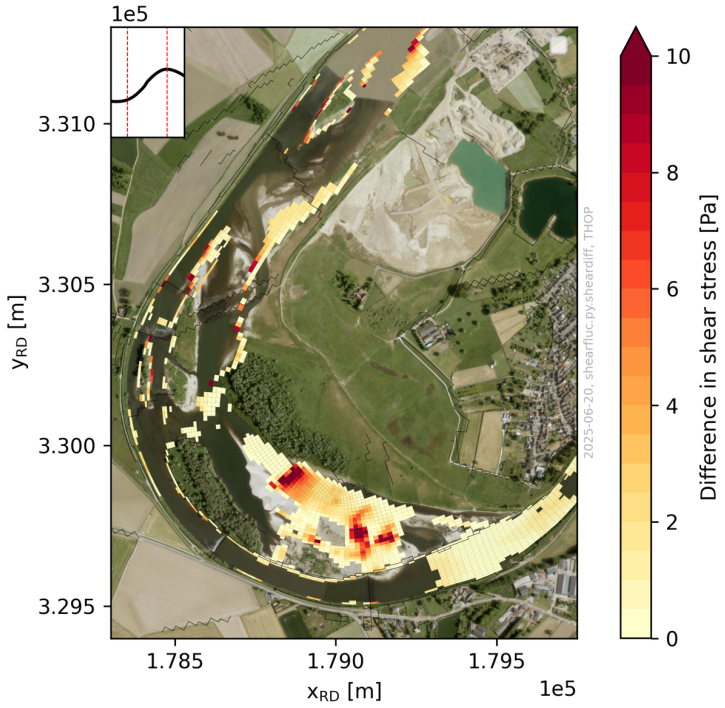

Figure 4.35: Difference in bed shear stress between base flow and peak of 95th percentile hydropeak at Meers at locations with low bed shear stress (< 1 Pa) before hydropeak. The moments in time are visualised in the hydrograph in the top left corner. Background map: Esri (2025b).

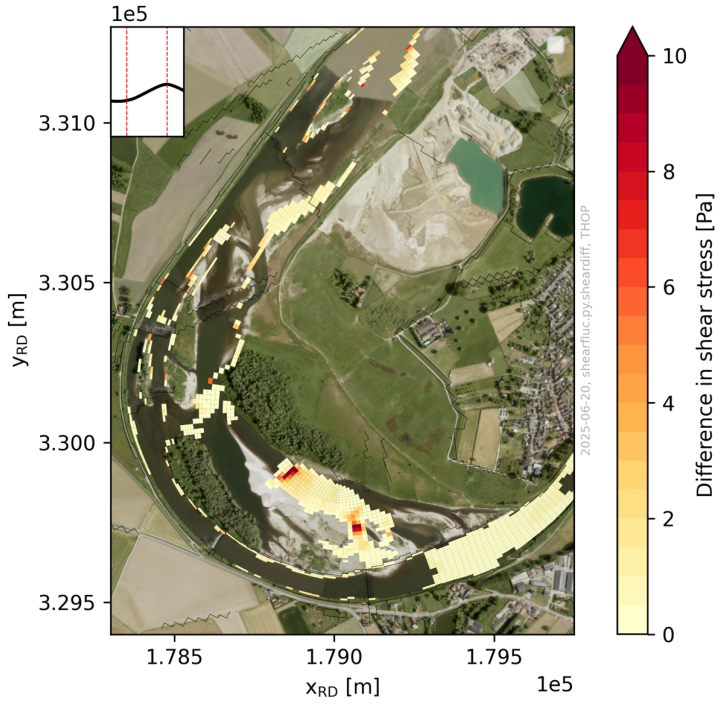

Figure 4.36: Difference in bed shear stress between base flow and peak of 95th percentile hydropeak with retention at Meers at locations with low bed shear stress (< 1 Pa) before hydropeak. The moments in time are visualised in the hydrograph in the top left corner. Background map: Esri (2025b).

Grevenbicht

At Grevenbicht, the hydropeak has diffused to such an extent that bed shear stresses at the gravel bars barely increase during any of the runs. The median hydropeak has 0 m^2 of high-risk areas (Figure 4.37). The 95th percentile hydropeak has 125 m^2 of high-risk area (Figure 4.38), which is fully resolved during the run with retention (Figure 4.39)

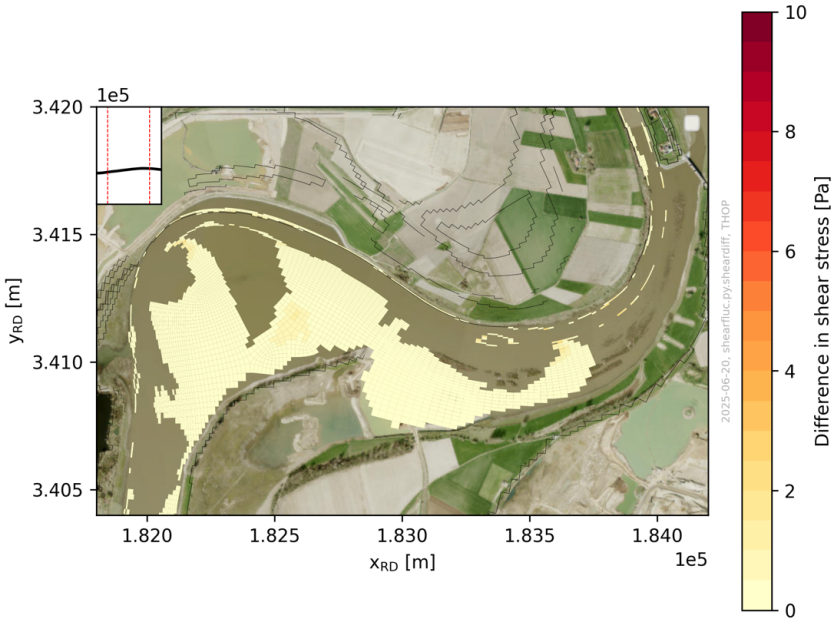

Figure 4.37: Difference in bed shear stress between base flow and peak of median hydropeak at Grevenbicht at locations with low bed shear stress (< 1 Pa) before hydropeak. The moments in time are visualised in the hydrograph in the top left corner. Background map: Esri (2025b).

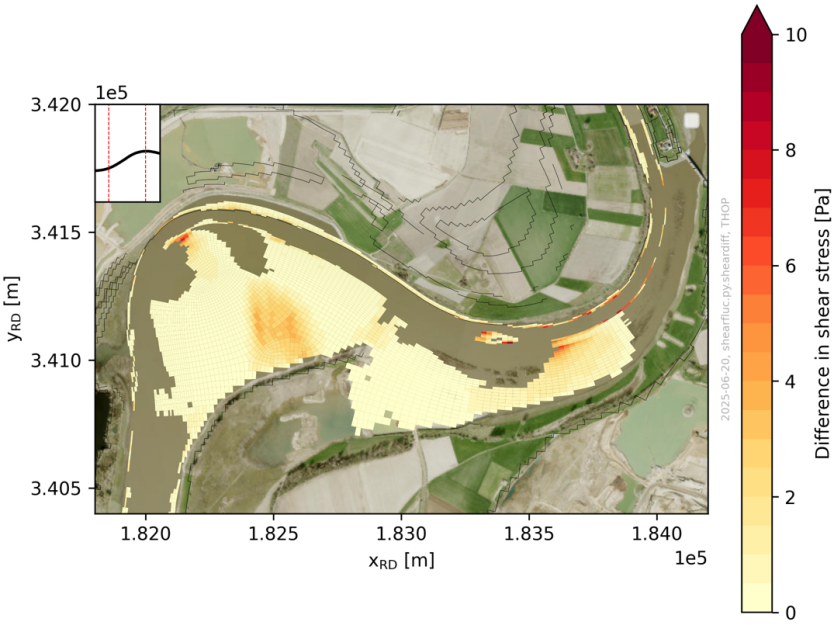

Figure 4.38: Difference in bed shear stress between base flow and peak of 95th percentile hydropeak at Grevenbicht at locations with low bed shear stress (< 1 Pa) before hydropeak. The moments in time are visualised in the hydrograph in the top left corner. Background map: Esri (2025b).

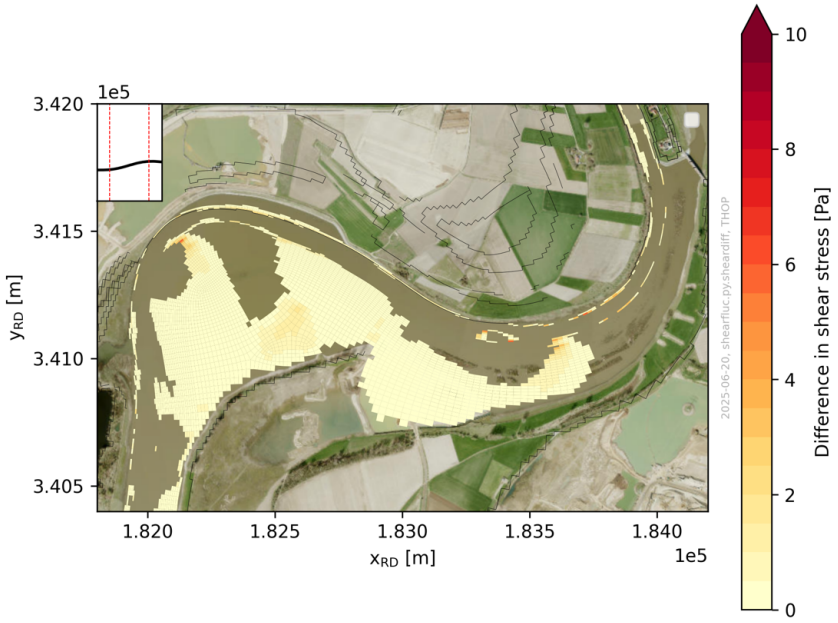

Figure 4.39: Difference in bed shear stress between base flow and peak of 95th percentile hydropeak with retention at Grevenbicht at locations with low bed shear stress (< 1 Pa) before hydropeak. The moments in time are visualised in the hydrograph in the top left corner. Background map: Esri (2025b).

Table 4.4 presents an overview of the drift-prone area per gravel bar and run. The reduction in bed shear stress fluctuations due to peak attenuation in downstream direction is clearly visible in this table.

Table 4.4: Drift-prone area (m^2) due to bed shear stress fluctuation per gravel bar and model run

Gravel bar	Median hydropeak (m^2)	95th percentile hydropeak (m^2)	Retention (m^2)	Difference (%)
Borgharen	3,004	15,166	7,047	-54%
Meers	136	5,165	574	-89%
Grevenbicht	0	125	0	-100%

5 Discussion

The aim of this chapter is to reflect on the study's findings and place them in a broader context. Section 5.1 interprets the results of this research. This is followed by an assessment of the study's limitations in Section 5.2. Finally, Section 5.3 discusses the implications of the results.

5.1. Interpretation of results

This section interprets the modelling results by comparing the ecological impact of the three modelled hydropeaks using the full set of established indicators. Instead of discussing the impact of a hydropeak per indicator, the focus now lies on the ecological impact of a hydropeak as a whole. This approach facilitates a link between separate hydropeaks and the protected species and habitats, which are the underlying motivation for the indicator establishment and the model simulations. Finally, the study results are placed into the context of existing literature.

5.1.1. Key findings and ecological relevance

A median hydropeak does not pose a large threat to ecology in the Dutch Meuse. Only limited pool formation occurs at two of the three studied gravel bars. The wetted river area variation does not exceed the 30% threshold anywhere in the Upper Meuse or Common Meuse, and only a relatively small area causes drift-prone conditions at one gravel bar.

A 95th percentile hydropeak causes substantial pool formation at two of the three studied gravel bars, exceeds the wetted river area variation threshold of 30% at 4 out of 61 reaches, and induces large bed shear stress fluctuations at two gravel bars. Clearly, a 95th percentile hydropeak causes more challenging conditions for the aquatic ecosystem than a median hydropeak.

Retention can significantly reduce the negative impact of extreme hydropeaking events on ecology in the Dutch Meuse. When a theoretical retention basin is implemented, pool formation at the two problematic gravel bars reduces by 61% and 67% in terms of total pool area. The number of reaches that exceed the wetted area threshold reduces from 4 to 1, a 75% reduction. Finally, areas that carry a high drift risk reduce by 54% and 89%.

95th percentile hydropeaks in combination with a low natural discharge are a larger stressor to the Meuse ecosystem than median hydropeaks in combination with the same natural discharge. The harmful hydropeaks usually occur between May and October. Within this half-year window, the return period of extreme hydropeaks is 9 days. Hydropeaks usually differ from natural peaks in their high frequency of occurrence and rapid change in conditions, whereas the low frequency of occurrence of extreme hydropeaks partially limits the threat they pose. This is because the wetted river area variation only is a stress factor when its frequency of occurrence is high. The rate of change of wetted river area is less relevant to ecological impact. If the large variation only occurs once every 9 days, the impact is smaller than if it were to occur more frequently. Nevertheless, the wetted river area variation caused by 95th percentile hydropeaks is still larger than the natural variation in a 9-day window in summer. Therefore, 95th percentile hydropeaks remain a relevant stressor to river lamprey larvae and the eggs of chabot bullheads.

The effects of the other two indicators, disconnected pool formation and bed shear stress fluctuation, also play an important role. Their impact is driven not only by the high frequency of occurrence of hydropeaking, but also by the high rate of change of conditions that hydropeaking induces. As a result,

extreme hydropeaks do substantially affect habitat suitability for chabot bullheads, macroinvertebrates, and large pondweed.

5.1.2. Comparison with previous research

The effects of specific hydropeaks on the local ecosystem of the Meuse had not been demonstrated before. Van Denderen (2024) identified and quantified hydropeaks in the Meuse and briefly assessed their relationship with increased bed shear stress and its variations, similar to the approach in this study. However, the present study focused more on the ecological effect of these variations, particularly drift, and adopted a more detailed approach to the variations by examining locations that rapidly transition from low to high bed shear stress. Van Neer (2016) assessed macroinvertebrate abundance in the Common Meuse and found more characteristic species downstream. However, the extent to which hydropeaking contributed to this outcome remained unclear, and no other species types were studied. The effectiveness of mitigation measures in reducing the ecological impact of hydropeaking had not yet been explored either.

5.2. Research limitations

This study focused on improving conditions for protected habitats and species along the Common Meuse, as defined by Natura 2000 guidelines (Rijkswaterstaat, 2023). Generalised indicators and thresholds were established to assess the impact of hydropeaking on these habitats and species. It is important to acknowledge that this approach results in a simplification of a complex ecosystem, addressing only a subset of its components. Impacts on other parts of the ecosystem may therefore be underrepresented in the findings of this study. Nevertheless, focus lay on the most vital part of the ecosystem, and the established indicators reflect the main stress factors associated with hydropeaking.

The method used to isolate hydropeaks from the hydrograph, the wavelet transform, also comes with limitations. The method implies that hydropeaks can be isolated based on the frequency of a reconstructed signal. In practice, however, hydropeaks will also have smaller and larger frequencies than the chosen frequency window, and natural signals will in reality also lie within the hydropeaking frequency window that was established. In addition, the separated 'natural' signal at Eijsden Grens cannot be validated with a truly natural signal. All nearby measurement stations with similar hydrological characteristics are also affected by hydropeaking and therefore cannot provide a natural hydrograph as a reference. As a result, the separated hydropeaking signal and the identified hydropeaking events should be interpreted with caution. Nevertheless, this was the most suitable signal processing technique, given the lack of quantitative information on the influence of hydropower plants on the hydrograph in the region of interest.

Using a hydrodynamic model to simulate hydropeaking effects brings certain limitations. Not all physical properties and phenomena can be accurately mimicked in a hydrodynamic model. For instance, there will be differences in bed shear stress between the model and reality, as a simplified, uniform Manning's friction coefficient is used in the model. Furthermore, model topography lacks detail, which may lead to an underestimation of disconnected pool formation. Additionally, the used submodel exhibits reduced peak attenuation (Deltares and Rijkswaterstaat, 2025b), causing the model to produce downstream results that are more severe than they would be in reality. This results in conservative findings; the ecological impact of the modelled hydropeaks is expected to be larger than the impact such hydropeaks would induce in practice, particularly downstream.

Two model runs have been performed to assess hydropeaking impact without mitigation. These runs, recreating a median hydropeak and a 95th percentile hydropeak, exhibit substantial impact differences. The median hydropeak causes little negative impact, whereas the 95th percentile hydropeak induces significant disruption of aquatic habitats. As no hydropeaks with intermediate magnitudes were simulated, it remains unclear how rapidly hydropeaking impact increases with increasing hydropeaking magnitude.

The extraction method used in this study is based on retrospective knowledge about the shape of a hydropeak. This approach provides a useful first approximation of the effectiveness of retention as a measure to reduce hydropeaking impact, but does not account for practical uncertainties. In practice, a

hydropeak's shape is not known in advance. This makes the release and extraction of water challenging, while this is a critical part of retention as a mitigation measure. When release is poorly timed and starts too early, a hydropeak will be amplified instead of attenuated, aggravating the problem that retention is supposed to solve. As a result, the effectiveness of retention in this study should be viewed as an idealised outcome that excludes the practical challenges associated with real-time implementation of retention.

5.3. Implications of findings

The results show that median hydropeaks pose only a limited burden to ecology, that 95th percentile hydropeaks cause a substantial burden, and that retention can significantly mitigate this burden. This study specifically focused on assessing hydropeaking influence on ecology and did not separately account for other contributing factors. In practice, hydropeaking is just one of various factors that influence the ecological state of a river. Thus, while an extreme hydropeak negatively affects ecological conditions, other drivers may still contribute positively to the overall ecosystem health. The same holds for the mitigation of ecological hydropeaking impact: minimising the impact does not necessarily mean that the desired ecosystem is reached. It will bring conditions closer to the desired system, but other negative influences may persist. Pollution coming from urban, industrial, and agricultural sources forms a continuous threat to water quality (Wageningen University & Research, n.d.). In addition, climate change will increase discharge extremes, aggravating the impact of pollutants as there is less dilution during prolonged low-flow periods (Asselman et al., 2019). The presence of river barriers such as hydropower plants and weirs will also continue to disturb ecosystem connectivity, despite efforts to reduce the unnatural flow regime they induce.

Currently, only 1 % of Dutch water bodies comply with WFD criteria regarding chemical and ecological properties (Rijksoverheid, 2022). It is unrealistic to expect that hydropeaking impact mitigation alone will dramatically improve the ecological state of the Meuse, and that the species and habitats that are protected according to Natura 2000 guidelines Rijkswaterstaat (2023) will all reach a satisfactory status. A comprehensive approach is required, targeting both water quality and specific species and habitats. This is particularly important as chemical pollutants may directly impact the ecosystem. This comprehensive view is adopted in the maintenance plan 'Natura 2000-ontwerpbeheerplan Grensmaas', which focuses on protecting specific species and habitats, while also aiming to contribute positively to the objectives regarding water quality set by the WFD (Rijkswaterstaat, 2023).

Hydropeaking impact mitigation should also be put into the context of the current vision for the Meuse. Asselman et al. (2019) state that efforts should be made to make the river more dynamic, like it used to be centuries ago. Part of a dynamic river are water level fluctuations and a strong floodplain connectivity (Asselman et al., 2019) — phenomena which are especially increased by hydropeaking. That is why it may seem contradictory to attenuate hydropeaks, while also actively enforcing dynamics in the Meuse. The difference, however, lies in the rate of change of conditions. Natural dynamics display a gradual change to which species are likely to be able to adapt, whereas a hydropeak causes excessively large variations within a matter of hours, causing a burden to aquatic species. Therefore, the high rate of change of water level and the high rate of change of bed shear stress that an extreme hydropeak causes may justify active attenuation of these hydropeaks, even if such events occur only weekly or even less frequently.

As this study has shown that extreme hydropeaks in summer are in particular responsible for ecological impact by hydropeaking, the issue could be addressed at its source by preventing the large hydropeaks from occurring in summer. Reducing the magnitude of the hydropeaks in summer could substantially reduce the ecological impact of hydropeaking. However, achieving this could prove to be challenging in practice, as impounding is particularly needed in summer due to a lack of base flow. Moreover, limiting the discharge diverted through a hydropower plant may quickly reduce the efficiency of electricity generation by hydropower turbines.

6

Conclusions and recommendations

This chapter presents the conclusions and recommendations of this research. In Section 6.1, conclusions are drawn by answering the research questions. Section 6.2 provides recommendations to local stakeholders and fellow researchers.

6.1. Conclusions

This study examined to what extent ecology in the Dutch Meuse is affected by hydropeaking and whether retention is a viable solution to mitigate the negative impact of hydropeaking on ecology. The three research questions that were introduced in Section 1.3 to support this examination are now addressed one by one.

"What part of the Dutch Meuse is affected by hydropeaking and what are the characteristics of these hydropeaks?"

Hydropeaking events were separated from the Meuse hydrograph using a wavelet transform. This showed that hydropeaking is predominantly present in the Upper Meuse and Common Meuse. Further downstream, hydropeaks attenuate due to bottom friction and the buffering effect of large ponds. Hydropeaks generally have a peak value between 0 m^3/s and 250 m^3/s, and an average duration of 9 hours. Hydropeaking mainly differs from natural flow in its increased frequency of occurrence and its higher rate of change of hydrological conditions (Meile et al., 2011). Hydropeaking has a significant influence on the hydrograph, especially when large hydropeaks occur during periods of low natural discharge. These harmful phenomena mainly occur between May and October.

"In what way is the ecology of the Dutch Meuse affected by hydropeaking?"

Hydrodynamic modelling showed that between May and October, an extreme (95th percentile) hydropeak is a significant stressor to the Meuse ecosystem. Median hydropeaks, which may occur every day, do not significantly affect any protected species or habitat in the Dutch Meuse. As the Common Meuse provides great ecological value, this study primarily focused on hydropeaking impact along this reach. The goal has been to accommodate satisfactory conditions for habitats and species which are protected according to Natura 2000 guidelines (Rijkswaterstaat, 2023). One of these species, chabot bullhead, is particularly affected by the falling stage of an extreme hydropeak, as rapidly dropping water levels cause disconnected pools with poor water quality. Large pondweed and macroinvertebrates are both exposed to abrupt fluctuations in bed shear stress during an extreme hydropeak, which reduces the amount of potential habitats significantly. River lamprey larvae and eggs of the chabot bullhead are affected by the large variations in wetted river area an extreme hydropeak induces. The magnitude of median hydropeaks is too small relative to natural base flow to make such hydropeaks significant stressors during any time of the year. From November to April, high base flows reduce the relative magnitude of extreme hydropeaks as well, minimising their impact during that period.

It is important to note that hydropeaking is only one of several factors influencing the ecological status of the Meuse; the above conclusions indicate only the ecological impact of hydropeaking.

"To what extent could retention be an effective measure to reduce the negative effects of hydropeaking in the Dutch Meuse?"

The results demonstrate that retention is theoretically effective, as it largely mitigates the negative impact of hydropeaking on the habitats of chabot bullheads, macroinvertebrates, and large pondweed.

However, because the practical implementation of retention is expected to be complicated, and because hydropeaking is only a part of several influences on ecology, retention alone is unlikely to offer a realistic solution to the ecological challenges the Dutch Meuse is facing.

6.2. Recommendations

It is recommended to assess whether the impact of hydropeaking justifies mitigation measures. Since median hydropeaks do not induce significant ecological issues, such measures would primarily target hydropeaks of a larger magnitude, although the exact magnitude at which hydropeaking impact becomes significant is uncertain. Upon implementation of measures, conditions are expected to significantly improve for chabot bullheads, macroinvertebrates, and large pondweed. However, impact mitigation should be weighted against required investments, which are uncertain at this stage. In addition, it is important to acknowledge that measures that target hydropeaking impact alone are unlikely to bring the ecological status of the Dutch Meuse to a satisfactory level. Other influences, such as water quality, climate change, and river fragmentation, persist when only hydropeaking is targeted. Instead, a broad, integrated approach is required to reach the ecological goals set by Natura 2000 guidelines (Rijkswaterstaat, 2023) and the Water Framework Directive (European Commission, 2000).

If measures are taken that target hydropeaking, it remains uncertain whether retention is the most appropriate type of measure, as its implementation is not straightforward. The design of a basin was not part of this study, but such a system would likely require a weir with a varying crest level that alters based on real-time data, an impermeable layer to prevent water from draining through the subsurface, and a pump or outlet structure to release water from the retention basin back into the river. An alternative to retention would be actively impounding with a weir to attenuate hydropeaks. This is in line with the recommendations made by Van Denderen (2024), who suggested using the weir of Borgharen for this purpose. When using impounding as a measure, crest level control is the only large challenge. No retention basin has to be prepared, and no pumping is required. This would significantly reduce investments, maintenance, and operational costs. Therefore, impounding can be considered as an alternative measure.

Future researchers are advised to investigate how real-time data monitoring can optimise peak attenuation. Translating upstream or local data into local hydropeak magnitude predictions could largely help in facing the problem of varying crest level control, regardless of the choice for retention or impounding. A local observation of rapidly increasing discharge levels or water levels may indicate the start of a hydropeak, allowing for a prediction of its shape. Upstream data will provide more information but also more uncertainty, as between the upstream measurement location and the retention site, the shape of a hydropeak may change significantly due to diffusion or due to artificial amplification when a hydropower plant is located in between. Enhanced communication between Rijkswaterstaat and Belgian hydropower plant operators could be valuable, as direct information on discharge diverted through hydropower plants in Belgium would provide valuable insight into the hydropeaks that can be expected in the Dutch Meuse. Subsequently, a well-informed decision can be made on whether the incoming hydropeaks require mitigation.

This study has treated hydropeaking primarily as a given condition, after which impact arises and measures can be taken to mitigate that impact. An alternative approach would be changing the way hydropower plants are operated to prevent the formation of hydropeaks directly at their source. The largest hydropeaks in summer appear to cause most of the ecological impact; therefore, limiting hydropeaking in that period may already resolve most of the issues that hydropeaking causes. However, this may be challenging in practice due to the limited availability of base flow in summer with which electricity can be generated. Moreover, the persisting demand for electricity generation would require alternative energy sources.

References

Airbus (2023). Satellite imagery of the Dutch Meuse. https://earth.google.com/web.

— (2024). Satellite imagery of the Dutch Meuse. https://earth.google.com/web.

AND (2007). OpenStreetMap. https://www.openstreetmap.org/.

Animalia (n.d.). Myoxocephalus scorpius. https://animalia.bio/fr/myoxocephalus-scorpius.

Asselman, N., Barneveld, H., Klijn, F., and Van Winden, A. (2019). Het Verhaal van de Maas. https://www.deltaprogramma.nl/documenten/publicaties/2019/09/05/het-verhaal-van-de-maas.

Auer, S., Zeiringer, B., Führer, S., Tonolla, D., and Schmutz, S. (2017). Effects of river bank heterogeneity and time of day on drift and stranding of juvenile European grayling (Thymallus thymallus L.) caused by hydropeaking. Science of the Total Environment 575, 1515–1521. https://doi.org/http://dx.doi.org/10.1016/j.scitotenv.2016.10.029.

Auer, S., Hayes, D. S., Führer, S., Zeiringer, B., and Schmutz, S. (2023). Effects of cold and warm thermopeaking on drift and stranding of juvenile European grayling (Thymallus thymallus). River Research and Applications 39(3), 401–411. https://doi.org/https://doi.org/10.1002/rra.4077.

Baumann, P., Kirchhofer, A., and Schälchli, U. (2012). Risanamento deflussi discontinui Pianificazione strategica. Ufficio federale dell'ambiente (UFAM).

Becker, A., Geerling, G., and Harezlak, V. (2022). Systeembeschouwing voor N2000 - Bovenmaas. https://open.rijkswaterstaat.nl/open-overheid/onderzoeksrapporten/@259464/systeembeschouwing-n2000-bovenmaas/.

Bipa, N. J., Stradiotti, G., Righetti, M., and Pisaturo, G. R. (2023). Impacts of hydropeaking: A systematic review. Science of The Total Environment 912. https://doi.org/https://doi.org/10.1016/j.scitotenv.2023.169251.

Bradford, M., Taylor, G., Allan, J., and Higgins, P. (1995). An Experimental Study of the Stranding of Juvenile Coho Salmon and Rainbow Trout during Rapid Flow Decreases under Winter Conditions. North American Journal of Fisheries Management 15(2), 473–479. https://doi.org/https://doi.org/10.1577/1548-8675(1995)015%3C0473:AESOTS%3E2.3.CO;2.

Brevé, N., Moquette, F., Vertegaal, D., Oyen, H., Belgers, T., and Budé, M. (2014). Grensmaas onder de maat. URL: https://edepot.wur.nl/319342.

Carolli, M., Vanzo, D., Siviglia, A., Zolezzi, G., Bruno, M., and Alfredsen, K. (2015). A simple procedure for the assessment of hydropeaking flow alterations applied to several European streams. Aquatic Sciences 77, 639–653. https://doi.org/https://doi.org/10.1007/s00027-015-0408-5.

Carter, G. (n.d.). Microphotograph of typical benthic animals. URL: https://www.flickr.com/photos/noaa_glerl/4076029220.

Céréghino, R., Legalle, M., and Lavandier, P. (2004). Drift and benthic population structure of the mayfly Rhithrogena semicolorata (Heptageniidae) under natural and hydropeaking conditions. Hydrobiologia 519(1), 127–133. https://doi.org/http://dx.doi.org/10.1023/B:HYDR.0000026499.53979.69.

Dam Removal Europe (2024). New Report: Dam Removal Movement Breaks Barriers and Records. URL: https://damremoval.eu/dre-report-2023/ (visited on 03/03/2025).

De Jong, J. and Asselman, N. (2019). Topvervlakking Maas; Het effect van golfvormen, bergingsgebieden en rivierverruiming. Rapport 11203684-003-ZWS-0002. Delft: Deltares.

Deltares (2025a). D-Flow Flexible Mesh User Manual. URL: https://content.oss.deltares.nl/delft3d/.

— (2025b). D-HYDRO Suite 2D3D. URL: https://www.deltares.nl/software-en-data/producten/d-hydro-suite-2d3d.

Deltares and Rijkswaterstaat (2025a). Baseline-NL. URL: https://iplo.nl/thema/water/applicaties-modellen/modelschematisaties/nederland/.

— (2025b). D-Flow FM 2D deelmodellen Maas. URL: https://iplo.nl/thema/water/applicaties-modellen/modelschematisaties/rivieren.

Déry, S., Hernández-Henríquez, M., Stadnyk, T., and Troy, T. (2021). Vanishing weekly hydropeaking cycles in American and Canadian rivers. Nature Communications 12. https://doi.org/https://doi.org/10.1038/s41467-021-27465-4.

DHI Group (2025). MIKE+ Rivers. URL: https://www.dhigroup.com/technologies/mikepoweredbydhi/mikeplus-rivers.

Directie Natuur & Biodiversiteit (2018). Ontwerp-wijzigingsbesluit Habitatrichtlijngebieden vanwege aanwezige waarden. https://www.natura2000.nl/gebieden/limburg/grensmaas/grensmaas-archief.

Elliot, J. and Elliot, J. (1995). The critical thermal limits for the bullhead, Cottus gobio, from three populations in north-west England. Freshwater Biology 33(3), 411–418. https://doi.org/https://doi.org/10.1111/j.1365-2427.1995.tb00403.x.

ENTSO-E (2025). ENTSO-E Transparency Platform. URL: https://transparency.entsoe.eu/dashboard/show.

Esri (2025a). Outdoor Map. https://www.arcgis.com/home/item.html?id=98beaa0b7d8a405eb0d8f799288b62c9.

— (2025b). World Imagery. https://www.arcgis.com/home/item.html?id=10df2279f9684e4a9f6a7f08febac2a9.

European Commission (2000). Water Framework Directive. URL: https://environment.ec.europa.eu/topics/water/water-framework-directive_en.

— (2020). EU Biodiversity Strategy for 2030 - Bringing nature back into our lives. URL: https://nl.chm-cbd.net/en/policy-biodiversity-netherlands/international-agreements/eu-biodiversity-strategy-2030-english.

— (2025). Natural Water Retention Measures. URL: https://www.nwrm.eu/measure/retention-ponds.

European Environment Agency (n.d.[a]). Basse Meuse et Meuse mitoyenne. https://eunis.eea.europa.eu/sites/BE33004C0.

— (n.d.[b]). Uiterwaarden langs de Limburgse Maas met Vijverbroek. https://eunis.eea.europa.eu/sites/BE2200037.

GeoWeb Rijkswaterstaat (2025). Waterbodematlas RWS ZN. URL: https://maps.rijkswaterstaat.nl/gwproj55/index.html?viewer=ZN_Waterbodematlas.Webviewer.

Glock, K., Tritthart, M., Habersack, H., and Hauer, C. (2019). Comparison of Hydrodynamics Simulated by 1D, 2D and 3D Models Focusing on Bed Shear Stresses. Water 11(2). https://doi.org/https://doi.org/10.3390/w11020226.

Grenzeloze Schelde (2016). Micro-waterkrachtcentrales: bron van groene stroom? https://www.gs-esf.be/mailer/mailer-GSNB-73/NL/GSNB73_T3.htm.

Grimardias, D., Faivre, L., and Cattaneo, F. (2012). Postemergence downstream movement of European grayling (Thymallus thymallus L.) alevins and the effect of flow. Ecology of Freshwater Fish 21(4), 495–498. https://doi.org/https://doi.org/10.1111/j.1600-0633.2012.00572.x.

Hauer, C., Unfer, G., Graf, W., Leitner, P., Zeiringer, B., and Habersack, H. (2012). Hydro-morphologically related variance in benthic drift and its importance for numerical habitat modelling. Hydrobiologia 683, 83–108. https://doi.org/10.1007/s10750-011-0942-7.

Herasimtschuk, D. (n.d.). Pacific Lamprey at the Oregon Zoo. https://www.flickr.com/photos/usfwspacific/7129322663.

Hoffarth, P. (2004). Evaluation of Juvenile Fall Chinook Salmon Entrapment in the Hanford Reach of the Columbia River, 56. URL: https://wdfw.wa.gov/publications/00185.

Jakubec, K. (n.d.). Planting and Growing Shining pondweed. URL: https://www.picturethisai.com/care/Potamogeton_lucens.html.

Jardim, P. and Colishonn, W. (2024). Sub-daily flow alterations (hydropeaking) due to reservoir operations in Brazil. Brazilian Journal of Water Resources 29(3). https://doi.org/https://doi.org/10.1590/2318-0331.292420230111.

Kenney, M., Sutton-Grier, A., Smith, R., and Gresens, S. (2009). Benthic macroinvertebrates as indicators of water quality: The intersection of science and policy. Terrestrial Arthropod Reviews 2, 99–128. https://doi.org/http://dx.doi.org/10.1163/187498209X12525675906077.

Kindle, H., Wendlinger, C., Frangez, C., Baumann, P., and Schneider, M. (2012). Alpenrhein: Quantitative Analyse von Schwall/Sunk-Ganglinien für unterschiedliche Anforderungsprofile. Zukunft Alpenrhein, 35.

Koninklijk Nederlands Meteorologisch Instituut (2025). Grafieken van het lopende jaar. URL: https://www.knmi.nl/nederland-nu/klimatologie/grafieken/jaar.

Kopecki, I., Schneider, M., and Schletterer, M. (2022). Modelling of Habitat Changes Related to Hydropeaking with CASiMiR. Novel Developments for Sustainable Hydropower, 147–156. https://doi.org/http://dx.doi.org/10.1007/978-3-030-99138-8_13.

Lancaster, J. and Hildrew, A. (1993). Characterizing In-stream Flow Refugia. Canadian Journal of Fisheries and Aquatic Sciences 50(8), 1663–1675. https://doi.org/https://doi.org/10.1139/f93-187.

Meile, T., Boillat, J.-L., and Schleiss, A. (2011). Hydropeaking indicators for characterization of the Upper-Rhone River in Switzerland. Aquatic Sciences 73, 171–182. https://doi.org/https://doi.org/10.1007/s00027-010-0154-7.

Miller, S. and Judson, S. (2014). Responses of macroinvertebrate drift, benthic assemblages, and trout foraging to hydropeaking. Canadian Journal of Fisheries and Aquatic Sciences 71, 675–687. https://doi.org/https://doi.org/10.1139/cjfas-2013-0562.

Ministerie van Landbouw, Visserij, Voedselzekerheid & Natuur (n.d.). Beschermde natuur. https://www.natura2000.nl/profielen.

Moore, K. and Gregory, S. (1988). Summer Habitat Utilization and Ecology of Cutthroat Trout Fry (Salmo clarki) in Cascade Mountain Streams. Canadian Journal of Fisheries and Aquatic Sciences 45(11). https://doi.org/https://doi.org/10.1139/f88-224.

Moreira, M., Hayes, D. S., Boavida, I., Schletterer, M., Schmutz, S., and Pinheiro, A. (2018). Ecologically-based criteria for hydropeaking mitigation: a review. Science of the Total Environment 657, 1508–1522. https://doi.org/https://doi.org/10.1016/j.scitotenv.2018.12.107.

Ouwerkerk, S., Versteegen, F., Silva, J. V., da, Visser, B., and Rudolph, M. (2021). Préverkenning waterberging Maas. https://www.deltaprogrammamaas.nl/algemeen/pre-verkenning-waterberging-maas-afgerond/.

Panthi, M., Lee, A., Dahal, S., Omer, A., Franca, J., and Crosato, A. (2022). Effects of sediment flushing operations versus natural foods on Chinook salmon survival. Scientific Reports 12. https://doi.org/https://doi.org/10.1038/s41598-022-19294-2.

Person, É. (2013). Impact of Hydropeaking on Fish and their Habitat. https://www.researchgate.net/publication/283488112_Impact_of_Hydropeaking_on_Fish_and_their_Habitat.

Programmadirectie Natura 2000 (2013). Natura 2000-gebied Grensmaas. https://www.natura2000.nl/gebieden/limburg/grensmaas/grensmaas-aanwijzing.

Reindl, R., Neuner, J., and Schletterer, M. (2023). Increased hydropower production and hydropeaking mitigation along the Upper Inn River (Tyrol, Austria) with a combination of buffer reservoirs, diversion hydropower plants and retention basins. River Research and Applications 39(3), 602–609. https://doi.org/https://doi.org/10.1002/rra.4052.

Rijksoverheid (2022). Nationaal Water Programma - Het nationale waterbeleid en de uitvoering in de rijkswateren. URL: https://www.rijksoverheid.nl/documenten/rapporten/2022/03/18/bijlage-nationaal-water-programma-2022-2027.

Rijkswaterstaat (2023). Natura 2000-ontwerpbeheerplan Grensmaas. https://rwsnatura2000.nl/gebieden/grensmaas/gm_documenten/default.aspx.

— (2025a). Bathymetrie Nederland. URL: https://geoweb.rijkswaterstaat.nl/ModuleViewer/?app=d22bec5b3e3244b19cdd20b308442683.

— (2025b). Betrekkingslijnen Maas versie 2023-2024. URL: https://open.rijkswaterstaat.nl/overige-publicaties/2023/betrekkingslijnen-maas-versie-2023-2024/.

— (2025c). De 7 Maasstuwen. URL: https://www.rijkswaterstaat.nl/water/waterbeheer/bescherming-tegen-het-water/waterkeringen/dammen-sluizen-en-stuwen/de-7-maasstuwen.

— (2025d). Normaal Amsterdams Peil (NAP). URL: https://www.rijkswaterstaat.nl/zakelijk/open-data/normaal-amsterdams-peil.

— (2025e). Rijkswaterstaat Waterinfo. https://waterinfo.rws.nl/thema/Waterbeheer.

Salmaso, F., Servanzi, L., Crosa, G., Quadroni, S., and Espa, P. (2021). Assessing the Impacts of Hydropeaking on River Benthic Macroinvertebrates: A State-of-the-Art Methodological Overview. Environments 8(7), 67. https://doi.org/https://doi.org/10.3390/environments8070067.

Saltveit, S. and Brabrand, Å. (2013). Incubation, hatching and survival of eggs of Atlantic salmon (Salmo salar) in spawning redds influenced by groundwater. Limnologica 43(5), 325–331. https://doi.org/https://doi.org/10.1016/j.limno.2013.05.009.

Schülting, L., Feld, C., Zeiringer, B., and Hudek, H. (2018). Macroinvertebrate drift response to hydropeaking: An experimental approach to assess the effect of varying ramping velocities. Ecohydrology 12(1). https://doi.org/http://dx.doi.org/10.1002/eco.2032.

Schweizer, S., Neuner, J., Ursin, M., Tscholl, H., and Meyer, M. (2008). Ein intelligent gesteuertes Beruhigungsbecken zur Reduktion von künstlichen Pegelschwankungen in der Hasliaare. Wasser Energie Luft 3, 1–10.

Scopus (2025). Scopus. URL: https://rb.gy/ycvskg (visited on 03/03/2025).

Sifuzzaman, M., Islam, M., and Ali, M. (2009). Application of Wavelet Transform and its Advantages Compared to Fourier Transform. Journal of Physical Sciences 13, 121–134.

Strijker, B., Asselman, N., Jong, J., de, and Barneveld, H. (2023). The 2021 flood event in the Dutch Meuse and tributaries from a hydraulic and morphological perspective. Journal of Coastal and Riverine Flood Risk 2(Article 6). https://doi.org/https://doi.org/10.59490/jcrfr.2023.0006.

TELEMAC (2025). TELEMAC-2D - Two-dimensional hydrodynamic. URL: https://www.opentelemac.org/index.php/presentation?id=17.

Tonolla, D., Bruder, A., and Schweizer, S. (2017). Evaluation of mitigation measures to reduce hydropeaking impacts on river ecosystems - a case study from the Swiss Alps. The Science of The Total Environment 574, 594–604. https://doi.org/https://doi.org/10.1016/j.scitotenv.2016.09.101.

Torrence, C. and Compo, G. (1998). A practical guide to wavelet analysis. Bulletin of the American Meteorological Society 79(1). https://doi.org/https://doi.org/10.1175/1520-0477(1998)079%3C0061:APGTWA%3E2.0.CO;2.

Van Denderen, P. (2024). Hydropieken in de Grensmaas: overzicht van de hydrodynamische effecten. https://open.rijkswaterstaat.nl/open-overheid/onderzoeksrapporten/@282844/hydropieken-grensmaas-overzicht/.

Van Duinhoven, G. (2004). Ruimte voor de rivier; Hoe zat dat ook al weer? URL: https://edepot.wur.nl/114410.

Van Looy, K., Jochems, H., Vanacker, S., and Lommelen, E. (2007). Hydropeaking impact on a riparian ground beetle community. River Research and Applications 23(2), 223–233. https://doi.org/https://doi.org/10.1002/rra.975.

Van Neer, R. (2016). A study on the border Meuse : the effect of hydropeaking on the gravel banks and its macroinvertebrates. https://open.rijkswaterstaat.nl/open-overheid/@112785/study-on-the-border-meuse-the-effect/.

Wageningen University & Research (n.d.). Een dikke onvoldoende voor waterkwaliteit. URL: https://www.wur.nl/nl/show-longread/een-dikke-onvoldoende-voor-waterkwaliteit.htm.

Zolezzi, G., Siviglia, A., Toffolon, M., and Maiolini, B. (2011). Thermopeaking in Alpine streams: event characterization and time scales. Ecohydrology 4(4), 564–576. https://doi.org/https://doi.org/10.1002/eco.132.